ABSTRACT

ABU-EL-HAIJA, LENA A. PRECiSE: PancREatic Cancer Prioritization and Screening Evaluation Tool. (Under the direction of Julie Ivy).

Pancreatic cancer (PC) is the fourth leading cause of death due to cancer in the US, and it is projected to be the second leading cause by 2030. While the incidence of PC is relatively low, it has been increasing in recent years. The mortality risk of PC is high with an 8% five-year survival rate. PC can be asymptomatic, which often leads to late diagnosis after the tumor has metastasized to other organs. The late diagnosis was initially perceived to be due to the tumor's rapid progression. However, recent findings have shown that there is an average of seven years from the start of the tumor until metastasis. This presents an opportunity for screening to detect PC patients earlier.

Chapter 2 presents a discrete event simulation model of pancreatic cancer progression, where the discrete events are (i) tumor volume at symptomatic detection, (ii) tumor volume at transition from the local stage to the regional stage, and (iii) tumor volume at transition from the regional stage to the distant stage. The model is personalized to race, gender, and age. Surveillance, Epidemiology and End Results data were used to parameterize the model. Pancreatic cancer is resectable if the tumor can be surgically removed. Resection is the best option for improving survival rates. In Chapter 2, a resectability prediction tool is introduced. With resection being the only true cure for PC, there is a call for screening policies to catch the disease at an early stage. However, current screening policies remain nonspecific with undetermined screening start age, screening interval, and screening end age. The general population has a lifetime risk of 1.3%. However, some are at a much higher risk than others. There are calls for PC screening of high-risk patients only rather than a population wide screening. The International Cancer of the Pancreas Screening Consortium defines high-risk as genetic mutation or first-degree family members with PC.

In Chapter 3, we present an extension to the progression model from Chapter 2, where the risk of a patient contributes to the incidence rate of PC. We overlay the progression model with different screening policies, where the screening start age is set at 50 years old, the screening end age is set at 100, and the screening interval was set at half a year, a year, two years, three years, four years, five years, and ten years. We created different homogeneous populations to study the effect of the screening policies and the effort associated with catching one pancreatic cancer by screening by race, gender, and patient PC risk.

In Chapter 4, we expand the resectability prediction tool and integrate it with the screening model. We test screening policies with varying screening start age, screening end age, screening interval, and screening modality. We test the different policies on homogeneous and heterogeneous populations. We estimate the effort to screen and the average five-year survival of each policy. We create an effort to five-year survival frontier and identify the efficient policies.

PRECiSE: PancREatic Cancer Prioritization and Screening Evaluation Tool

by
Lena A. Abu-El-Haija

A dissertation submitted to the Graduate Faculty of
North Carolina State University
in partial fulfillment of the
requirements for the Degree of
Doctor of Philosophy

Industrial Engineering

Raleigh, North Carolina

2019

APPROVED BY:

Maria Mayorga

Yunan Liu

Reha Uzsoy

Karen Hicklin

Julie Ivy
Chair of Advisory Committee

DEDICATION

To my parents and my five older siblings that have provided all forms of support.

TABLE OF CONTENTS

LIST OF TABLES

LIST OF FIGURES

CHAPTER

1

INTRODUCTION

1.1 Background and Motivation

The pancreas is one of the digestive system organs that is responsible for producing digestive enzymes and hormones, such as insulin [Abo]. Due to the pancreas location in the upper abdomen behind the stomach as shown in Figure 1.1, symptoms of pancreatic disorders can be nausea and abdominal pain which are common to other conditions, such as food poisoning. Given the vague symptoms of pancreatic disorders, diagnosis can be a challenge. Pancreatic disorders include acute pancreatitis, chronic pancreatitis, hereditary pancreatitis, and pancreatic cancer [Abo]. Acute pancreatitis is inflammation of the pancreas that causes a surge in the production of digestive enzymes. Chronic pancreatitis is the permanent damage of the pancreas after multiple episodes of acute pancreatitis. Pancreatic cancer is the existence of malignant cells with abnormal growth inside the pancreas.

The most challenging disease of the pancreatic disorders is pancreatic cancer. Pancreatic Cancer (PC) is the fourth leading cancer cause of death in the United States, and it is projected to be the second by year 2030 [Rah14]. Pancreatic cancer has a low incidence rate; approximately 1.6% of the population will get pancreatic cancer in their lifetime [NCISP]. For 2018, it was estimated there would be 55,440 new cases of PC and 44,330 deaths due to PC with a low 5-year survival of 8.5% [NCISP].

The dismal 5-year survival rate is partly driven by late diagnosis of the disease. Less than 20% of

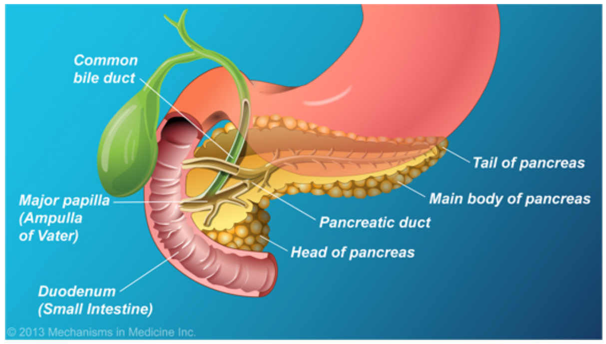

Figure 1.1 Anatomy of the Pancreas [Abo]

PC patients are diagnosed with localized disease, 30% are diagnosed with regional disease, and the remaining 50% are diagnosed with metastatic disease [McA17]. The stage at diagnosis contributes significantly to the 5-year survival rate. The 5-year survival is 34.3%, 11.5%, or 2.7% if the patient was diagnosed in the local, regional, or distant stage, respectively. Surviving pancreatic cancer is further complicated by the fact the only true cure for the disease is surgery (resecting part or all of the pancreas), and it is estimated that only 10% to 20% of patients have a resectable disease at diagnosis [Hol14]. This highlights the need to detect pancreatic cancer early to increase the chance of survival [Tam14]. The goal is to detect cancer at a local or resectable state such that a cure becomes an option for the patient.

There is a debate in the literature as to whether early diagnosis of pancreatic cancer will truly increase survival rates; whether efforts to catch the disease early would be worthwhile given the low survival rates. It was observed that within a sample of 500 patients, as expected the survival of patients with stage I PC was higher than all other stages [Por13]. Moreover, the 1-year and 5-year survival rates for PC increased from the late 1970's to the early 2000's, and the increase is believed to be due to the better imaging technology and surgical methods for detecting and resecting the cancer [Por13]. There is also discussion regarding the detection of precancerous lesions. This was deemed successful for colon cancer to surgically remove the lesions before they become harmful [Len14].

While early detection does not equal survival, there is evidence suggesting that early detection was a factor in the increasing survival rates over the last few decades. However, the survival rates are still very low and hence the motivation for this dissertation. We aim to understand the current status of pancreatic cancer screening and to use the available resources in the literature to develop screening policies for pancreatic cancer.

1.2 Pancreatic Cancer

Cancer is the abnormal growth of cells with mutation, and pancreatic cancer is the growth of such cells within the pancreas. Similarly to colon cancer, pancreatic cysts can be precancerous cells in some cases of pancreatic cancer, especially intraductal papillary mucinous neoplasm cysts [PRM18]. However, only 1% to 2% of pancreatic cysts become cancerous [Fou17]. In fact, when a patient presents with a pancreatic cyst, the treatment option is not always to remove it since most pancreatic cysts have been shown to be harmless and can essentially stay within the pancreas for the rest of the patient's life without complications [Tan12]. Given the distinctions between the problems of pancreatic cyst and pancreatic cancer, we focus on the progression of pancreatic cancer regardless of the path to the first cancerous cell.

1.2.1 Types of Pancreatic Cancer

There are two main types of pancreatic cancer: exocrine and endocrine [Zho10]. Exocrine cells produce enzymes in the pancreatic duct, and a tumor typically develops in the duct [Ame]. Endocrine cells produce hormones, such as insulin, and there are fewer endocrine cells than exocrine cells in the pancreas. Therefore, exocrine and endocrine cells produce different tumors, where the two types have distinctly different biological composition and placement within the pancreas. Exocrine pancreatic cancer, also referred to as pancreatic ductal adenocarcinoma, represents about 95% of the pancreatic cancer population, and it has a lower survival rate than the endocrine type.

1.2.2 Risk Factors

Pancreatic cancer is believed to have different causes, a summary of the risk factors along with their risk is listed in Table 3.1. One of the main causes is genetic mutation. Some of the genes that have been studied and found to have causal effect are *BRCA1/BRCA2* (hereditary breast and ovarian cancer syndrome), *MLH1/MSH2/MSH6/PMS2* (Lynch syndrome), *TP53* (Li-Fraumeni syndrome), *CDKN2A/p16* (familial atypical multiple mole melanoma syndrome), *STK11* (Peutz-Jeghers syndrome), and *PRSS1* (hereditary pancreatitis syndrome) [McA17]. Carriers of any of these genetic mutations are considered to be at high-risk for pancreatic cancer.

Patients with first degree relatives (FDRs - parent, sibling, or child) that have/had pancreatic cancer are also considered to be at high-risk, and the more FDRs with PC the higher the risk for the patient. However, hereditary factors, such as FDRs and genetic mutations, seem to account for only 10% of the pancreatic cancer population [McA17]. The question remains, who else is at risk for pancreatic cancer? There are other recognized risk factors that are mentioned in the literature and are believed to contribute to pancreatic cancer, such as chronic pancreatitis, diabetes, and cigarette and alcohol use. We will elaborate on each of those risk factors and how they contribute to pancreatic cancer.

Chronic Pancreatitis is irreversible damage of the pancreas as a result of inflammation after one or more episodes of acute pancreatitis, where acute pancreatitis is an episode of inflammation of the pancreas [Abo]. If chronic pancreatitis was due to hereditary pancreatitis (when the cause of pancreatitis is genetic instead of environmental), then it is believed that chronic pancreatitis evolves through the same mechanism that is involved in the development of pancreatic cancer [Bec14]. However, hereditary pancreatitis is very rare, where only 2% to 4% of chronic pancreatitis patients had hereditary pancreatitis [Sol93]. The most common cause of chronic pancreatitis in adults is alcohol or cigarette abuse which is also a risk factor for pancreatic cancer [McA17]. This relationship makes it difficult to determine if chronic pancreatitis itself is a risk factor since alcohol and cigarette abuses play major roles in the development of both diseases [Dha15]. In addition, the exact mechanism that turns chronic pancreatitis to pancreatic cancer has not yet been defined [Rai10]. Raimondi et al. conducted a meta-analysis to quantify the relative risk associated with chronic pancreatitis and found that the disease increases pancreatic cancer risk by 13.3 (6.1-28.9 95% CI) fold [Rai10].

Diabetes is when the pancreas cannot produce insulin (Type I) or overproduces it (Type II). Diabetes has been linked to pancreatic cancer. However, there is debate about whether it should be recognized as a risk factor especially given that the prevelance of diabetes is much higher than that for pancreatic cancer. Diabetes can be an early indicator of the onset of pancreatic cancer where some studies have shown that 25% to 50% of pancreatic cancer patients have developed diabetes 6-36 months before they developed pancreatic cancer [Sal15]. The Centers for Disease Control and Prevention estimated that there are 30.2 million diabetics in the US as of 2015 [Cen17a]. However, it is not clear that all 30.2 million diabetic patients are at risk for pancreatic cancer. There is the debate as to whether diabetes could cause the cancer or if the early stages of the cancer cause diabetes.

Smoking has been linked as a cause of different pancreatic disorders, such as pancreatitis and pancreatic cancer [YL13]. In fact, "cigarette smoking has been consistently associated with risk of pancreatic cancer" [Sch14], and it accounts for about 25% of pancreatic cancer cases [YL13]. Similarly, **alcohol** was also recognized to be a cause of pancreatic disorders, especially pancreatitis. However, only heavy alcohol consumption was found to increase the risk to pancreatic cancer [Zak15].

The literature does well in identifying the high-risk population of pancreatic cancer as the group with genetic mutations or first degree family history. Some literature specifies that a patient must have at least two FDRs with pancreatic cancer, or one FDR and genetic mutation are needed to classify the patient at high risk. Following the same logic of combining risk factors, a patient with diabetes that smokes and drinks alcohol could be classified as a high-risk patient. Therefore, these risk factors should not be neglected when advising patients to screen for pancreatic cancer.

Table 1.1 Risk Factors of Pancreatic Cancer and their Associated Relative Risks

Risk Factor	Gene Associated	Increased Relative Risk
Familial Pancreatic Cancer, 1 FDR	Unknown	4.5
Familial Pancreatic Cancer, 2 FDR	Unknown	6.4
Familial Pancreatic Cancer, 3 FDR	Unknown	32
Hereditary breast and ovarian cancer syndrome	BRCA1	2.3
Hereditary breast and ovarian cancer syndrome	BRCA2	3.5
Lynch syndrome	MLH1, MSH2, MSH6, PMS2	8.6
Familial atypical multiple mole melanoma pancreatic carcinoma syndrome	p16	13
Peutz-Jeghers syndrome	STK11/LKB1	132
Hereditary pancreatitis	PRSS1, SPINK1	69
Cystic fibrosis	CFTR	3.5
Chronic Pancreatitis		13.3
Type-I Diabetes		2
Type-II Diabetes		1.8
Cigarette Use		1.7
More than 3 alcoholic drinks per day		1.2

1.2.3 Pancreatic Cancer Symptoms and Diagnosis

About half of the pancreatic cancer population are diagnosed at the metastatic stage [McA17], and the late diagnosis is mostly due to the asymptomatic nature of the disease. Moreover, symptoms of PC are not distinct enough to steer diagnositic tests towards pancreatic cancer directly. The most commons symptoms are abdominal pain and nausea, which are also the symptoms for appendicitis, pancreatitis, gallstones, kidney stones, lactose intolerance, or many other digestive problems. These common symptoms might be accompanied with other symptoms, such as jaundice, unwanted weight loss, or a new onset of diabetes [Ame].

Once pancreatic cancer, or pancreatic disorders in general, are suspected, imaging is performed to the abdominal area and the pancreas, such as a computed tomography (CT) scan or a magnetic resonance image (MRI). If a mass is found in the pancreas and suspected to be a tumor, then usually an endoscopic ultrasound (EUS) procedure is performed as a confirmation test. Each of these testing mechanisms or modalities can be used for pancreatic cancer screening and diagnosis.

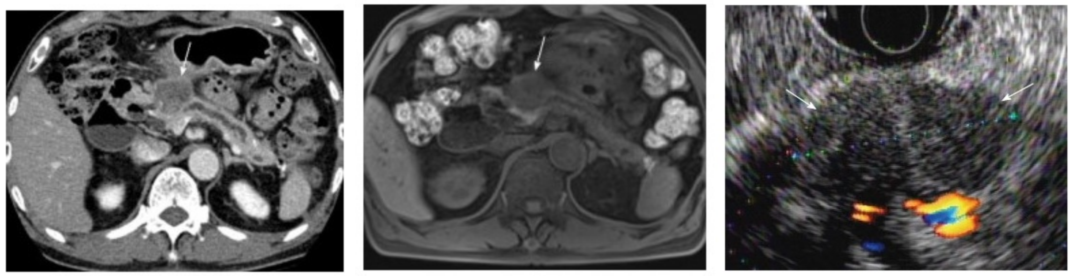

(a) CT Scan **(b)** MRI **(c)** EUS

Figure 1.2 Images of Pancreatic Cancer using Different Screening Modalities [LL14]

1.2.4 Screening Modalities for Pancreatic Cancer

Diagnosing pancreatic disorders requires imaging techniques due to the fact that the pancreas is an organ that is difficult to view since it is embedded behind other organs. Some of the different imaging techniques are computed tomography scan, magnetic resonance imaging, and endoscopic ultrasound. Each of the modalities has individual features that would lead medical personnel to choose one over another.

Computed Tomography scan (CT) is an imaging mechanism that uses x-ray and often dye that can detect legions [201a]. A patient getting a CT scan must lie still on a table while the image is being taken. CT scan is noninvasive imaging that has a reported sensitivity (true positive) of 76% to 92% [Tum11].

Magnetic Resonance Imaging (MRI) is an imaging mechanism that uses strong magnets connected to computers [201a]. MRI is better at differentiating lesions than a CT scan. For example, if a mass was detected by a CT scan it is not uncommon to order an MRI for further diagnosis [Tum11]. However, the sensitivity of the imaging for detection of pancreatic cancer is only 84%, and hence MRI is not always perceived to have a diagnostic advantage over CT Scans [Tum11].

Endoscopic Ultrasound (EUS) is a procedure that requires inserting a tube orally to examine a patient's digestive system and nearby organs, where the end of the tube is an ultrasound device [201b]. Ultrasound uses sound waves to image the pancreas. If a lesion is found, **Fine Needle Aspiration (FNA)** is used to biopsy the mass during the scope. EUS requires the patient to be sedated, and it is an invasive screening modality. Despite the invasive nature of EUS, it is the most accurate for diagnosing pancreatic lesions with a reported sensitivity of 86.8% to 92.0% [LL14; Tum11]. EUS is commonly used to confirm diagnosis after a lesion is detected by a CT scan or an MRI since the lesion can be biopsied using FNA.

Detection of pancreatic cancer leads to assessing the patient's cancer stage and potential treatment options. The imaging techniques discussed are used to view the location, the spread, and the size of the tumor.

1.2.5 Resectability of Pancreatic Cancer

The treatment options for pancreatic cancer are limited. Radiation and chemotherapy can have some effect in reducing tumor size within the pancreas, or prolonging a patient's life [Tam14]. However, they only have limited effect in curing the tumor. Therefore, the main measure of the tumor's curability is whether it can be surgically removed, i.e., resection. Pancreatic cancer is said to be resectable if it can be surgically removed. Pancreatic cancer can be *resectable*, *borderline resectable*, or *unresectable*.

The definitions of the three resectability categories are constantly being refined in the literature as surgical advances take place. *Resectable* pancreatic cancer is when the cancer is confined to the pancreas and has not reached any major blood vessels [Tem17]. Another criterion for a tumor to be resectable is that the patient's health state would permit enduring a pancreatectomy (surgical removal of the pancreas) [Tam14]. A *borderline resectable* tumor is usually classified as one that has some contact with a major artery or blood vessel that does not enclose more than half of the artery ($\leq 180°$ enclosement) [Tem17]. An *unresectable* tumor is one that has spread to major blood vessels or metastasized to distant locations, such as the liver or lungs [Tem17]; even if the tumor was surgically removed, there cannot be a guarantee that another tumor onset did not occur in another location.

Generally, pancreatic cancer recurrence is possible after a successful resection. However, resection still remains the best option for surviving pancreatic cancer. Therefore, screening for pancreatic cancer is vital to detecting the tumor at a resectable state.

1.3 Pancreatic Cancer Screening

Given the low incidence rate of PC, population level screening is not thought to be efficient [CMHFHR13]. Therefore, population screening guidelines have not been configured. This is due, in part, to the belief that pancreatic tumors are aggressive and unlikely to be caught at an early stage. However, recent studies have shown that there is a window for early detection [YID13]. Therefore, the problem of early detection of PC has been gaining traction in recent years, and studies have elaborated on whom to screen and what screening modalities should be used [DC14; Bec14; Lin].

Moreover, there are multiple centers that have conducted case studies recruiting high-risk patients and screening them. One study recruited 51 patients at high risk for PC, and after the first round of screening, they found two patients with pancreatic cancer, one with local cancer and one with metastatic cancer [Ver10]. Canto et al. (2006) recruited 78 patients and found one patient with a pancreatic lesion and nine patients with pancreatic cysts or dilated ducts [Can]. Al-Sukhni et al. (2012) conducted an eight-year study where they recruited and annually screened 262 patients finding three patients with PC (one local, and two metastasized) and fifteen patients with pancreatic cysts [AS12].

The International Cancer of the Pancreas Screening (CAPS) consortium calls for screening high-risk patients for pancreatic cancer [CMHFHR13]. The consortium consists of 50 experts in the field, and their meeting in 2013 was targeted towards defining the high-risk population and discussing the potential screening for the disease. The produced guidelines are the main source of guidance when it comes to screening for PC. The questions of when to start screening, how frequently, and when to stop screening still remain unanswered. In 2013, the consortium suggested to start screening at the age of 50; however, only 51% of the consortium agreed on that age. Moreover, there was not a consensus on the screening modality, screening interval or screening end age. The CAPS definition of high-risk individuals focused on genetic mutation and the number of FDRs with pancreatic cancer. They mentioned that a high-risk individual is anyone with an increased relative risk of five-fold.

The question of whom to screen was only partially answered by the CAPS guidelines. For example, an individual with a five-fold relative risk can be a chronic pancreatitis patient. However, non-hereditary pancreatic disorders are not necessarily considered when defining the population at high risk. Moreover, family history only accounts for about 10% of the pancreatic cancer population, and genetic mutation is not necessarily observed unless other risk factors are present. This results in a high-risk group that does not fully cover the pancreatic cancer population. This highlights the need for an expanded definition of high risk to include a broader spectrum of pancreatic cancer risk factors.

The other three major questions are (i) when to start screening, (ii) how frequently should the screenings be, and (iii) when to stop screening? The CAPS guidelines have touched on some answers, but a screening policy has yet to be developed. Screening start age will heavily depend on the age distribution at pancreatic cancer incidence. It could be appropriate to start screening the high-risk group at age 50 without missing a large portion of the pancreatic cancer population. The time interval between screenings will likely depend on the progression rate of the tumor, and how quickly a patient might transition out of the curable stage. Lastly, the screening stop age could be a function of resectability. For example, if we cannot resect tumors in patients over 80 years old then should we screen them?

1.4 Problem Definition

The overarching goal of this dissertation is to develop methods for identifying policies that allow for the detection of pancreatic lesions at a clinical stage when surgery may be an option. Pancreatic cancer is the fourth leading cause of death due to cancer, and it is expected to be the second by 2030 [Rah14]. The asymptomatic nature of the disease leads to late symptomatic detection after the tumor has metastasized. However, asymptomatic may not mean the tumor is fast growing and that the window for screening is small. In fact, there is evidence that there is an average of a seven year interval from the beginning of the cancer until it reaches metastasis [Yac10].

Even with the time opportunity to screen, a population wide screening program would be exhaustive and would result in many benign screenings. The pancreatic cancer incidence rate in the US typically ranges between 50,000 and 60,000 cases per year [NCISP]. Therefore, it becomes clear that only the high-risk population should be considered. However, the current definition of the high-risk population is mostly restricted to individuals with genetic mutation or FDRs with pancreatic cancer. The CAPS guidelines defined a high-risk individual as anyone with a relative risk of 5 [CMHFHR13], while other literature views a high-risk individual as someone with a relative risk of 10 [Har16]. The high-risk group for pancreatic cancer is not well defined, although risk factors are extensively discussed in the literature.

Screening policies for pancreatic cancer are also ill defined. Because the incidence rate is relatively low, and population wide screening is out of the question, screening policies have not been studied. There are case study reports of hospitals recruiting patients and screening them over some period of time [Can; Ver10; AS12]. However, these screening trials are not screening policies. A screening policy would specify the screening start age, screening interval, and screening end age.

The curability of the disease after it is detected remains unresolved as well. If screening was employed in a perfect matter, we still cannot claim that everyone with a screening detected pancreatic cancer has a resectable cancer. The stage of the cancer, spread of the tumor, and age of the patient affect the resectability status of the cancer. However, it is unknown the degree to which each of these factors affect resectability.

Pancreatic cancer is a unique disease where it combines low incidence, late diagnosis, and high mortality with a potential for increased survival if it is detected early. Pancreatic cancer problems are new to the simulation and optimization world. This dissertation seeks to answer the following questions:

1. Who is at high risk for developing pancreatic cancer?
2. When should screening start for high-risk individuals?
3. How often should high-risk individuals be screened?
4. What screening modality should be used?
5. When should screening stop?
6. What is the role of gender, race, and age in personalizing screening policy?
7. How does resectability influence screening policy?
8. Can we categorize patients into resectable and nonresectable?

9. Given the answers to the above, what should the optimal screening policies for pancreatic cancer be?

1.5 Dissertation Organization

The remainder of this dissertation is organized as follows. Chapter 2 presents a discrete event simulation progression model of pancreatic cancer. Chapter 3 presents a simulation-based screening policy evaluation tool. Chapter 4 presents a simulation-based screening policy evaluation tool with resectability prediction incorporated. Chapter 5 discusses dissertation findings, key contribution, and directions for future work.

CHAPTER

2

SEER BASED PANCREATIC CANCER PROGRESSION MODEL

2.1 Introduction

Pancreatic Cancer (PC) is the fourth leading cause of mortality due to cancer in the US, and it is projected to be the second by 2030 [Rah14]. The general populations' lifetime risk is a low 1.6%. It was projected that in 2018 there would be 55,440 new cases and 44,330 deaths from pancreatic cancer (7.3% of all cancer deaths) [NCISP]. Pancreatic cancer tends to be asymptomatic leading to late symptomatic detection often after the cancer has metastasized to other organs [Xu14]. As a result, metastasis is common in PC, accounting for up to 90% of its mortality and the dismal 5-year survival rate of 8% [YID13]. Initially, it was thought that PC is aggressive, fast growing in nature, and hence unlikely to be caught at an early stage. However, it was found that there is an average of 6.8 years from the first parental clone to metastasis in the progression of PC [Yac10]. The late diagnosis of PC is actually due to the asymptomatic nature of the tumor rather than its fast progression. Therefore, the problem of early detection of PC has been gaining traction recently [DC14; Bec14; Lin].

Pancreatic cancer is further complicated by the fact that the only known cure is through surgery (resection), and the cancer is only resectable if it has not metastasized to other organs or major blood vessels. It was estimated that only 10-20% of PC patients are candidates for resection at diagnosis [Hol14]. This can be due to the late symptomatic detection of the tumor, where its resectability can be viewed as a property that is lost as the tumor ages. A formal definition of "resectable" pancreatic cancer is imprecise as resectability is determined on a case-by-case basis. Resectability seems to be related to age, stage of the tumor, and the spread of the tumor. A patient that is considered to have a resectable cancer may still not be fit for surgery due to the risk of mortality from the pancreatectomy because of their age [Tam14]. The tumor stages may also be viewed from the perspective of resectability where the tumor can be *resectable*, *borderline resectable*, and *unresectable*.

Producing effective screening policies for PC requires an understanding of the tumor's progression and behavior. Research devoted to understanding the pathogenesis of the disease is growing [Old17]. Most PC progression models take a molecular view on the evolution of PC and consider the series of mutations until a cancer cell is created in the pancreas [Hru00]. Of the mathematical growth models for PC, most describe cell interactions rather than milestones within the disease [Lou14]. We develop a progression model that predicts the time when the tumor is symptomatic and the times when the tumor transitions from local to regional and regional to distant stages. In this chapter, we present a discrete event simulation model of the natural history of PC simulating the potential cancer progression paths in cancer free patients.

2.2 Literature Review

Pancreatic cancer research has been gaining traction as mortality risk drives efforts to enhance treatment and survival rates. Oldfield et al. conducted a literature review on the molecular behavior and the natural history of pancreatic cancer [Old17]. Their work presented a genetic background of the tumor's progression and provided a base for improvement in detection and management of PC. Louzoun et al. developed a mathematical model that describes the interaction between pancreatic cancer and the immune system [Lou14]. Hruban et al. analyzed the progression of PC from normal pancreas cells that become lesions and undergo a series of mutations before they become cancerous cells [Hru00].

Yachida et al. studied pancreatic cancer samples and estimated a 10-year window between the first cancer cell and a parental clone, and a 7-year interval until metastasis, suggesting a slower progression of PC than initially believed [Yac10]. Sun et al. conducted similar work where they developed a mathematical model to replicate pancreatic cell mutations from the first lesion to cancer [Sun14]. Sun et al. used their model and the patient summary data presented in Yachida et al. to evaluate the timeline of the tumor progression as well as the tumor doubling time [Yac10; Sun14]. The model yielded a tumor doubling time with an average of 94.3 days (ranged between 84 and 105 days) before metastasis and an average tumor doubling time of 36 days after metastasis [Sun14]. Furukawa et al. studied the pancreatic cancer tumor growth rate in nine patients before metastasis, and their sample yielded a doubling time of the tumor that ranged between 64 and 255 days [Fur01]. Notta et al. developed an algorithm, Chrom-AL, that was designed to look at the chromosomal levels of pancreatic cancer progression [Not16].

Haeno et al. developed a cell replication model for PC that starts with a single tumor cell without metastatic ability that can multiply into a tumor cell with metastatic ability which, in turn, can multiply into a metastatic tumor cell at a distant location [Hae12]. This model assumes that all rates are associated with exponential distributions due to the exponential nature of tumor growth and cell division. Weekes et al. also considered the exponential nature of tumor growth by developing differential equations that describe the cell replication behavior for a non-cancer specific model [Wee14]. This model assumes two types of cancer cells: stem and non-stem cells. Cancer stem cells are the tumor initiation cells with replication ability. Non-stem cells are the tumor cells with a shorter lifespan and lower ability to multiply. The model considered the possible paths of a stem cell dividing into two stem cells, one stem cell and one non-stem cell, or two non-stem cells [Wee14]. Pandharipande et al. developed a pancreatic cancer screening simulation model where the model also includes a natural history model for pancreatic cancer [Pan15]. Peters et al. expanded on the natural history model presented by Pandharipande et al. by incorporating precancerous stages know as *PanIN* cells [Pet18]. The Peters et al. and the Pandharipande et al. models used the summary statistics from the Surveillance, Epidemiology, and End Results (SEER) databases but not the patient level data.

Cancer progression models have been developed for various cancers. Roberts et al. developed a discrete event simulation model of colorectal cancer progression: the *Vanderbilt/NC State* model [Rob07]. The underlying distribution for most of the random variables in the simulation model was assumed to be the Johnson SB. However, if the variable was time dependent then it was assumed to follow a nonhomogeneous Poisson process [Rob07]. Shen et al. developed a continuous Markov chain model to estimate the time until symptomatic detection using periodic screening data of lung cancer patients [She17]. The study aimed to understand the effect of the tumor's time until symptomatic detection on personalized screening policy effectiveness [She17]. Plevritis et al. derived probability models of symptomatic detection and the transition between stages of cancer [Ple07]. While their model was tumor independent, it was only implemented on breast cancer [Ple07]. Tejada et al. developed a simulation model for natural history of breast cancer that used the result of Plevritis et al. to evaluate the probability that the tumor is in a certain stage given its volume [Tej15].

In parallel with the tumor progression research, the study of the curative state of pancreatic cancer has been ongoing. The National Comprehensive Cancer Network (NCCN) 2017 guidelines for pancreatic cancer gave a criteria for the three resectability categories depending on the tumor position in the pancreas and the spread of the tumor [Tem17]. Resectable pancreatic cancer is confined to the pancreas, a boarderline resectable tumor has some contact with major arteries, and an unresectable tumor is no longer contained to the pancreas and neighboring organs. The true criteria for borderline resectable cancer is constantly being refined in the literature [Lop14]. Management of the tumor changes with the degree of resectability, and with technological advances in surgery, the hope is to be able to resect more borderline resectable tumors.

One of the main challenges when trying to understand PC is the lack of large databases on the evolution of the disease; the incidence of the disease is low. The Surveillance, Epidemiology, and End Results (SEER) databases are the publicly available patient level data in the US that have been used to study pancreatic cancer. These studies have explored the associated trends in incidence and mortality of PC over time [Wu18; Gd18; Saa18]. The studies found a rising trend in incidence of PC even when the data was stratified by gender, race, and age. Other studies explored the racial, gender, and age disparities in PC [Nip17; Zho17]. The studies found that African Americans are more likely to be diagnosed at a later stage of the cancer and have lower survival rates than whites. Most pancreatic cancer research to date has been descriptive in nature, where little modeling work has been developed to characterize the evolution of pancreatic cancer within a patient. To the best of our knowledge, a pancreatic cancer growth model based on population level data such as SEER has not been developed. In this chapter, we utilize SEER data, the framework presented by Plevritis et al., and the findings of Furukawa et al. to develop a pancreatic cancer growth model that is personalized by race, gender, and age.

2.3 Methods

For this study, we analyzed pancreatic cancer data from SEER. Moreover, we utilized the PC progression timeline introduced by Yachida et al., and the progression models by Haeno et al. and Plevritis et al. We created a discrete event simulation of the model based on Haeno et al. and evaluated the time until metastasis. We modified the progression model presented by Plevritis et al. and created a discrete event simulation of the resulting model. We validated the model by comparing the time until metastasis produced by the model against that presented by Yachida et al. and the result of the simulation of Haeno et al. The simulation models were implemented using Python 3.6. The remainder of this section introduces the pancreatic cancer data in SEER and our extension of the progression model by Plevritis et al. using the SEER data for PC.

2.3.1 SEER Data

The SEER databases are registries by the National Cancer Institute and consist of data collected from 18 different registries around the US. The SEER databases have millions of records, where each record corresponds to a patient and multiple records could correspond to the same patient at different points in time. Each record contains 133 fields with patient and tumor information including primary tumor, age at diagnosis, gender, race, tumor size, tumor stage, and treatment. We filtered the data by primary tumor, and only studied the set of patients whose primary tumor was pancreatic cancer. Table 2.1 summarizes the characteristics of pancreatic cancer patients in the

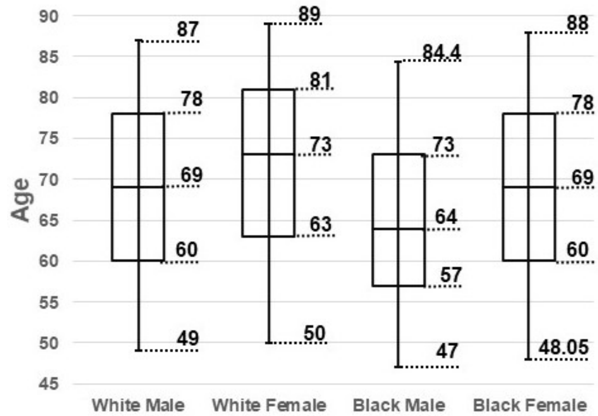

Figure 2.1 Box Plots of Age Distribution by Race and Gender

SEER data.

2.3.2 SEER Data Analysis

Given the lack of screening for the disease, we assumed the pancreatic cancer entries that were not death records and did not undergo treatment to be symptomatic detection records. We remove the treatment records since the recorded tumor size can be post surgery. We have identified that the records prior to 2004 were missing the tumor volume where SEER data created that field in 2004 and there did not exist an equivalent field with tumor size prior to 2004. The records prior to 2004 were about 47% of the total PC records. After filtering the data and removing the rows with missing information, we had 40,587 records of white patients, 6,355 records for African American, and 3,906 records for the other races. We excluded the records for the other races since they were not enough to train the progression model. The resulting data spanned the years 2004 till 2014. We segmented the filtered data by gender and race then analyzed the age distribution within each subset. The box plots in Figure 2.1 suggests that the age distribution within each subgroup is different. In fact, the white female's 50^{th} percentile of 73 years old is the same as the black male's 75^{th} percentile. Based on this heterogeneity, we further segmented the gender/race populations by age percentiles in each group resulting in sixteen disjoint subsets. Each subset was converted into frequency contingency tables of cancer stage (local, regional, and distant) against tumor size (groups by: ≤ 1cm, 1-2cm, ..., 9-10cm, 10-12cm, 12-15cm, 15-20cm, and ≥ 20cm in diameter).

Table 2.1 SEER Data Summary Statistics for Pancreatic Cancer Records

Category	Subcategory	Count	Percentage
Gender	Male	110,510	49.82%
	Female	111,313	50.18%
Race	White	180,549	81.39%
	Black	25,714	11.59%
	Other	15,214	6.86%
	Unknown	346	0.16%
Ethnicity	Hispanic	17,708	7.98%
	Non-Hispanic	204,115	92.02%
Gender by Race	Males, white	90,604	40.85%
	Females, white	89,945	40.55%
	Males, black	12,189	5.49%
	Females, black	13,525	6.10%
Age at Diagnosis	≤ 34	1,180	0.53%
	35-39	1,527	0.69%
	40-44	3,450	1.56%
	45-49	7,177	3.24%
	50-54	12,954	5.84%
	55-59	19,473	8.78%
	60-64	25,505	11.50%
	65-69	30,161	13.60%
	70-74	32,702	14.74%
	75-79	32,486	14.65%
	80-84	27,812	12.54%
	≥ 85	27,388	12.35%
	unknown	8	0.00%
Tumor Size	Blank field	103,806	46.80%
	Unknown	34,921	15.74%
	No mass found	681	0.31%
	< 1cm	815	0.37%
	1-1.9cm	5,255	2.37%
	2-2.9	16,225	7.31%
	3-3.9	21,136	9.53%
	4-4.9	16,382	7.39%
	≥ 5	22,525	10.15%

Table 2.1 SEER Data Summary Statistics for Pancreatic Cancer Records (continued)

Category	Subcategory	Count	Percentage
Stage	In-Situ	676	0.30%
	Local	20,470	9.23%
	Regional	55,891	25.20%
	Distant	111,010	50.04%
	Unstaged	33,776	15.23%
Total records		221,823	

We also explored two fields in the SEER data: reason for no surgery and which surgery was performed (if any) to identify resectable disease. The first field has a category "surgery not recommended", and the second field has a category for "no surgery" was performed. We filtered the set of patients that were not recommended for surgery and did not have a surgery performed and assumed the set to include patients with *unresectable pancreatic cancer*. Similarly, we filtered the set of patients that had a surgery on the primary tumor site to be the set of patients with *resectable/borderline resectable pancreatic cancer*. We created two databases of *resectable* and *unresectable* cancer for further analysis as described in Section 2.3.4. Table 2.2 summarizes the characteristics of the two databases created.

2.3.3 Progression Model

The tumor growth model was developed based on the work by Plevritis et al. One of the key assumptions in our work is that tumor progression is gender, race, and age dependent. We developed a simulation model that imitates the natural history of PC in high-risk patients. Table 2.3 and Figure 2.2 present the logic of the simulation model. The simulation starts by creating a patient with either an assigned or randomly sampled race and gender, and using the race and gender of the patient, an age of cancer initiation is generated according to a cancer initiation age distribution we obtain from SEER. We used the White male to White female to Black male to Black female ratio from the SEER data when generating a new patient. Using the complete records of the SEER data, we utilized the age at diagnosis and the tumor volume fields with the progression model described in Section 2.3.3.1 to reverse the tumor progression to the age at which the tumor would have been initiated for each race and gender. With a simulated cancer patient, we sample tumor volumes of the cancer progression as explained in the next section. The model assumes that cancer stages progress from local to regional to distant. We assume that it is not possible to move from local to distant without passing through the regional stage.

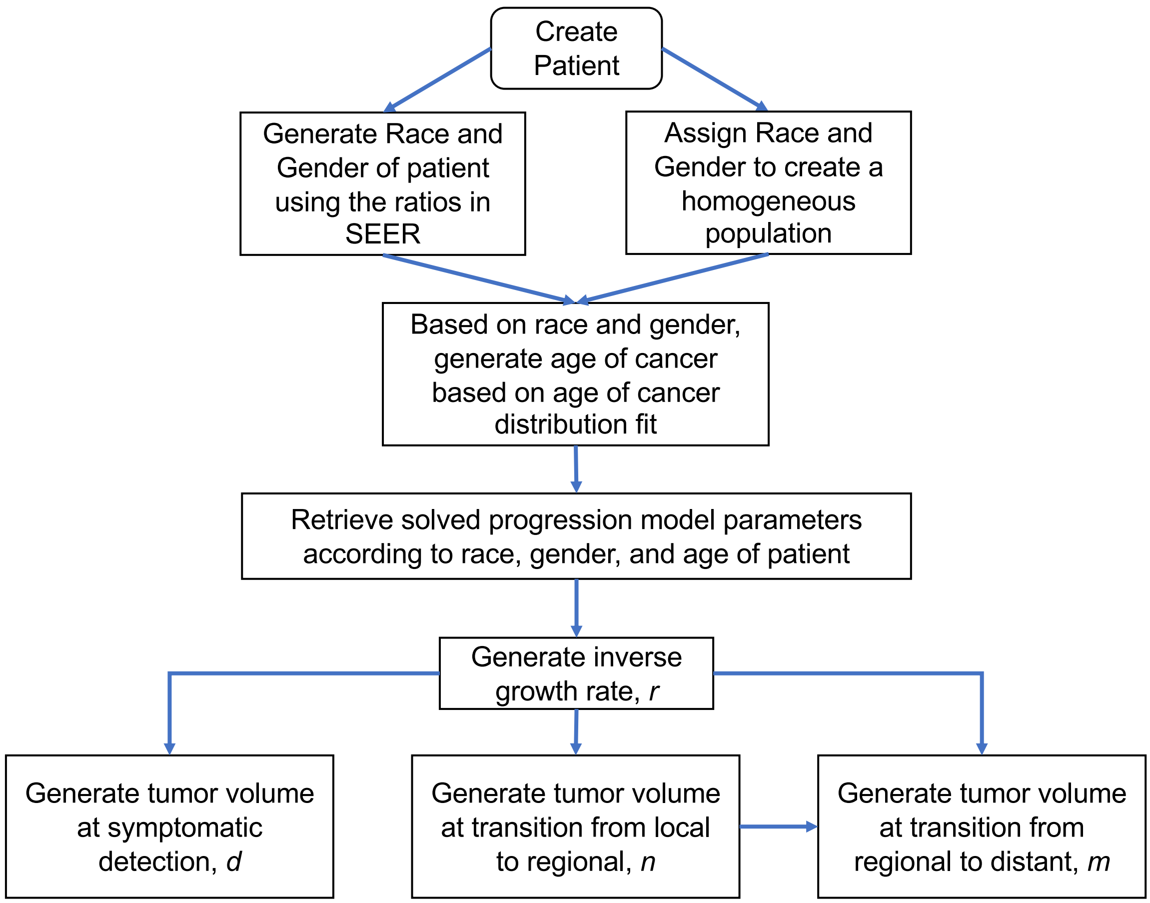

Figure 2.2 Cancer Progression Model

Table 2.2 Summary Statistic of the Resectable and Unresectable Populations Created

		Resectable		Unresectable	
		Count	Percentage	Count	Percentage
Total		19,281		52,499	
Race and Gender	White Male	8,189	42.47%	21,641	41.22%
	White Female	7,620	39.52%	20,361	38.78%
	Black Male	859	4.46%	3,022	5.76%
	Black Female	1,025	5.32%	3,292	6.27%
	Other Male	752	3.90%	2,030	3.87%
	Other Female	836	4.34%	2,153	4.10%
Age at Diagnosis	≤ 34	297	1.54%	172	0.33%
	$35-39$	254	1.32%	266	0.51%
	$40-44$	485	2.52%	704	1.34%
	$45-49$	976	5.06%	1,725	3.29%
	$50-54$	1,642	8.52%	3,277	6.24%
	$55-59$	2,311	11.99%	5,180	9.87%
	$60-64$	2,917	15.13%	6,687	12.74%
	$65-69$	3,189	16.54%	7,157	13.63%
	$70-74$	2,990	15.51%	7,306	13.92%
	$75-79$	2,474	12.83%	7,326	13.95%
	$80-84$	1,346	6.98%	6,686	12.74%
	≥ 85	400	2.07%	6,013	11.45%
Stage	Local	3,626	18.81%	4,602	8.77%
	Regional	12,707	65.90%	12,794	24.37%
	Distant	2,948	15.29%	35,103	66.86%

2.3.3.1 Model Framework

This section presents the methodology of the progression model, and Table 2.4 summarizes the model parameters used. The tumor volume is assumed to follow an exponential growth function according to:

$$V(t) = c_0 e^{t/R}, \tag{2.1}$$

where c_0 is the spherical initial tumor volume with a diameter of 2mm. We calculate the time where a tumor is at a certain volume, V, with the inverse of Equation 2.1:

$$T(V) = R \ln\left(\frac{V}{c_0}\right) \tag{2.2}$$

The inverse growth rate of the tumor, R, is assumed to follow a Gamma distribution [Ple07; Atk83]:

Table 2.3 Pancreatic Cancer Progression Model Simulation Run

Step 1	Create Patient: • For a heterogeneous population: Using the distribution of race/gender in the SEER data patients, sample a race and gender. • For a homogeneous population: Specify a race and gender. • Using the race/gender sampled, identify the appropriate distribution of cancer age initiation. Sample an age.
Step 2	Using the race, gender, and age generated in Step 1, retrieve progression model parameters
Step 3	From the distribution of the inverse growth rate, R, generate a sample r
Step 4	Create Tumor: 1. Generate tumor volume at symptomatic detection, d, using Equation 2.5. 2. Generate tumor volume at transition from local to regional, n, using Equation 2.6. 3. Generate tumor volume at transition from regional to distant, m, using Equation 2.7.
Step 5	Translate tumor volumes generated to time in years using the Equation 2.2 and record the time stamps of the events generated.

$$\Gamma_R(\alpha,\beta) = \frac{\beta^{\alpha}}{\Gamma(\alpha)} r^{\alpha-1} e^{-\beta r}, \tag{2.3}$$

where the parameters α and β are solved for in the model using the method presented in Plevritis et al. [Ple07]. The tumor volume doubling time is proportional to the inverse growth rate R, where doubling time (DT) is:

$$DT = \ln(2) \times R. \tag{2.4}$$

To represent tumor progression, Plevritis et al. introduced three conditional tumor volume probability distributions given an inverse growth rate, R, as follows:

1. Distribution of tumor volume at symptomatic detection, D:

$$F_{D|R}(d|r) = 1 - e^{-\gamma r(d-c_0)} \tag{2.5}$$

Table 2.4 Model Parameters

Parameter	Description
t	time in years
c_0	tumor starting (spherical) volume of diameter 2mm
$V(t)$	tumor volume, in mm^3, at time t
R	the inverse growth rate
r	a realization of R
α, β	shape parameters of the distribution of R
DT	tumor doubling time
a, b	input parameters of uniform distribution
D	the tumor volume at symptomatic detection
d	a realization of D
F_D	cumulative density function of D
N	the tumor volume at transition from local to regional
n	a realization of N
F_N	cumulative density function of N
M	the tumor volume at transition from regional to distant
m	a realization of M
$F_{M\|N}$	cumulative density function of M given N
γ, η, ω	parameters of the distributions of $D, N,$ and M
K	number of categories of discretized tumor volumes
d_k	realized volume at the k^{th} category, $1 \leq k \leq K$
I	tumor stage, 0 for local, 1 for regional, and 2 for distant

2. Distribution of tumor volume at transition from local stage to regional stage of cancer, N:

$$F_{N|R}(n|r) = 1 - e^{-\eta r(n-c_0)} \tag{2.6}$$

3. Distribution of tumor volume at transition from regional stage to distant stage of cancer, M:

$$F_{M|N,R}(m|n,r) = 1 - e^{-\omega r(m-n)} \tag{2.7}$$

We note that the distribution of tumor volume at detection is assumed to be independent of the distributions of tumor volume at transitions between the local, regional, and distant tumor stages. These three distributions are used to create the three events in the simulation, given a specific R value generated for each patient. The parameters γ, η, and ω were estimated by maximizing the likelihood function:

$$L = \prod_{k=1}^{K-1} \mathbf{P}(D \in (d_k, d_{k+1}), I = 0)^{p_k} \mathbf{P}(D \in (d_k, d_{k+1}), I = 1)^{q_k} \mathbf{P}(D \in (d_k, d_{k+1}), I = 2)^{s_k}, \tag{2.8}$$

where K denotes the number of discretized tumor size categories; I the tumor stage where 0 is local, 1 is regional, and 2 is distant; $\mathbf{P}(D \in (d_k, d_{k+1}), I)$ the probability a pancreatic cancer patient experiences symptomatic detection at a tumor volume in the range (d_k, d_{k+1}) in stage I; and p_k, q_k, and s_k correspond to the frequency of tumor volume within the range d_k to d_{k+1} for stage 0, 1, and 2, respectively. Since these frequencies can be high, we maximize the log-likelihood function instead:

$$\log(L) = \sum_{k=1}^{K-1} p_k \log(\mathbf{P}(D \in (d_k, d_{k+1}), I = 0)) \\ + q_k \log(\mathbf{P}(D \in (d_k, d_{k+1}), I = 1)) + s_k \log(\mathbf{P}(D \in (d_k, d_{k+1}), I = 2)) \tag{2.9}$$

The conditional joint density functions for detection volume and stage conditional on the inverse tumor growth rate were given as follows [Ple07]:

$$f_{D,I|R}(d, 0|r) = \gamma r e^{-(\gamma+\eta)r(d-c_0)} \tag{2.10}$$

$$f_{D,I|R}(d, 1|r) = \frac{\eta\gamma}{\eta-\omega} r[e^{-(\gamma+\omega)r(d-c_0)} - e^{-(\gamma+\eta)r(d-c_0)}] \tag{2.11}$$

$$f_{D,I|R}(d, 2|r) = f_{D|R}(d|r) - f_{D,I|R}(d, 0|r) - f_{D,I|R}(d, 1|r) \tag{2.12}$$

Plevritis et al. derived the unconditional discretized distributions of $\mathbf{P}(D \in (d_k, d_{k+1}), I)$ for each stage to solve for the parameters of the tumor growth model by maximizing Equation 2.9. The parameters were estimated using the SEER frequency data under the assumption that R follows a Gamma distribution with unknown parameters. The assumed Gamma distribution of R does not specify the time unit of the inverse growth rate. While Furukawa et al. found that the tumor doubling time ranges between 64 and 255 days [Fur01], a distribution fit for the tumor doubling time was not provided. Using the result of Furukawa et al., we performed two analyses where we assume R follows (i) a Uniform distribution, and (ii) a Gamma distribution.

R ~Uniform. Since the result of Furukawa et al. was based on only nine patient samples, we assume that $DT \sim \text{Uniform}(64/365, 255/365)$. A uniform distribution has the property of giving equal weight to the different possible values within the given range including extreme values. Hence, we assume R to be uniformly distributed:

$$R \sim \text{Uniform}(a, b), \text{ where } a = \frac{64}{365 \cdot \ln(2)} \text{ and } b = \frac{255}{365 \cdot \ln(2)}. \tag{2.13}$$

The derivation of the unconditional discretized distributions under the uniform distribution assumption is shown in Appendix A. The unconditional joint distributions of volume and stage at symptomatic detection are as follows:

$$f_D(d) = \frac{1}{b-a} \cdot \left[\frac{a \cdot e^{-\gamma \cdot a(d-c_0)} - b \cdot e^{-\gamma \cdot b(d-c_0)}}{d-c_0} + \frac{e^{-\gamma \cdot a(d-c_0)} - e^{-\gamma \cdot b(d-c_0)}}{\gamma(d-c_0)^2} \right] \tag{2.14}$$

$$\begin{aligned} f_{D,I}(d,0) = \frac{1}{b-a} \Bigg[& \frac{\gamma \cdot a \cdot e^{-(\gamma+\eta)a(d-c_0)} - \gamma \cdot b \cdot e^{-(\gamma+\eta)b(d-c_0)}}{(\gamma+\eta)(d-c_0)} \\ & + \frac{\gamma \cdot e^{-(\gamma+\eta)a(d-c_0)} - \gamma \cdot e^{-(\gamma+\eta)b(d-c_0)}}{(\gamma+\eta)^2(d-c_0)^2} \Bigg] \end{aligned} \tag{2.15}$$

$$\begin{aligned} f_{D,I}(d,1) = \frac{1}{b-a} \cdot \frac{\eta\gamma}{\eta-\omega} \Bigg[& \frac{a \cdot e^{-(\gamma+\omega)a(d-c_0)} - b \cdot e^{-(\gamma+\omega)b(d-c_0)}}{(\gamma+\omega)(d-c_0)} + \frac{b \cdot e^{-(\gamma+\eta)b(d-c_0)} - a \cdot e^{-(\gamma+\eta)a(d-c_0)}}{(\gamma+\eta)(d-c_0)} \\ & + \frac{e^{-(\gamma+\omega)a(d-c_0)} - e^{-(\gamma+\omega)b(d-c_0)}}{(\gamma+\omega)^2(d-c_0)^2} + \frac{e^{-(\gamma+\eta)b(d-c_0)} - e^{-(\gamma+\eta)a(d-c_0)}}{(\gamma+\eta)^2(d-c_0)^2} \Bigg] \end{aligned} \tag{2.16}$$

$$f_{D,I}(d,2) = f_D(d) - f_{D,I}(d,0) - f_{D,I}(d,1) \tag{2.17}$$

Equations 2.15-2.17 are used to find $\mathbf{P}(D \in (d_k, d_{k+1}), I)$ as the discretized version of the distribution (shown in Appendix A), which, in turn, were used to maximize the likelihood function and estimate the parameters γ, η, and ω.

R ~Gamma. We develop two models under the assumption of a Gamma distributed inverse growth rate with unknown parameters, α and β, as used by Plevritis et al. and Atkinson et al. One uses the derivation of Plevritis and the other incorporates the tumor doubling time. [Ple07; Atk83]. We maintain the tumor doubling time range of 64 to 255 days; however, we now assume that about 80% of the tumors have a doubling time in the range (64,255) days. We set the distribution of R to be Gamma, where the 10th percentile is $64/(\ln(2)\times 365)$, the 90th percentile is $255/(\ln(2)\times 365)$, and the expected value to be the midpoint of $319/(2\times\ln(2)\times 365)$ and solve for the distribution parameters. The form of the Gamma is distribution is as follows:

$$f_R(x) = \frac{\beta^\alpha}{\Gamma(\alpha)} x^{\alpha-1} e^{-\beta x} \tag{2.18}$$

where α and β are the parameters to be solved for according to the assumptions:

$$F_R(a) = \frac{\gamma(\alpha, \beta a)}{\Gamma(\alpha)} = 0.1 \tag{2.19a}$$

$$F_R(b) = 0.9 \tag{2.19b}$$

$$\mathbf{E}[X] = \frac{\alpha}{\beta} = \frac{a+b}{2} \tag{2.19c}$$

where

$$a = \frac{64}{365 \cdot \ln 2} \text{ and } b = \frac{255}{365 \cdot \ln 2}.$$

Given the nature of the cumulative density function of the Gamma distribution (shown in Equation 2.19a), the two percentile points are insufficient to have a unique solution for α and β. Therefore, we also assume the relationship between the two (or in this case, a value for the mean). The cumulative density function also does not have a closed form solution, so we approach the problem of solving for the parameters iteratively. We express the equations in terms of α using the assumed value of the mean. We set α at a starting value of 0.0001 with increments of 0.0001 and a ceiling of 10. Using the built-in CDF function for Gamma in MATLAB, we iteratively evaluate $F_R(a)$ and $F_R(b)$ until they are equal to 0.10 and 0.90 rounded to two decimal places and a value for α is returned. Using this iterative method, we found that $\alpha = 5.1590$, and $\beta = 8.1832$.

The model was parameterized under three assumptions: (i) $R \sim \text{Gamma}(\alpha, \beta)$ with unknown parameters with the derivations provided by Plevritis et al., (ii) $R \sim \text{Gamma}(\alpha, \beta)$ where $\alpha = 5.1590$ and $\beta = 8.1832$, and (iii) $R \sim \text{Uniform}(a, b)$ with known parameters. To solve for the parameters, we used TensorFlow™, a machine learning open source package for Python. Specifically, we used the application of the stochastic optimization algorithm: Adam [KLB].

The developed simulation model of the tumor progression uses the parameters under $R \sim$ Uniform for each race, gender, and age group. Using the tumor volume Equation 2.1, for each patient in the SEER data, we performed ten trials where we sampled an inverse growth rate according to the distribution in Equation 2.13. We solved for the tumor initiation time, i.e., the time it took for the tumor to grow from a 2mm wide cancer to its recorded diameter in SEER. We averaged ten trials and fit the average ages. The simulation uses the resulting age distribution when creating a patient.

2.3.4 Resectability of Pancreatic Cancer

We used the sets of resectable and unresectable pancreatic cancers to develop a model that uses a patient's age, cancer stage (local, regional, or distant), and cancer size to predict the resectability of the tumor. For example, we would input patient X's information who is 74 years old with regional stage tumor of size 31mm, and use the model to predict the probability this patient has a resectable cancer. We used four different tools to develop a resectability prediction tool: *Ridge Regression, Logistic Regression, Support-vector Classification (SVC), and Support-vector Regression (SVR).* For all techniques, we used the machine learning package Scikit-learn [Ped11]. The Ridge Regression model minimizes a linear least squares function that is regularized by the L-2 norm by adjusting the weights w such that:

$$\min_{w} ||Xw - y||_2^2 + \psi ||w||_2^2, \tag{2.20}$$

where the vector X is the input data, w are the regression coefficients, y is the variable to be

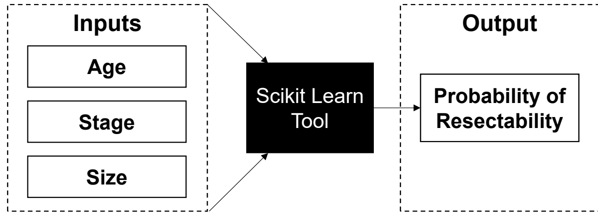

Figure 2.3 Flow of inputs and outputs to the prediction model

predicted, and ψ is an error term. On the other hand, Logistic Regression minimizes the following function:

$$\min_{w,c} \frac{1}{2} w^T w + C \sum_{i=1}^{n} \log(\exp(-y_i(X_i^T w + c)) + 1). \tag{2.21}$$

where C is a lower bound. Support vector machines are a set of supervised learning tools that are used for classification and regression problems.

We tested our data through a classification tool and a regression tool. Classification algorithms in general will return a class to which a variable should belong (black or white), while regression will return a combination of the different classes (grey scale). For each of the fitting techniques, we set the dependent variable equal to 1 if the patient's tumor was deemed resectable, and 0 if surgery was not recommended for the patient. We reformatted the input data to the models, X, into categorical values such that the independent variable is a vector of 0-1 entries with exactly three positions that are 1:

- $X = [H, A, S]$
- H is a row vector that corresponds to the tumor stage, where:

$$H_i = \begin{cases} 1 & \text{if tumor stage is } i, i \in \{\text{local, regional, or distant}\}; \\ 0 & \text{otherwise.} \end{cases}$$

- A is a row vector that corresponds to the patient's age, where:

$$A_i = \begin{cases} 1 & \text{if patient's age is within the category } i, \\ & i \in \{\leq 40, 41-43, 44-46, \ldots, 92-94, \text{ and } \geq 95\}; \\ 0 & \text{otherwise.} \end{cases}$$

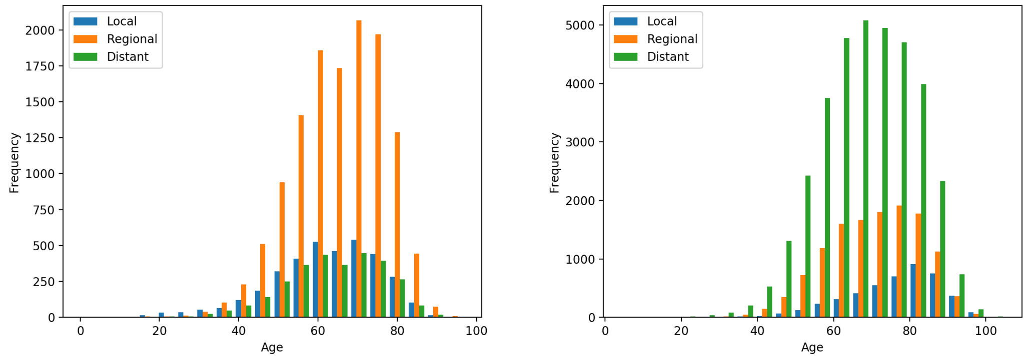

(a) Resectable **(b)** Unresectable

Figure 2.4 Bar Charts of Age by Tumor Stage in the Resectable and Unresectable Groups

- S is a row vector that corresponds to the tumor diameter, where:

$$S_i = \begin{cases} 1 & \text{if the tumor diameter is within the category } i, \\ & i \in \{\leq 5mm, 6-10mm, 11-15mm, ..., 96-100mm, \text{ and } \geq 101mm\}; \\ 0 & \text{otherwise.} \end{cases}$$

Ridge Regression is often used when there is believed to be a relationship between the input variables as well as their relationship to the output variable. In our case, tumor size is related to tumor stage. We plotted the age distribution by stage for the resectable and unresectable groups as shown in Figure 2.4. We also plotted the age and tumor size scatter plot by stage for the resectable and unresectable groups as shown in Figure 2.5. We can see that the relationships are not linear. Therefore, categorizing tumor volume and stage would approximate the non-linear relationship with a piece-wise linear one. Hence, we converted all input variables into categorical entities. Moreover, we cannot assume that age or tumor size to have a linear relationship with resectability. We divided the data where we used 80% for training and 20% for testing and consistently used the same training set for all models. The Ridge Regression and SVR models output a value that is not necessarily 0 or 1, where the predicted value could also be negative since they are hyper-plane fits. On the other hand, the Logistic Regression and SVM models output 0 or 1 only. We compared the output of the four models using the 20% testing set, refer to Table 2.5. For the predictions of the regression models, we assume that an output that is greater than 0.5 is resectable. The regression models also can return a negative fractional value or a value that is greater than 1 since the output is not restricted to be between 0 and 1. For example a ninety year old patient with distant cancer would result in a negative value as we can infer from the weights summarized in Table 2.6.

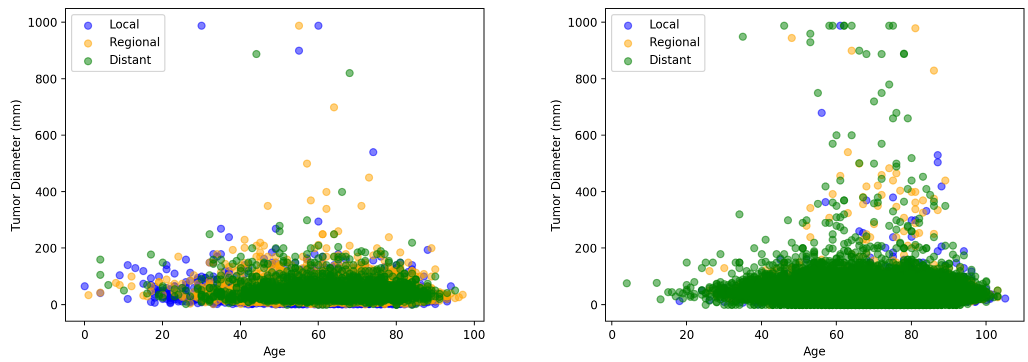

(a) Resectable **(b)** Unresectable

Figure 2.5 Scatter Plot of Age and Tumor Size by Stage in the Resectable and Unresectable Groups

Table 2.5 Comparison of the Resectability Prediction Tools

	Type of Output	Correct Predictions (%)
Ridge Regression	fraction (possibly negative)	79.88
SVR	fraction (possibly negative)	79.91
Logistic Regression	binary	79.97
SVC	binary	78.52

We further compared the two regression models since they output a spectrum of values, and we identified the set of patients whose predicted resection was negative. For the Ridge Regression model, the model returned 1337 patients with a negative prediction, where all patients had a distant stage cancer, were 77 years old or older, and had a tumor that was at least 16mm in diameter. On the other hand, the SVR model returned 1240 patients with a negative value, where the patients had different stages of cancer, were at least 77 years old, and had a tumor that was at least 6mm in diameter.

The literature defines an unresectable cancer as one that has spread beyond the pancreas and neighboring organs. Therefore, we choose the Ridge Regression model as the tool to predict the probability of resectability, where we set negative values to zero and values over one to one. The Ridge Regression model is a linear model. Table 2.6 shows the resulting ridge coefficients for each X_i, i.e., the weight of each pancreatic cancer patient attribute of tumor stage, age, and tumor diameter. The probability of resectability output can be calculated according to the formula:

$$y = Xw. \tag{2.22}$$

Resectability of pancreatic cancer is key to survival, and screening is key to detection at re-

Table 2.6 Results of the Ridge Regression and the Weight of each Patient Attribute to the Probability of Resectability

X	Local	Regional	Distant	$\leq$ 40 y.o.	41-43 y.o.	44-46 y.o.	47-49 y.o.
w	0.0616	0.1425	-0.2547	0.2603	0.1529	0.1335	0.1089
X	50-52 y.o.	53-55 y.o.	56-58 y.o.	59-61 y.o.	62-64 y.o.	65-67 y.o.	68-70 y.o.
w	0.0912	0.0848	0.0787	0.0567	0.0659	0.0629	0.0591
X	71-73 y.o.	74-76 y.o.	77-79 y.o.	80-82 y.o.	83-85 y.o.	86-88 y.o.	89-91 y.o.
w	0.0441	0.0293	-0.0166	-0.0550	-0.1193	-0.1723	-0.2041
X	92-94 y.o.	$\geq$ 95 y.o.	$\leq$ 5mm	6-10mm	11-15mm	16-20mm	21-25mm
w	-0.2188	-0.2372	0.3759	0.3397	0.2849	0.1907	0.1706
X	26-30mm	31-35mm	36-40mm	41-45mm	46-50mm	51-55mm	56-60mm
w	0.0773	0.0926	0.0412	0.0414	0.0175	0.0452	0.0247
X	61-65mm	66-70mm	71-75mm	76-80mm	81-85mm	86-90mm	91-95mm
w	0.0621	0.0375	0.0637	0.0536	0.0623	0.0715	0.1176
X	96-100mm	$\geq$101mm					
w	0.0638	0.1446					

sectability. The progression model and the resectability prediction tool open the path to modeling screening and possibly treatment of the disease. However, before using these models as building blocks for future work, we use independently developed models to validate our model.

2.4 Model Validation

To validate our model, we chose to study the model presented by Haeno et al. and its tumor growth timeline. We also compared the model to the timeline suggested by Yachida et al. Although the resulting timelines were derived using different methodologies, with the exception of the tumor doubling time that we adopted, our model is the only one of the three that was not *entirely* built from the genetic behavior of pancreatic cancer samples.

We simulated the model presented by Haeno et al. The model is a computational and cell division model of pancreatic cancer [Hae12]. Figure 2.6 shows the model framework where:

- n_0 is the number of type 0 tumor cells. Type 0 tumor cells are in the main body of the tumor and they lack metastatic ability. During cell division, the cell either divides into another type 0 cell with probability $1-u$, or with probability u it divides into type 1.

- n_1 is the number of type 1 tumor cells. Type 1 tumor cells are in the main body of the tumor with the ability to metastasize. During cell division, the cell either divides into type 1 cell with probability $1-q$, or with probability q it divides into type 2.

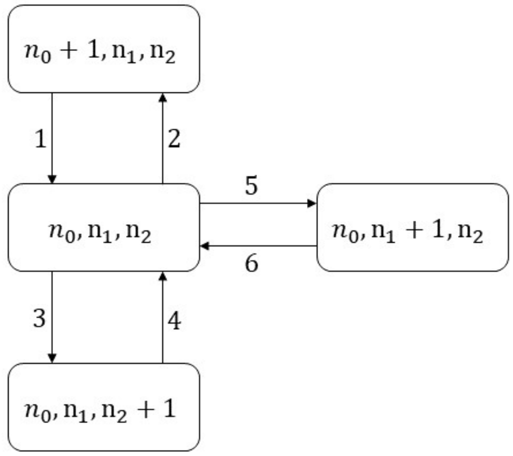

Figure 2.6 Cell divisions model, n_0 is type 0 tumor cell and the core of the tumor, n_1 is type 1 tumor cell that has metastatic ability, and n_2 is type 2 tumor cell that is metastatic

- n_2 is the number of type 2 tumor cells. Type 2 tumor cells are metastatic cells outside the main body of the tumor.

All of the cell divisions were assumed to be exponentially distributed where the probability distribution function is:

$$f(x) = \lambda e^{-x\lambda}. \tag{2.23}$$

Therefore, the rate for each arc in Figure 2.6 has an exponential distribution with λ equal to:

1. $(1-u)a_0 n_0 t$,
2. $b_0(n_0+1)t$,
3. $b_2(n_2+1)t$,
4. $(a_2 n_2 + q a_1 n_1)t$,
5. $((1-q)a_1 n_1 + u r n_0)t$,
6. $b_1(n_1+1)t$,

where time, t, is in months. We maintained the memoryless property of the exponential distributions and we developed a simulation model that mimics the cell division behavior presented in Haeno et al. The memoryless property of a random variable, X, that is exponentially distributed means that:

$$\mathbf{P}(X > s + t | X > t) = \mathbf{P}(X > s).$$

Table 2.7 Haeno et al. Model Parameters [Hae12]

Parameter	Description	Value
a_0	division rate of type 0 cells	0.16
a_1	division rate of type 1 cells	0.16
a_2	division rate of type 2 cells	0.58
b_0	death rate of type 0 cells	$0.01a_0$
b_1	death rate of type 1 cells	$0.01a_0$
b_2	death rate of type 0 cells	$0.01a_2$
u	probability that type 0 cell division yields a type 1 cell	6.31×10^{-5}
q	probability that type 1 cell division yields a type 2 cell	6.31×10^{-7}

In other words, if an exponential event has not happened yet, then the distribution of the time remaining until the event happens is still exponential. The simulation model begins with one tumor cell of type 0 (parental clone) and simulates the cell divisions until the tumor develops its first type 2 cell (metastasis). In the simulation, we generate the times of the possible events that can occur and we choose the event that occurs first. For example, if we have x_0 and x_1 cells of type 0 and type 1, we have four competing events: (i) division of a type 0 cell, (ii) death of a type 0 cell, (iii) division of a type 1 cell, or (iv) death of a type 1 cell (arcs 1, 2, 5, or 6 in Figure 2.6). Since we maintain the memoryless property, after we chose the event that happened sooner than the others, we reset the clocks on the other events and generated all possible events from that point. This is equivalent to distribution of the minimum of four exponential random variables which is also exponentially distributed. Therefore, we expect the resulting timeline to be conservative and to overestimate the time between the first cell and metastasis. The simulation was coded using Python 3.6.

2.5 Results

After refining the SEER PC data to include complete records with age, tumor size, and stage, we segmented the data by race, gender and age quantiles within each subgroup. Table 2.8 shows the percentiles of each gender/race group. In general, the female diagnosis age distribution is higher than the male diagnosis age distribution, and the distribution for White patients is higher than the distribution for Black patients. The diagnosis age distribution of Black females is similar to that of White males, while those of White females and Black males are the farthest apart. Black males are the youngest cohort in the pancreatic cancer population and White females are the oldest.

We investigated the incidence of pancreatic cancer by gender, race, and age. Within a given gender and race subgroup, the older the patient the more likely his/her cancer was detected at an earlier stage. Using the distribution of tumor size and stage from the SEER data for each subgroup, we calculated the probability that a patient's tumor was detected at a particular tumor stage and size $\mathbf{P}(D \in (d_k, d_{k+1}), I = i)$, by dividing the number of patients with tumor size in (d_k, d_{k+1}) and in stage i by the total number of patients in a certain group. Figure 2.7 shows the joint probability distributions of tumor volume and stage at detection calculated from the contingency tables for each age quantile in each of the race/gender subgroup. Across all subgroups, there is a higher proportion of patients detected at the distant stage. Within each race/gender subgroup, the fourth age quantile has a higher proportion detected at the local stage and a lower proportion detected at the distant stage than the other age groups (the fourth quantile corresponds to the yellow line in all the charts). As patients age, they are more likely to have their cancer detected at an earlier stage.

Table 2.8 Age Percentiles by Race/Gender Group

	White Male	White Female	Black Male	Black Female
5^{th} Percentile	49	50	47	48
25^{th} Percentile	60	63	57	60
50^{th} Percentile	69	73	64	69
75^{th} Percentile	78	81	73	78
95^{th} Percentile	87	89	84.4	88

2.5.1 Growth Models Analysis

We filtered the age at diagnosis and tumor size fields from the SEER data records to trace back the tumor initiation age. We found that the cancer initiation age (when the tumor is at the initial diameter of 2mm) follows a Johnson SB distribution with $\zeta = -1.01$, $\delta = 1.90$, $\lambda = 105.27$, and $\xi = -1.37$, where Johnson SB has the probability density function:

$$f(x) = \frac{\delta}{\lambda\sqrt{2\pi}z(1-z)} e^{\left(-\frac{1}{2}\left(\zeta+\delta\ln\left(\frac{z}{1-z}\right)\right)^2\right)}, \text{ where } z = \frac{x-\xi}{\lambda}.$$

We found that the average diagnosis age is 69.8 years old while the average cancer initiation age is 64.2 years old. Under this distribution fit, about 13.6% of patients had their cancer start before the age of 50, while only 6.4% of patients were diagnosed before age 50. We are aiming to test the CAPS guideline's recommendation as to start screening at age 50. The lead time between cancer initiation and symptomatic detection is shown in Figure 2.8. It is important not to base screening policy decisions on the age distribution of symptomatic detection alone. Experts have indicated that detecting a lesion using Endoscopic Ultrasound (the most sensitive screening tool) is operator and tumor location dependent and not only tumor size dependent.

Experts noted that a lesion that is less than 5mm would most likely not be detectable even using

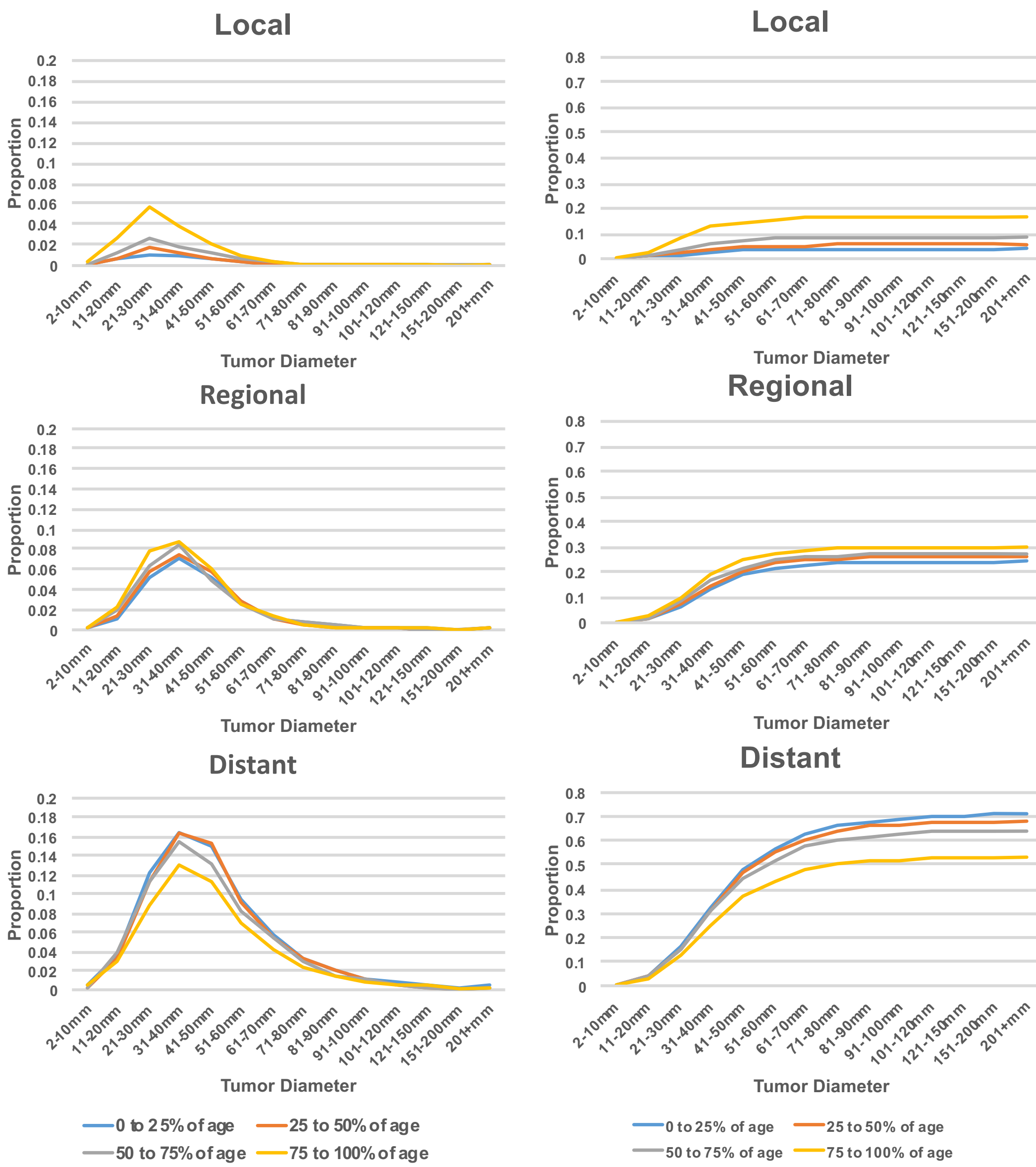

(a) White Male, PDF **(b)** White Male, CDF

Figure 2.7 The Proportional Distribution of Volume Detection at each Stage under each Age Group

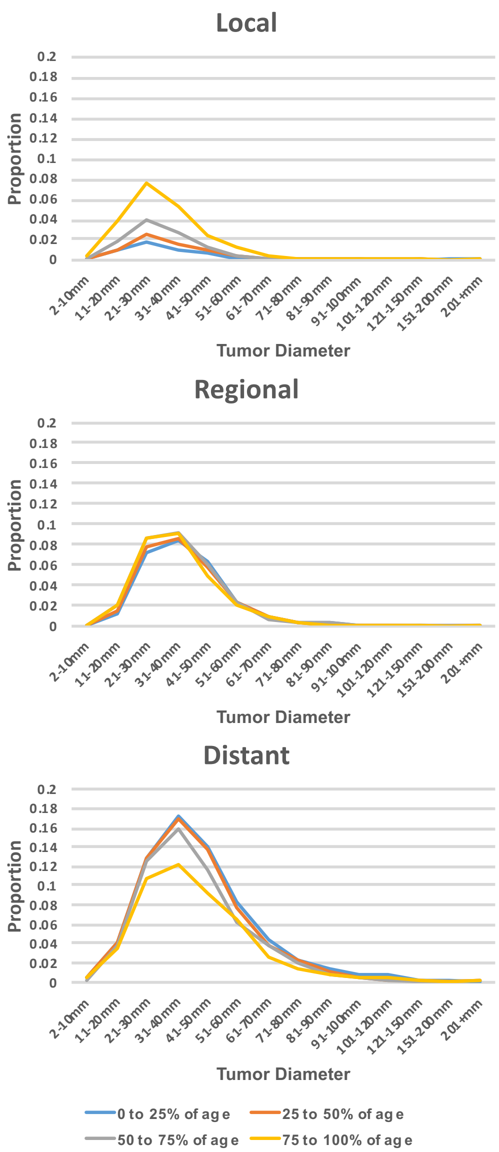

(c) White Female, PDF

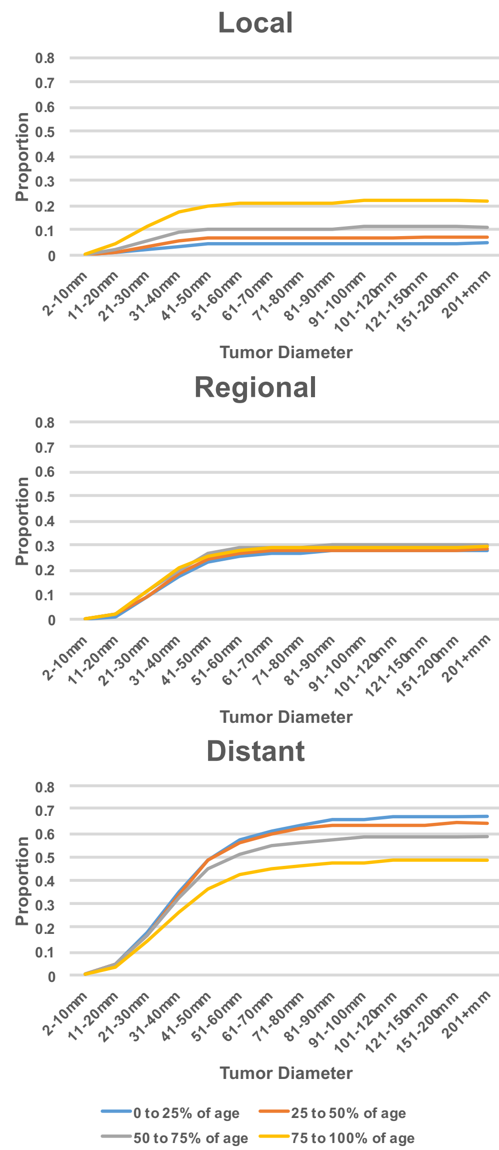

(d) White Female, CDF

Figure 2.7 (continued) The Proportional Distribution of Volume Detection at each Stage under each Age Group

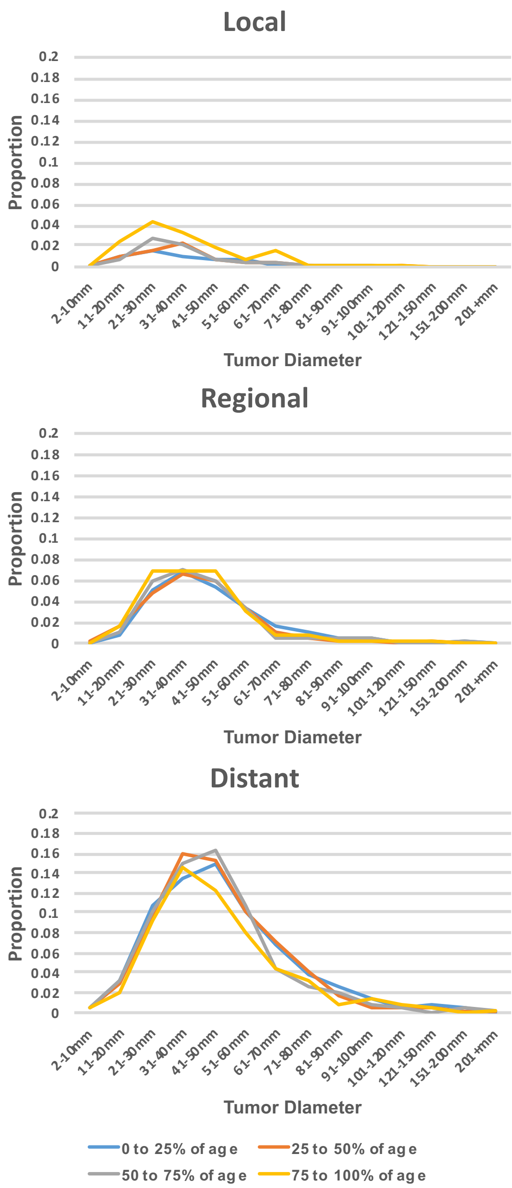

(e) Black Male, PDF

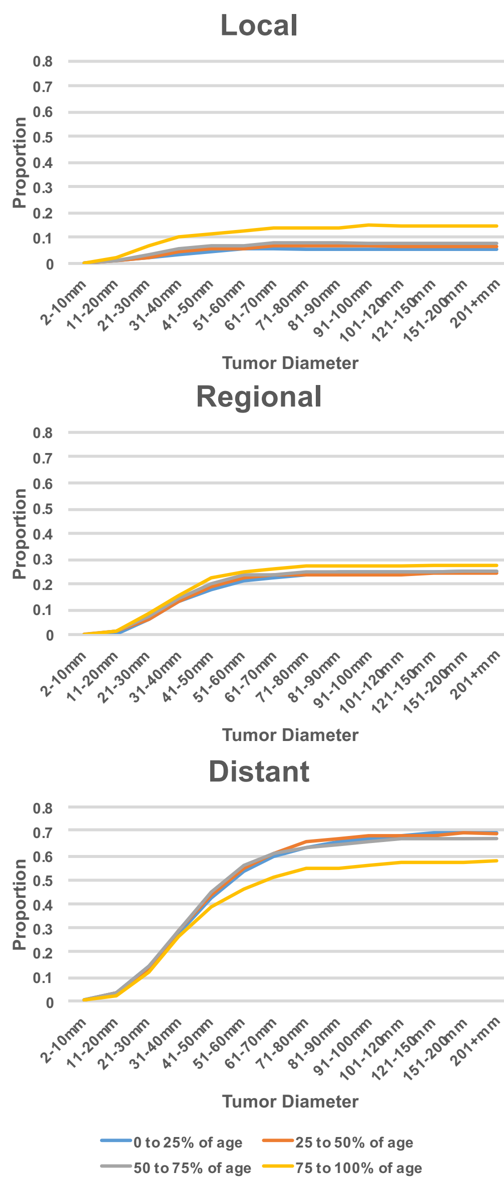

(f) Black Male, CDF

Figure 2.7 (continued) The Proportional Distribution of Volume Detection at each Stage under each Age Group

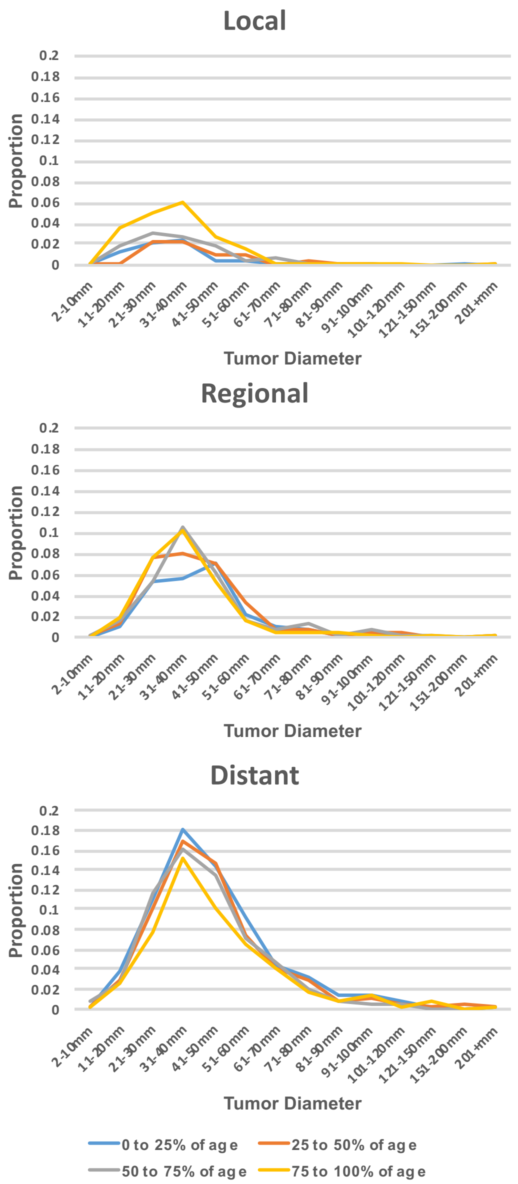

(g) Black Female, PDF

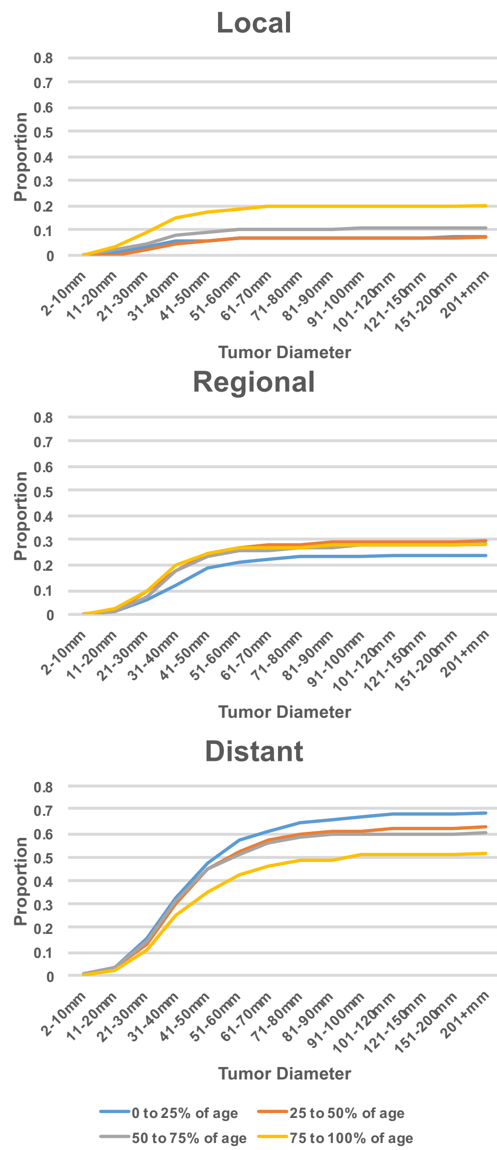

(h) Black Female, CDF

Figure 2.7 (continued) The Proportional Distribution of Volume Detection at each Stage under each Age Group

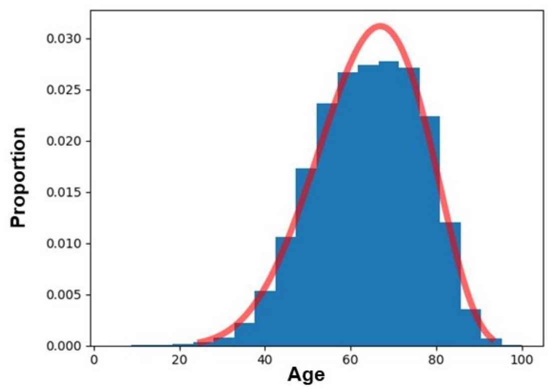

(a) Cancer Initiation Age Distribution

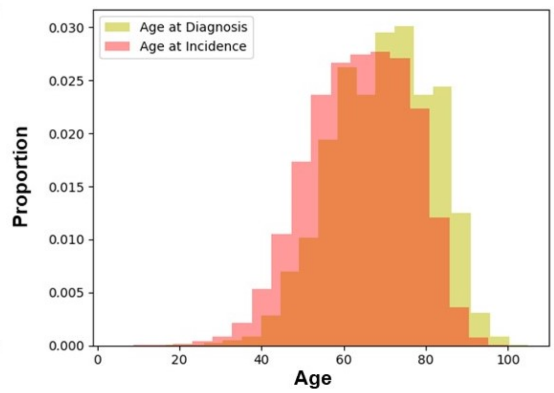

(b) Cancer Initiation versus Diagnosis Age

Figure 2.8 Age of Cancer Initiation Distribution with Plot Fit and Comparison to Age of Diagnosis

Table 2.9 Percentage of patients age 50 years old or younger with a tumor of a certain diameter

R	Tumor Size	White Male	White Female	Black Male	Black Female
Uniform	2mm	14.9	10.5	22.0	15.4
	5mm	12.0	8.6	12.9	12.1
Gamma	2mm	15.0	10.6	22.2	15.5
	5mm	12.1	8.5	17.9	12.6

EUS. Therefore, we also examined the age distribution when the tumor is 5mm in diameter since this would be the minimum volume that is detectable. Table 2.9 summarizes the percentage of patients with a detectable tumor under each inverse growth R distribution assumption in each of the race/gender groups. For the simulation, we separated the age at diagnosis and tumor volume fields based on race and gender, and we repeated the procedure to find a distribution for age at cancer initiation given a race and gender.

We compared the original model presented by Plevritis et al. and our modifications by changing the distribution of R from Gamma with unknown parameters that were fit by SEER data to Uniform and Gamma distributions with known parameters. Figure 2.9 shows, in each graph, the unconditional joint probability distributions of volume and stage at detection ($f_{D,I}(d,i)$, for $i = 0,1,2$) that were 1) extracted from the SEER data within each race/gender/age subgroup (blue line), 2) the model solution assuming R follows a Gamma distribution with unknown parameters (orange line), 3) the model solution assuming R follows a Uniform distribution shown in Equations 2.15, 2.16, and 2.17 (grey line), and 4) the model solution assuming R follows a Gamma distribution with known parameters (yellow line). We compared the solutions by calculating the Kullback-Leibler Divergence:

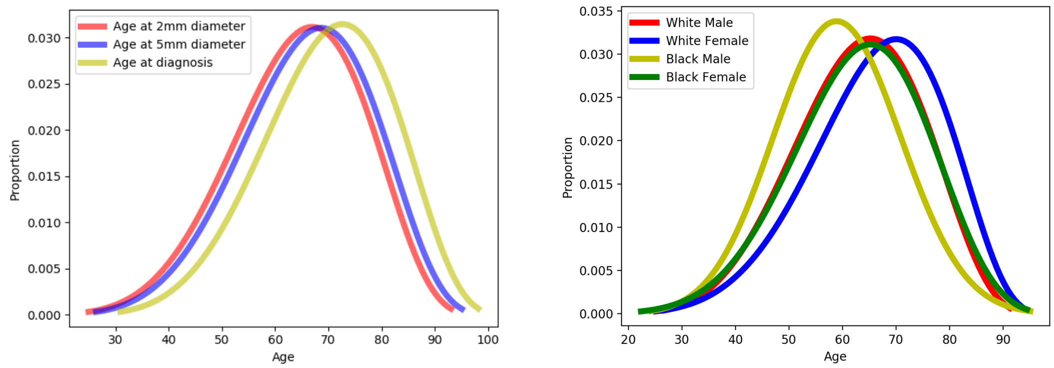

(c) Cancer Initiation Age Distribution

(d) Cancer Initiation Age Distribution Given Race and Gender

Figure 2.8 (continued) Age of Cancer Initiation Distribution with Plot Fit and Comparison to Age of Diagnosis

$$D_{KL}(P||Q) = \sum_{x \in \chi} P(x) \log\left(\frac{P(x)}{Q(x)}\right) \tag{2.24}$$

where $P(x)$ represents the probability distribution derived from the SEER data, $Q(x)$ represents the probability distribution be used to model the data, and $D_{KL}(P||Q)$ is a measure of how "far" Q is from P. Table 2.10 summarizes the divergence of the resulting models from the SEER data distribution. The model with $R \sim$ Uniform performs worse in all cases than the other two fitted models. The original model has the lowest divergence of among the three models. However, the inverse growth rate, R, in the original model does not have an identified time unit. The second best model fit is the model with $R \sim$ Gamma with $\alpha = 5.1590$ and $\beta = 8.1832$. We focus on the results of the models using the doubling time result of Furukawa et al. because they carry the information of time.

The fit of the model parameters for each of the subgroups is in Table 2.11. We found that the White male: White female: Black male: Black female ratio to be 446:419:65:70 in the PC population. We used the fit of the model, the appropriate proportions of each race and gender combination, and the age of cancer initiation fits shown in Figure 2.8 to simulate 100,000 patients of a heterogeneous pancreatic cancer population. We assumed that the generated population does not die before the cancer is initiated or detected, and that all transitions happen while the patient is alive. We fit the distributions of the time (in years) it takes for the cancer to grow from 2mm diameter tumor until its transitions to i) regional stage, ii) distant stage, and iii) symptomatic detection. The distribution that was the best or second best fit for all is the Johnson SB and the parameters are specified in Table

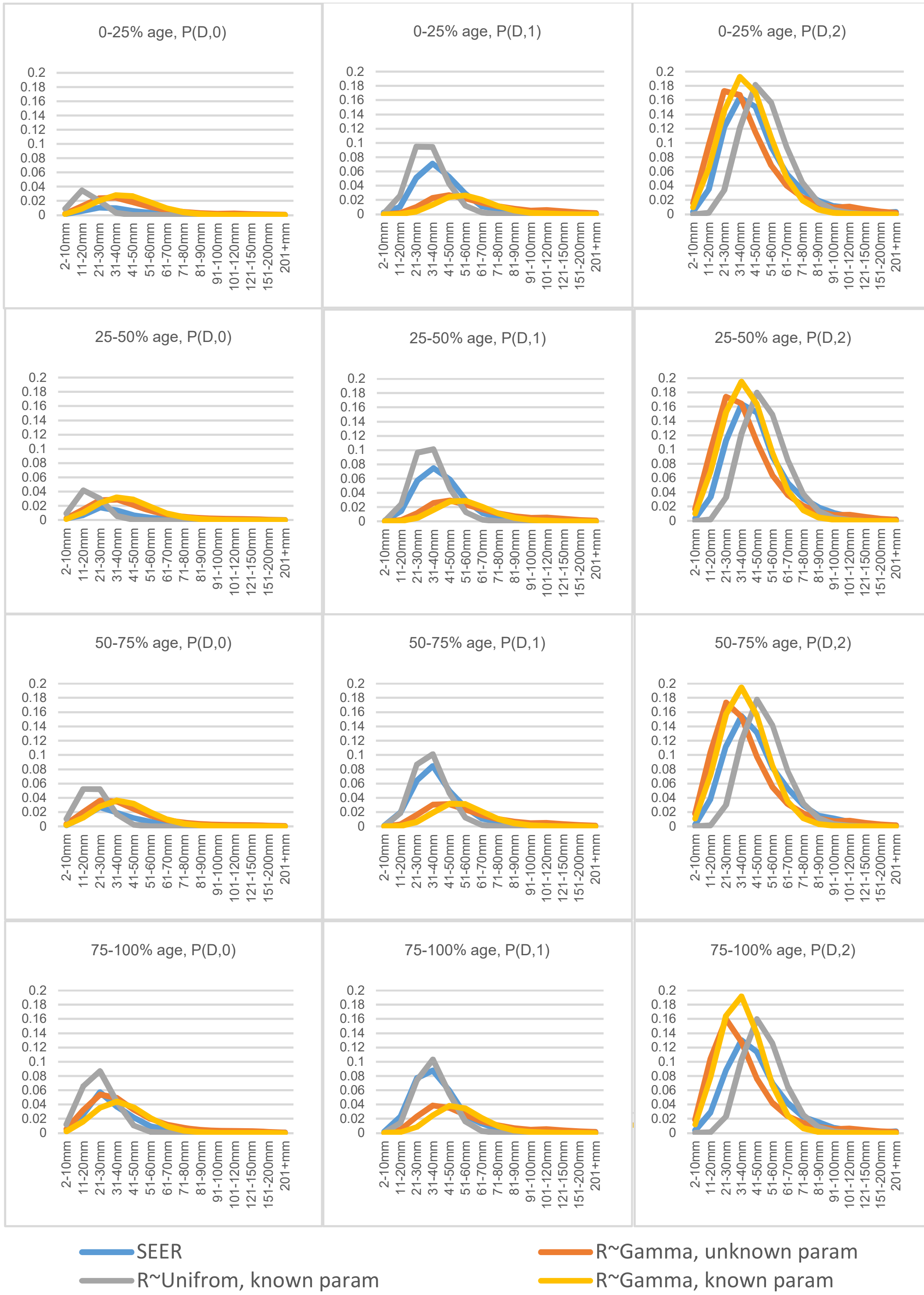

(a) White Male

Figure 2.9 The Probability of Detection at a Certain Volume and stage from the SEER Frequencies, Fit with $R \sim$ Gamma and Fit with $R \sim$ Uniform

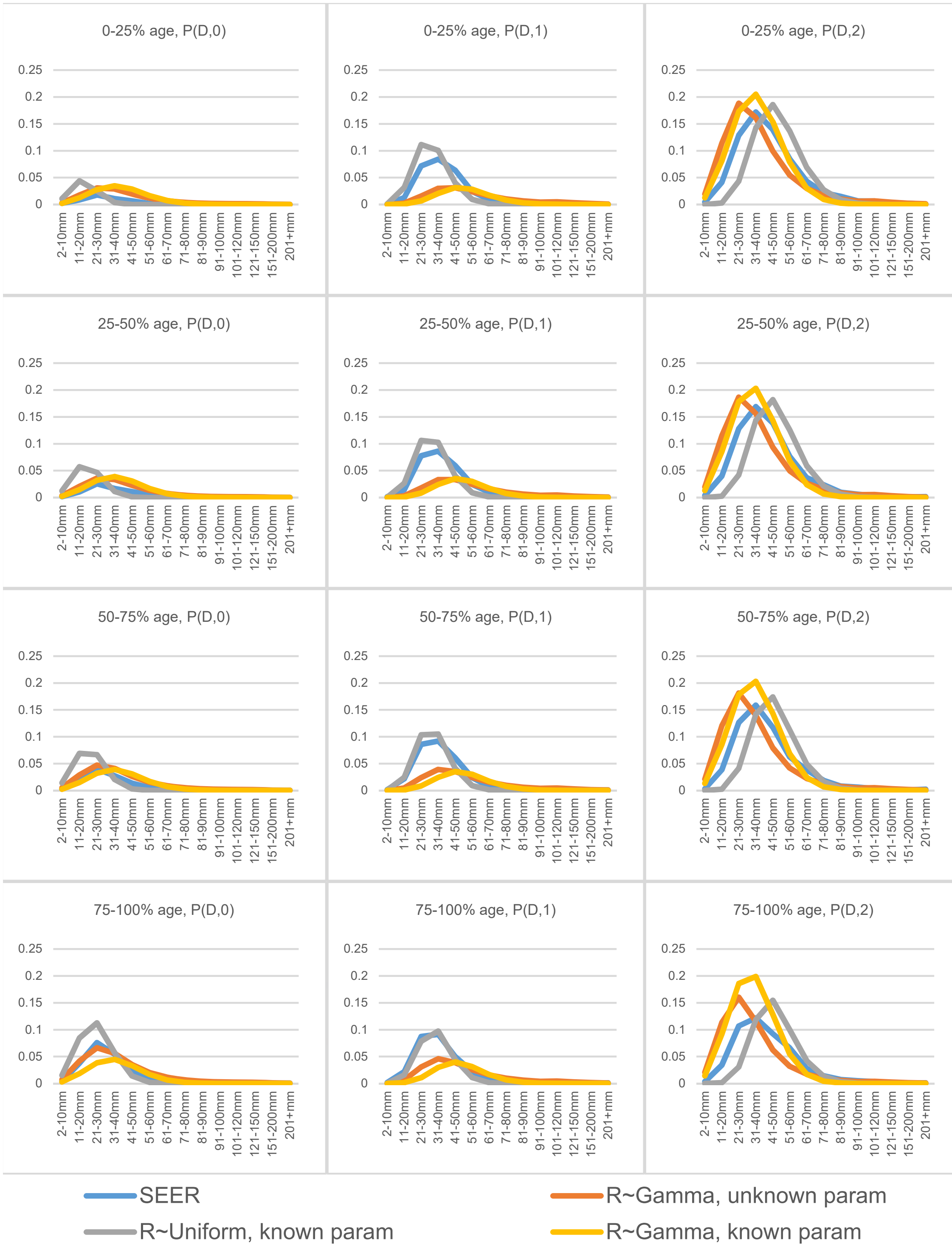

(b) White Female

Figure 2.9 (continued) The Probability of Detection at a Certain Volume and stage from the SEER Frequencies, Fit with $R \sim$ Gamma and Fit with $R \sim$ Uniform

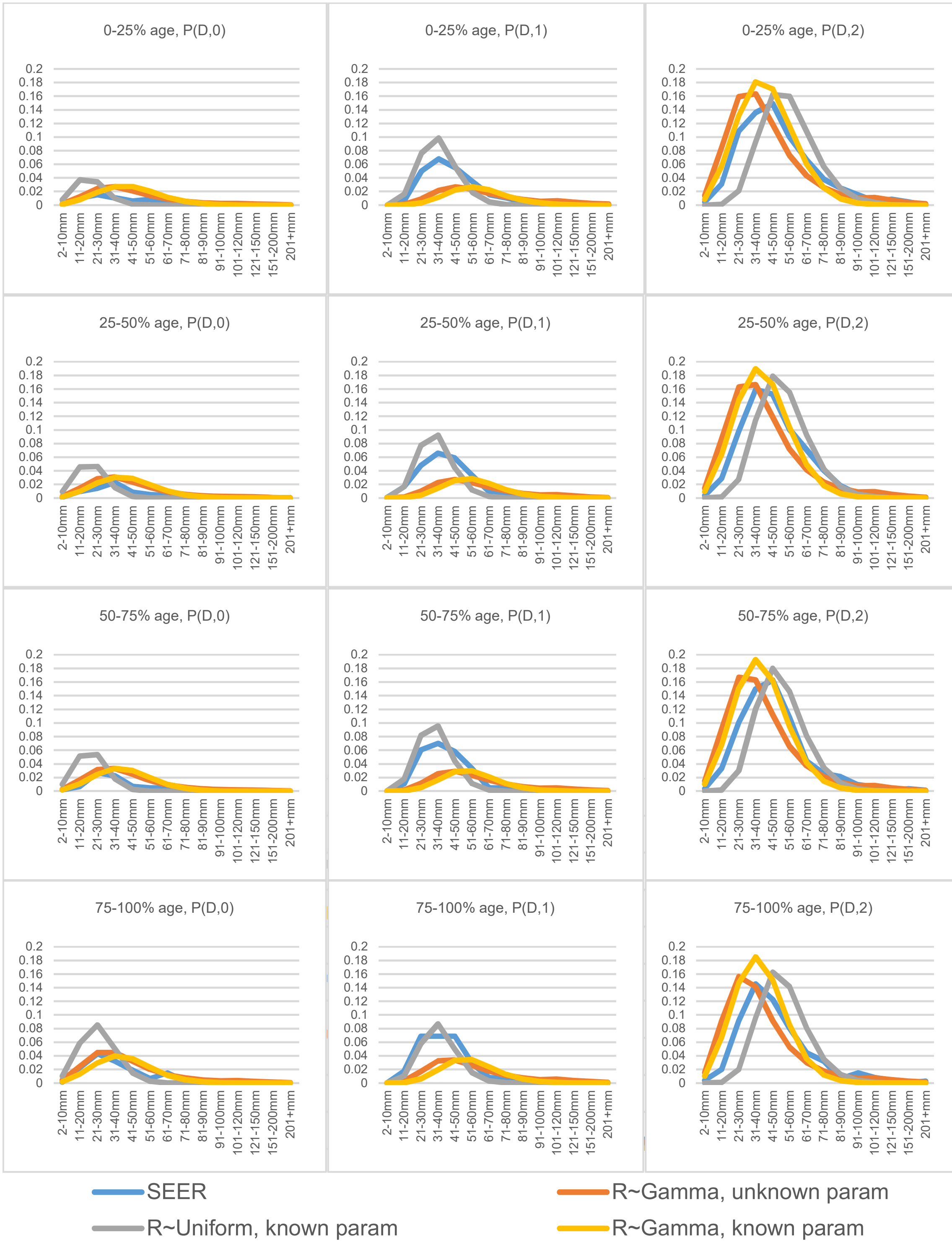

(c) Black Male

Figure 2.9 (continued) The Probability of Detection at a Certain Volume and stage from the SEER Frequencies, Fit with $R \sim$ Gamma and Fit with $R \sim$ Uniform

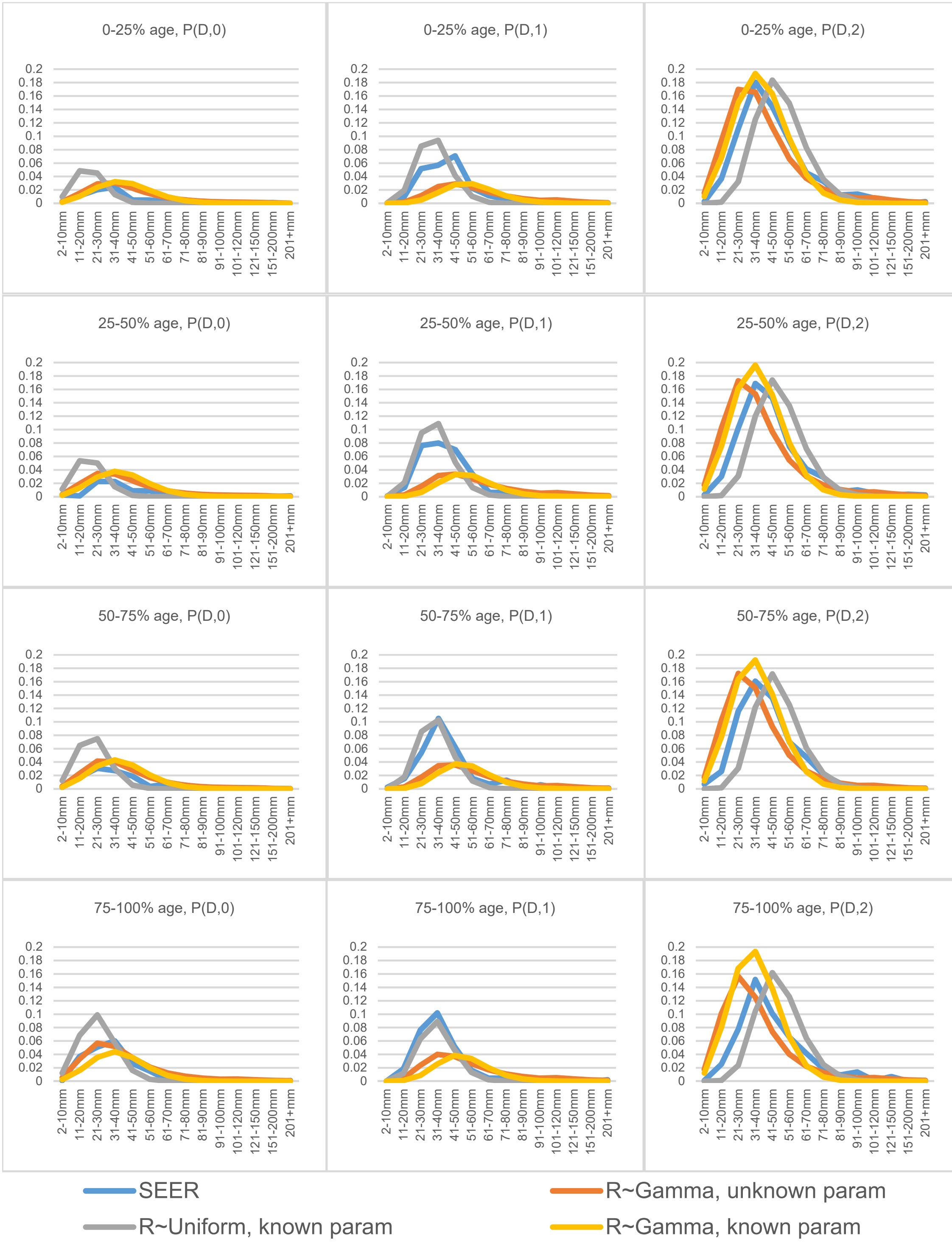

(d) Black Female

Figure 2.9 (continued) The Probability of Detection at a Certain Volume and stage from the SEER Frequencies, Fit with $R \sim$ Gamma and Fit with $R \sim$ Uniform

Table 2.10 The Kullback-Leibler Divergence of the Fitted Models under Different Assumptions for R

Race, Gender	Age Group	$R\sim$ **Gamma, unknown parameters**	$R\sim$ **Uniform, known parameters**	$R\sim$ **Gamma, known parameters**
White Male	$0^{th}-25^{th}$	0.202	0.530	0.362
	$25^{th}-50^{th}$	0.221	0.428	0.345
	$50^{th}-75^{th}$	0.210	0.451	0.358
	$75^{th}-100^{th}$	0.216	0.426	0.439
White Female	$0^{th}-25^{th}$	0.230	0.431	0.364
	$25^{th}-50^{th}$	0.220	0.429	0.343
	$50^{th}-75^{th}$	0.221	0.423	0.385
	$75^{th}-100^{th}$	0.180	0.407	0.391
Black Male	$0^{th}-25^{th}$	0.206	0.475	0.331
	$25^{th}-50^{th}$	0.228	0.376	0.312
	$50^{th}-75^{th}$	0.224	0.440	0.325
	$75^{th}-100^{th}$	0.218	0.463	0.387
Black Female	$0^{th}-25^{th}$	0.183	0.496	0.292
	$25^{th}-50^{th}$	0.263	0.572	0.436
	$50^{th}-75^{th}$	0.218	0.504	0.320
	$75^{th}-100^{th}$	0.239	0.415	0.471

2.12. We found the average time in years from the start of the tumor until transition into regional stage is 4 years, while average time to transition from regional to distant stage to be 1.4 years for a heterogeneous pancreatic cancer population.

We repeated the experiment to examine the tumor growth in each race and gender by creating 100,000 homogeneous pancreatic cancer populations. We ran the simulation described in Section 2.3.3 for each race and gender for all 100,000 replications and sampling from the age of cancer initiation for the simulated race/gender subgroup. We calculated the average age of cancer initiation, time until transition to regional, time to transition from regional to distant, time from tumor start until transition to distant, and time from tumor start until symptomatic detection. Table 2.13 summarizes the simulation results.

From the simulation of the Haeno et al. model, we measured the time until metastasis starting with one and with 1000 primary tumor cells. We found that under the Haeno et al. model, it takes an average of 7.7 years from the first tumor cell and 6.9 years from 1000 cells until metastasis. The model timeline presented by Yachida et al. of 6.8 ± 3.4 years was from the first parental clone to metastasis. The resulting timelines of the Haeno et al. model are longer (but within range) to the one presented by Yachida et al. The resulting timelines of our models are also within the range of the one presented by Yachida et al. The time until metastasis was measured from the initial tumor diameter of 2mm. We estimated the average time for a tumor to grow from 1mm to 2mm to be half

Table 2.11 Progression Model Parameters with R with known parameters in the Order γ, η, ω, (10^{-5})

Age Group		**White Male** Unif	Gam	**White Female** Unif	Gam	**Black Male** Unif	Gam	**Black Female** Unif	Gam
$0^{th}-25^{th}$	γ	2.84	0.405	3.62	0.593	2.45	0.370	3.18	0.487
	η	39.6	2.98	39.3	3.85	25.0	2.61	23.6	3.15
	ω	6.84	2.88	7.55	3.75	5.78	2.51	7.88	3.05
$25^{th}-50^{th}$	γ	3.10	0.487	4.00	0.703	2.90	0.441	3.51	0.616
	η	32.0	3.21	27.0	4.09	21.5	2.96	23.2	3.53
	ω	6.84	3.11	8.16	3.99	7.51	2.86	6.88	3.43
$50^{th}-75^{th}$	γ	3.33	0.577	4.46	0.703	3.23	0.505	3.89	0.728
	η	21.5	3.39	21.3	4.09	20.4	3.17	16.8	3.66
	ω	7.39	3.29	8.50	3.99	7.80	3.07	7.93	3.56
$75^{th}-100^{th}$	γ	3.71	0.753	4.77	0.870	3.19	0.607	3.75	0.766
	η	13.1	3.70	11.9	4.44	11.2	3.13	10.9	3.81
	ω	7.17	3.60	8.90	4.34	7.92	3.03	8.51	3.71

Table 2.12 Distribution Parameters of Milestones from the Start of the Cancer in a Simulated Heterogeneous Population

		μ	σ	ζ	δ	λ	ξ
$R \sim$ Uniform	Time until Regional	4.17	1.53	0.54	1.54	-0.22	10.44
	Time until Distant	5.29	1.74	0.34	1.15	1.24	9.27
	Time until Symptomatic Detection	5.45	1.89	0.23	1.35	0.22	11.34
$R \sim$ Gamma	Time until Regional	5.43	2.29	3.99	2.33	-0.97	39.83
	Time until Distant	6.07	2.46	3.75	2.33	-0.96	40.13
	Time until Symptomatic Detection	6.58	2.77	3.79	2.26	-0.99	45.60

a year if we assume an average tumor doubling time of 159.5 days. Our model with $R \sim$ Gamma yielded an average of six years until metastasis, and our model with $R \sim$ Uniform yielded an average of 5.3 years until metastasis. Figure 2.10 shows the comparison of the timelines of the Yachida et al. model, the Haeno et al. model, and our models. The fact that the starting points of the models differ may account for the differences in the timelines.

2.6 Discussion and Conclusion

We adopted the framework that was presented by Plevritis et al. integrated with the pancreatic cancer doubling time from Furukawa et al. to develop a personalized pancreatic cancer progression model that is based on population level data. While there are pancreatic cancer progression models built on the cellular level using pancreatic cancer samples, to the best of our knowledge, this is the first model using population data. Our model creates a basis for pancreatic cancer modeling and

Table 2.13 Models Average Timeline in Years and Stage Distribution at Symptomatic Detection per Race and Gender Subgroups

R ~ Uniform	**White Male**	**White Female**	**Black Male**	**Black Female**
Average age of cancer	63.00	66.34	59.12	63.02
Time until Regional	4.13	4.17	4.34	4.35
Time from Regional to Distant	1.18	1.09	1.05	0.98
Time until Distant	5.31	5.26	5.39	5.33
Time until Symptomatic Detection	5.54	5.37	5.57	5.45
Percent Detected at Local	10.22	13.93	12.24	15.34
Percent Detected at Regional	27.37	28.38	25.65	26.35
Percent Detected at Distant	62.41	57.69	62.11	58.31
R ~ Gamma	**White Male**	**White Female**	**Black Male**	**Black Female**
Average age of cancer	63.00	66.34	59.12	63.02
Time until Regional	5.49	5.34	5.57	5.45
Time from Regional to Distant	0.64	0.64	0.64	0.64
Time until Distant	6.13	5.97	6.20	6.09
Time until Symptomatic Detection	6.67	6.46	6.74	6.55
Percent Detected at Local	13.22	14.29	13.30	14.95
Percent Detected at Regional	11.79	12.41	11.87	12.71
Percent Detected at Distant	74.99	73.30	74.83	72.34

a pathway to explore screening and treatment policies. We validated our model against models presented in the literature by comparing timelines of the cancer from initiation until metastasis.

We found that tumor progression depends on race, gender and age. We personalized the growth model by solving for the model parameters for each group race, gender, and age quantile. The choice of age quantiles instead of pre-set age cuts across all race/gender subgroups was due to the differences in the age distributions at diagnosis for each subgroup. One-size-fits-all age cutoffs would not describe each demographic accurately. We aimed to personalize our progression model to capture gender, race, and age dependence of pancreatic cancer.

This chapter creates a foundation for the remainder of this dissertation. In Chapter 3, we present a screening tool that was overlayed on the progression model presented in this chapter.

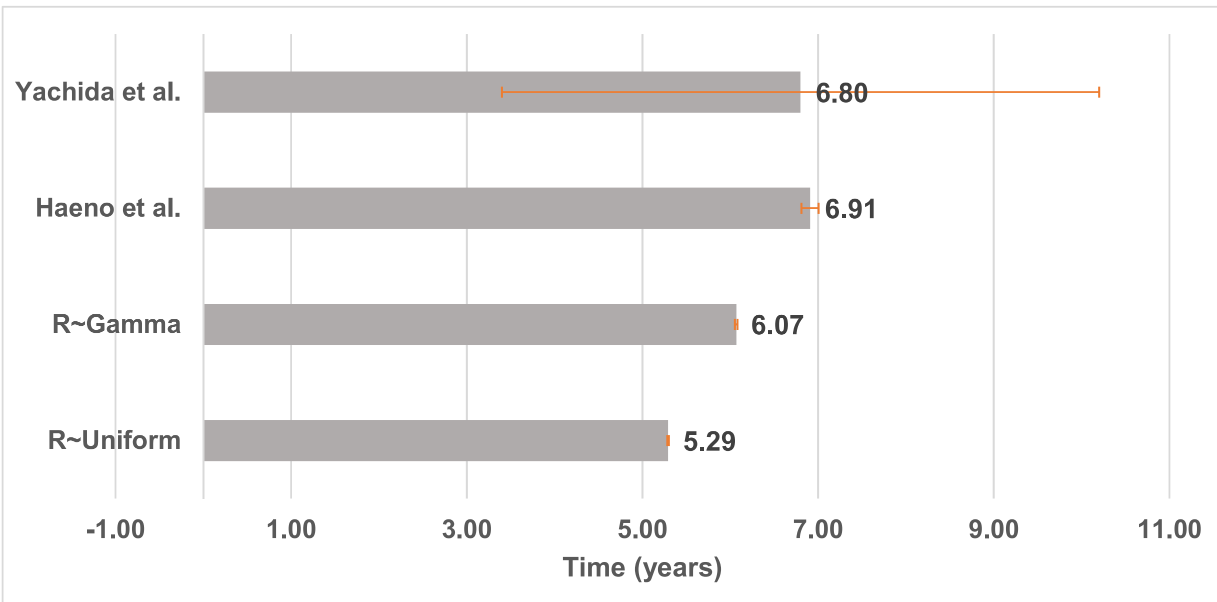

Figure 2.10 The Timelines of First Cancerous Cell to Metastasis of Three Different Models

CHAPTER

3

EVALUATION OF PANCREATIC CANCER SCREENING POLICIES

3.1 Introduction

The asymptomatic nature of pancreatic cancer often leads to its late diagnosis, where symptoms occur after the tumor has metastasized. From the tumor timeline presented by Yachida et al., and the work presented in Chapter 2, it is evident that pancreatic cancer does not quickly approach metastasis. There is a time window where pancreatic cancer could be detected before it becomes symptomatic.

Screening for pancreatic cancer is a reasonable solution to the late diagnosis. However, there are only 50-60,000 new cases annually; making any population wide screening exhaustive and inefficient. Therefore, experts in the field call for screening high-risk patients *only* [Bec14; CMHFHR13; McA17]. Patients with first degree relatives (FDRs) with pancreatic cancer or a genetic mutation that leads to pancreatic cancer are considered to be at high risk [CMHFHR13]. However, less than 10% of patients with PC have family members with pancreatic cancer, and it was estimated that 20% of pancreatic cancer cases are due to smoking [Vin11]. The 2013 CAPS guidelines state a general threshold of 5-folds relative risk to be identified as high-risk for pancreatic cancer, while other literature state a threshold of 10-fold [Har16]. Whether the 5- or 10-fold risk is used to define the high-risk population, there is a segment of at risk individuals that is being ignored by focusing on patients with genetic mutation and family history. There are studies that introduce the wider spectrum of pancreatic cancer risk factors [Bec14]. However, the other risk factors are not publicized as much in the literature when discussing screening high-risk patients. Therefore, the definition of high-risk patients needs to be expanded to explicitly include other risk factors that seem to be relevant when determining whom to screen.

The studies that recruited patients classified to be at high risk and performed screening on them have yielded some success in detecting pancreatic cancer cases among their recruited patients [Ver10; Can; AS12]. Verna et al.'s screening cohort included patients with family history of pancreatic cancer [Ver10]. Canto et al. included patients with strong family history and Peutz-Jeghers syndrome [Can]. Al-Sukhni et al. included patients with first- or second- degree relative with pancreatic cancer, genetic mutation, Peutz-Jeghers syndrome, or hereditary pancreatitis [AS12]. These studies could not test different screening policies since they were using human subjects. Therefore, we propose a simulation model that can test screening policies and measure outcomes such as benign screenings, false positives, and false negatives in addition to the number pancreatic cancer cases that could be detected by screening as a function of the number of cancer patients. In this chapter, we evaluate the effect of risk factors on screening policy outcomes.

3.2 Literature Review

Using simulation to approach screening for pancreatic cancer is not novel by itself. Pandharipande et al. developed simulation model to compare policies of one-time screening at different ages using MRI [Pan15]. The model was self-calibrated, where they used SEER data and calibrated the simulation model parameters such that it can replicate the data. The study found that patients at higher risk of pancreatic cancer could benefit from MRI screenings. Our model differs from the Pandharipande et al. model by evaluating different recurring screening policies rather than a one-time screening. Cucchetti et al. developed a Monte Carlo simulation to estimate the benefits of PC screening [Cuc16]. The simulation estimated the increase in the number of PC patients that might undergo surgery if 20%, 30%, and 50% reductions in diagnosis of PC at stage III/IV were to successfully happen due to screening. They have estimated the lead-time bias of early diagnosis of pancreatic cancer as a measure screening effectiveness.

There are studies that have used simulation as a method to study cancer screening for other cancers. Comas et al. developed a discrete event simulation model to reproduce screening policies for breast cancer that were employed in Spain along with a model of breast cancer natural history [Com14]. The model was developed to study long term costs of screening and treatment when policies are employed on a population level. Greuter et al. developed a simulation model for breast cancer screening using mammograms and incorporated the risk of developing breast cancer due to the radiation in mammography [Gre10]. Forastero et al. developed a Monte Carlo simulation tool to explore the potential detection rate of breast cancer via screening in women over 50 years old [For09]. Their work had an underlying tumor growth model that consisted of a single formula that depends on the tumor growth rate, symptomatic detection to occur at tumor size between 15mm and 20mm, and screening detection to occur at tumor size of 2mm. Rajapakshe et al. developed a micro-simulation model to optimize breast cancer screening based on the potential care paths of patients [Raj14]. The different care pathways were constructed using expert opinion and breast cancer patient data, and they were used to inform successes in screening policies [Raj14]. Tejada et al. developed a screening and treatment simulation model for breast cancer [Tej14]. As Tejada et al. focused on screening for older women, their two-part work presented a natural history model that used the findings of Plevritis et al. and evaluated different screening strategies that varied by screening interval and patient risk [Ple07; Tej14].

Similar extensive work has been published for colorectal cancer screening. Loeve et al. published one of the earlier studies in colorectal cancer screening producing the MISCAN-COLON simulation model [Loe99]. Their work simulated colon cancer patients as a heterogeneous population and two possible screening strategies [Loe99]. Taffazzoli et al. expanded on the Vanderbilt/NC State discrete-event simulation model of natural history to test and compare multiple screening policies for pancreatic cancer [Taf09]. The study compared their simulation results against the Minnesota study; a colorectal cancer screening case study from 1975 to 1977 [Taf09]. Li et al. presented a partially observed Markov chain model for colorectal cancer screening to evaluate strategies [Li14].

This chapter presents a screening evaluation tool, where we compare screening policies that vary by screening interval on different homogeneous populations. Our model utilizes simulation techniques to model the natural history of pancreatic cancer which uses a personalized progression model. We aim to personalize cancer screening to race, gender and relative risk. The remainder of this chapter presents the model and discusses the simulation results of the different screening policies.

3.3 Methods

We used the pancreatic cancer progression model presented in Chapter 2 as a tool for understanding tumor behavior. We expanded the model to evaluate high-risk patient's potential outcomes including death and pancreatic cancer incidence under different relative risks and screening policies. The simulation model starts with a 35 year-old cancer free patient, and each year, the patient either dies from any cause or develops PC. If the patient develops PC, the cancer will progress from local stage to regional and from regional to distant until the tumor is detected in one of those stages. We overlaid the patient's simulation with screening policies that start at age 50 and occur according to a predetermined interval. The simulation stops if the patient dies from any cause or if cancer is detected. Figure 3.1 shows the flow of one simulation run, where if the patient gets cancer then the

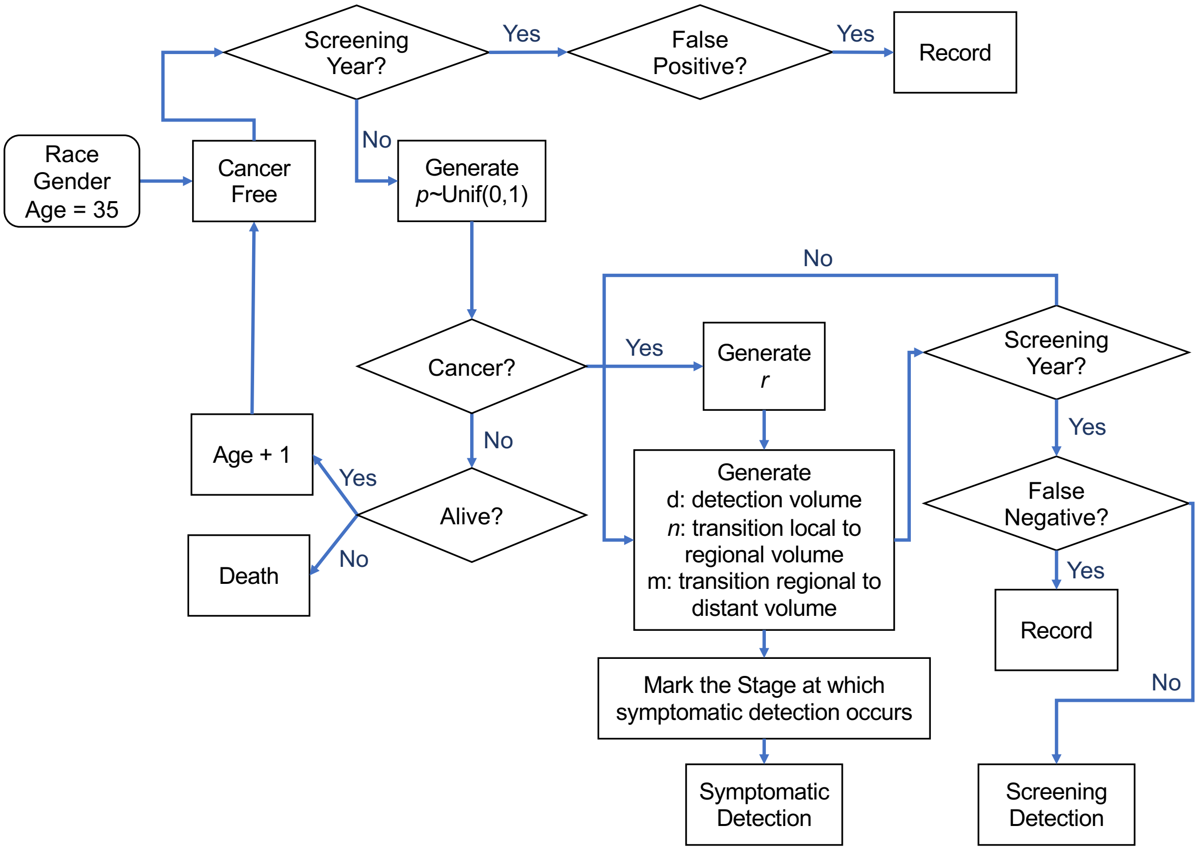

Figure 3.1 Flow Diagram of a Single Simulation Run

simulation of the progression model is identical to that in Chapter 2.

3.3.1 Death and Cancer Incidence Rates

The US Social Security Administration published an Actuarial Life Table that has probability of death at every age from 0 to 119 given a gender but not race [Soc]. In our simulation, we used these probabilities as a threshold to create the event of death for a patient in the simulation for each living and cancer free year. We determine the event of death by sampling a probability uniformly and then comparing it to the probability of death from the life tables, such that if the probability generated was less than the probability of death, then the event of death occurs. The Actuarial Life Table is an average given an age and gender. Therefore, we do not have the probability of death given other attributes a patient might have such as acute or chronic diseases.

The SEER databases also include cancer incidence rates per 100,000 that are a function of age, race, and gender (Figure 3.3). In our model, the probability of developing cancer every year is represented as:

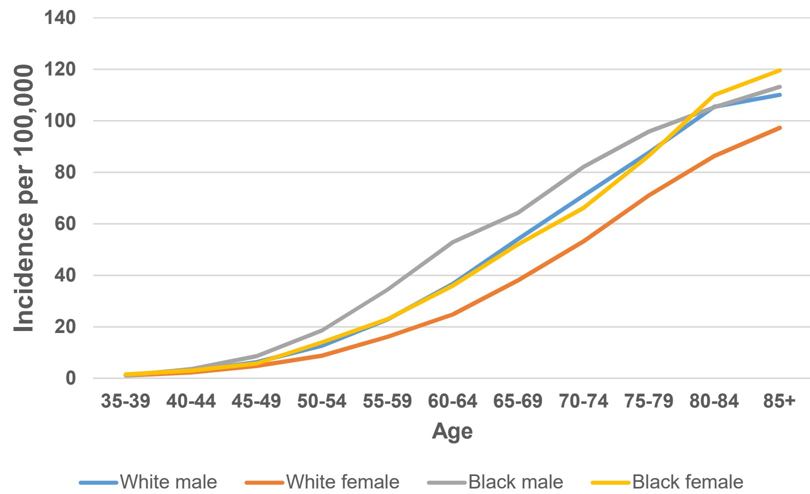

Figure 3.2 SEER Incidence Rates per 100,000 for Pancreatic Cancer

$$\mathbf{P}(\text{developing cancer in } [t, t+1] | \text{no cancer} < t, \text{ age, gender, race, and } RR) = RR \times (\text{Incidence rate per 100,000}|\text{age, gender, and race}), \quad (3.1)$$

where RR is the patient's relative risk of getting pancreatic cancer to the general population. For example, smoking was found to be a risk factor for pancreatic cancer with an associated risk of 1.7 (Table 3.1). This means that a smoker is 1.7 times more likely to get pancreatic cancer than a non-smoker. There are many other risk factors that were found to be associated with increased pancreatic cancer risk, and Table 3.1 highlights some of the risk factors that are frequently mentioned in the literature [CMHFHR13; Bec14]. The tumor growth model that we presented in Chapter 2 did not depend on the patient's comorbidities; we assumed that tumor growth only depends on the patient's age, gender, and race. Therefore, the relative risk will only affect the probability that a patient develops pancreatic cancer.

A patient's total relative risk is a function of the patient's comorbidities and collective risk factors. For example, a patient with Type-II diabetes ($RR = 1.8$) who also smokes ($RR = 1.7$) has a collective relative risk of 3.5 if having Type-II diabetes and smoking are independent events. This patient's relative risk of 3.5 is equivalent to that of a patient with cystic fibrosis. These two patients with the same collective relative risks are identical from the perspective of the simulation model, since the probability of cancer will be equal given all other factors being identical. Therefore, when creating a patient for simulation, we assign a RR value instead of specifying the patient's comorbidities.

Table 3.1 Risk Factors of Pancreatic Cancer and their Associated Relative Risks, [Bec14]

Risk Factor	Gene Associated	Increased Relative Risk
Familial Pancreatic Cancer, 1 FDR	Unknown	4.5
Familial Pancreatic Cancer, 2 FDR	Unknown	6.4
Familial Pancreatic Cancer, 3 FDR	Unknown	32
Hereditary breast and ovarian cancer syndrome	BRCA1	2.3
Hereditary breast and ovarian cancer syndrome	BRCA2	3.5
Lynch syndrome	MLH1, MSH2, MSH6, PMS2	8.6
Familial atypical multiple mole melanoma pancreatic carcinoma syndrome	p16	13
Peutz-Jeghers syndrom	STK11/LKB1	132
Hereditary pancreatitis	PRSS1, SPINK1	69
Cystic fibrosis	CFTR	3.5
Chronic Pancreatitis		13.3
Type-I Diabetes		2
Type-II Diabetes		1.8
Cigarette Use		1.7
More than 3 alcoholic drinks per day		1.2

3.3.2 Screening

For this model, we use Endoscopic Ultrasound (EUS) with sensitivity of 89% and specificity of 96% as the screening modality when evaluating screening policies. We chose EUS since it has the highest accuracy for detecting pancreatic cancer. Screening modalities with high sensitivity and specificity could be the key to justifying the effectiveness of pancreatic cancer screening. The simulation model was built with the following assumptions:

- A screening start age of 50 years old is appropriate as per the recommendation of the International Cancer of the Pancreas Screening Consortium (CAPS) guidelines.
- If a patient gets cancer, they stay alive until symptomatic detection. We did not model the transition from the undetected stages of cancer to death.

In our simulation model, screening is an action that is performed at set years. For example, the first screening year is always at age 50, and the next screening year is set based on the screening policy. At every screening, if the patient was cancer free then the model either simulates a false positive or a true negative, and if the patient had cancer then the model either simulates a true positive and record detection or a false negative and the patient remains in the simulation.

3.3.3 Simulation Experiments

We created a set of homogeneous populations of 100,000 with preset race, gender, and relative risk. We evaluated different screening policies for each homogeneous population measuring the following outcomes:

- Total number of benign screenings
- The number of false positive results from benign screenings; and the distribution of patients in the population that had 0, 1, 2, 3, 4, ..., false positive screenings in their lifetime.
- The number of false negative results from screenings in patients with cancer; and the number of patients in the population that had 0, 1, 2, 3, 4, ..., false negative screenings before a screening or symptomatic detection.
- The distribution of pancreatic cancer stages, local, regional, and distant, at symptomatic detection.
- The distribution of pancreatic cancer stages screen detected cancers in local, regional, or distant stage before symptomatic detection.

We expanded the simulation from Chapter 2 as shown in Figure 3.1. At the beginning of each simulation run we set the following:

- The number of patients to be generated at 100,000.
- The homogeneous population's demographic in race and gender.
- The population's relative risk.
- The number of replications of the homogeneous population that was created to 10.
- The screening interval to be employed at half a year, one year, two years, three years, four years, five years, or ten years.
- Screening start age was set at 50 years old.
- Screening stop age was set at 100 years old.
- Screening modality was set to be EUS, with a set sensitivity of 89% and specificity of 96%.

A Simulation Run

Each simulation run occurs as follows:

1. For the chosen homogeneous population, we personalize some components of the simulation. We set up the distributions used to create the events that transition a patient from cancer free to death or cancer:

   - Using the gender information of the population, the appropriate Actuary Life table is used to estimate the probability of death given patient's age.
   - Using the gender and race information, the incidence parameters corresponding to the patient's race, gender, and age are used to estimate the probability of cancer incidence.

2. Set the patient's age at 35 and start simulation.

3. While the patient is still alive and cancer free, at each time step (a year), t:

   - Generate a random probability, p, and:
     - Evaluate the probability of cancer given the current age, race, and gender of the patient, $\mathbf{P}(\text{cancer}|\text{age, race, gender})$, and check if p is less than that probability.

       If $p < \mathbf{P}(\text{cancer}|\text{age, race, gender})$, then the patient gets cancer at this age. Move to step 4.
     - Evaluate the probability of death given the gender and current age of the patient, $\mathbf{P}(\text{death}|\text{age, gender})$, and check if p is less than the retrieved probability.

       If $p < \mathbf{P}(\text{death}|\text{age, gender})$, then the patient dies at this age. **Stop the simulation**.
     - If $\mathbf{P}(\text{cancer}|\text{age, race, gender}) > p$ and $\mathbf{P}(\text{death}|\text{age, gender}) > p$, increment age by one year and this step is repeated.

4. If the patient develops cancer:

   - Generate an inverse growth rate, r, according to the distribution:

   $$R \sim \text{Uniform}(a, b), \text{ where } a = \frac{64}{365 \cdot \ln(2)} \text{ and } b = \frac{255}{365 \cdot \ln(2)}.$$

   - Using the age of cancer initiation, race, gender, and the inverse growth rate generated retrieve the progression model parameters γ, η, and ω and set the starting tumor spherical volume at $c_0 = \frac{2^3\pi}{6} = 4.19mm^3$, and generate:
     (a) The tumor volume at symptomatic detection, d, according to the distribution:

   $$F_{D|R}(d|r) = 1 - e^{-\gamma r(d-c_0)}$$

(b) The tumor volume at transition from local stage to regional stage, n, according to the distribution:

$$F_{N|R}(n|r) = 1 - e^{-\eta r(n-c_0)}$$

(c) The tumor volume at transition from regional stage to distant stage, m, according to the distribution:

$$F_{M|N,R}(m|n,r) = 1 - e^{-\omega r(m-n)}$$

- Translate each tumor volume to time in years using $T(V) = r\ln(V/c_0)$ where V is tumor volume, and evaluate age of symptomatic detection ($A(d)$ =age of cancer initiation+$T(d)$), age of transition from local to regional ($A(n)$ =age of cancer initiation+$T(n)$), and age of transition from regional to distant ($A(m)$ =age of cancer initiation+$T(m)$):
  - If $A(d) < A(n)$, then symptomatic detection occurs at the local stage.
  - If $A(d) > A(n)$ and $A(d) < A(m)$, then symptomatic detection occurs at the regional stage.
  - If $A(d) > A(m)$, then symptomatic detection occurs at the distant stage.
  - Record the stage at which symptomatic detection occurs.

5. When the patient becomes 50 years old, initiate screening. Throughout the simulation, a variable labeled *screening age*, that is initialized at 50 years old and updated after every screening with an increment of the screening interval, is used to intercept the natural history and perform a screening. When a screening is executed:
   - If the patient was cancer free at the time of a screening:
     - Record the benign screening as part of the effort to pancreatic cancer detection
     - Check if the patient triggered a false positive screening by generating a probability, p, and using the specificity of EUS equal to 0.96:
       - If $p < 0.96$, then the screening yields a true negative.
       - If $p > 0.96$, then the screening yields a false positive. Record it.
   - If the patient had cancer at the time of a screening:
     - Check if the patient triggered a false negative screening by generating a probability, p, and using the sensitivity of EUS equal to 0.89:
       - If $p < 0.89$, then the screening yields a true positive.
       - If $p > 0.89$, then the screening yields a false negative. Record it.
     - If screening detects the cancer (true positive), check the stage at which the screening is taking place:
       - If *screening age* $< A(n)$, then the tumor is detected at the local stage.

    - If *screening age* $> A(n)$ and *screening age* $< A(m)$, then the tumor is detected at the regional stage.
    - If *screening age* $> A(m)$, then the tumor is detected at the distant stage.
    - Record the stage at which screening detection occurs.
  - Screening can still miss the tumor and symptomatic detection would occur instead in one of the scenarios:
    - Symptomatic detection occurs before the first screening age after the cancer initiation age.
    - A screening occurs and yields a false negative, and symptomatic detection occurs before the next screening.

6. Terminate the simulation at tumor detection.

Experiment Scenarios

As previously mentioned, we created a set of homogeneous populations with size 100,000 and 10 replications for each. The simulation model was run for each of the combinations of the patient attributes:

- Different race and gender groups: White males, White females, Black males, and Black females;
- Different relative risk values of 5, 7, 10, 15, and 32;
- Under each of the following screening policy with the intervals of 0.5, 1, 2, 3, 4, 5, and 10 years.

After running the different simulations, we recorded the outcomes to compare them for each race, gender, relative risk, and screening policy. The resulting comparisons are discussed in the next section.

3.4 Results

Each screening policy was compared in terms of the associated effort for successfully detecting pancreatic cancer. Therefore, we record the benign screenings, false positives, false negatives, as well as the tumor stage at which successful screening detections and symptomatic detections occurred under each policy. We measured the effects of race, gender and relative risk on the incidence of pancreatic cancer in the homogeneous populations. Figure 3.3 shows the expected upward trend of increased incidence with increased relative risk, and it also shows that Black males are the most sensitive group to increased relative risk.

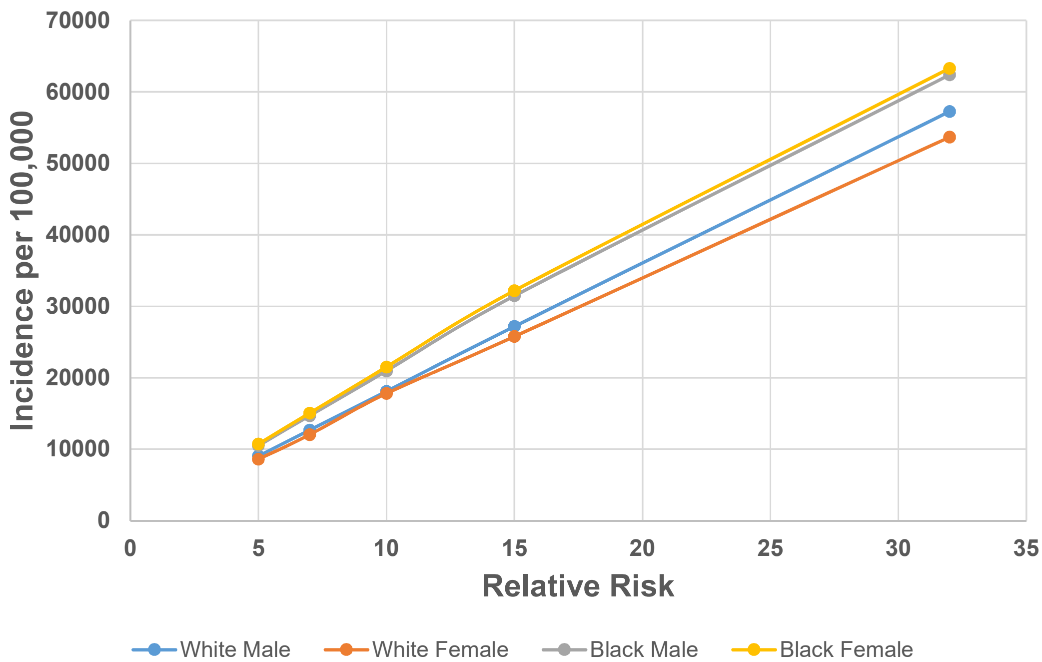

Figure 3.3 The Incidence Rate in Race, Gender, and Relative Risk Homogeneous Populations

We studied the burden of false positive screening when EUS is the screening modality. We recorded the distribution of patients by number of false positives over their lifetime under each screening policy. Figure 3.4 shows the frequencies of patients by number of false positive results during their lifetime under each of the screening policies. The largest group, consistently across the different screening policies, is the group where all of their benign screenings resulted in a true negative result; i.e. the proportion of patients that had zero false positive result. However, even under the screening policy with the screening interval of ten years, less than 90% of the patients underwent the policy with zero false positive results.

We examined the percentage of pancreatic cancer detections due to screening under each of the screening policies. The percentage of screening detections across different relative risks remained relatively the same since relative risk affects the total number of cancer patients but not the progression of the cancer. Therefore, when considering stage distributions at detection, we focus on the relative risk of five. Figure 3.5 shows the effect of the screening interval on the proportion of pancreatic cancer cases that would be detected by screening. The trend as approximated by MS Excel are polynomial lines of third degree. The screening intervals of half a year and a year do not differ in the proportion of pancreatic cancer cases detected by screening where each is around 96%. Moreover, Figure 3.6 shows the effect of the screening interval on the proportion of symptomatic detections complementing Figure 3.5. With a screening interval of ten years, more than half of the

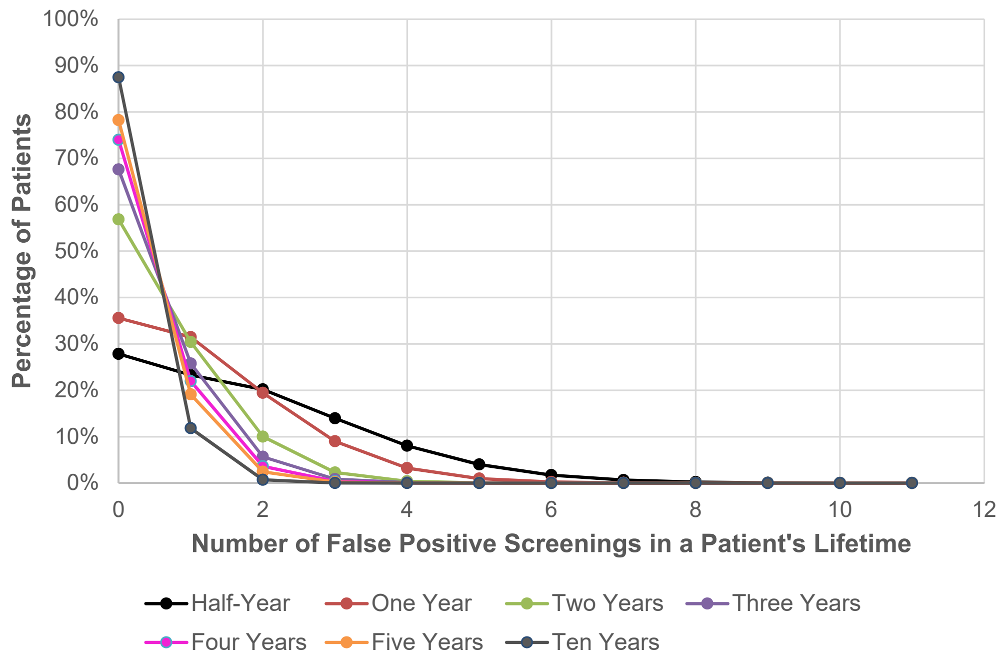

Figure 3.4 Frequency of False Positive Result Under Different Screening Policies

patients would be missed by the screening leading to symptomatic detections.

We took a closer look at the stage distribution at detection for symptomatic detection without any screening employed and screening detection under the different screening intervals. Figures 3.7, 3.9, 3.8, and 3.10 show the stage distribution at detection under no screening, half a year, one-year, two-year, three-year, four-year, five-year, and ten-year screening intervals for White males, White females, Black males, and Black females with a relative risk of five, respectively. The stage distribution at symptomatic detection without any screening seems to be similar within gender where females have higher proportions in symptomatic detection at the local and regional stages. The stage distributions under the half-year and one-year screening intervals only differ by at most 1%, suggesting that there is little benefit in screening more frequently than annually.

To further understand the effort required for screening, we measured the ratio of the number of benign screenings in the homogeneous populations by the total number of detections by screening. Figure 3.11 displays the benign to detection by screening ratio for each race, gender, and relative risk. White females require the most effort while Black males require the least. A policy maker could set a limit on the effort spent to detect a cancer by screening; a threshold for the number of benign screenings required for one cancer detection by screening. Given a threshold of that effort, T_{effort}, we can identify the screening policy with the shortest screening interval such that the benign to screening detection ratio is less than T_{effort}. For example, if we select the screening policy with the

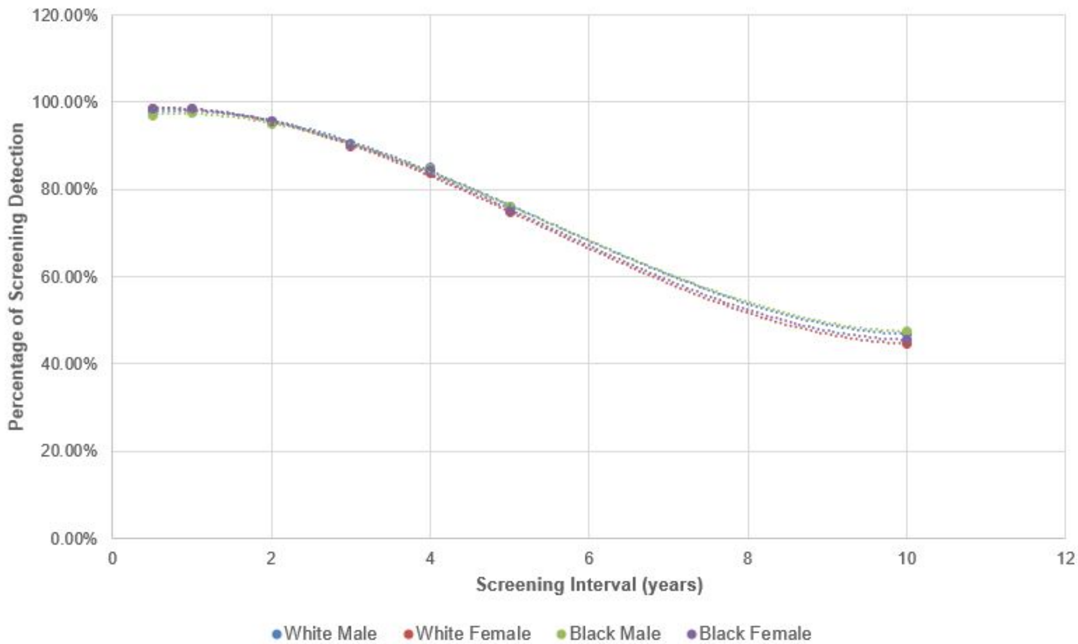

Figure 3.5 The Proportion of Pancreatic Cancer Cases that would be Detected by Screening for each Gender and Race

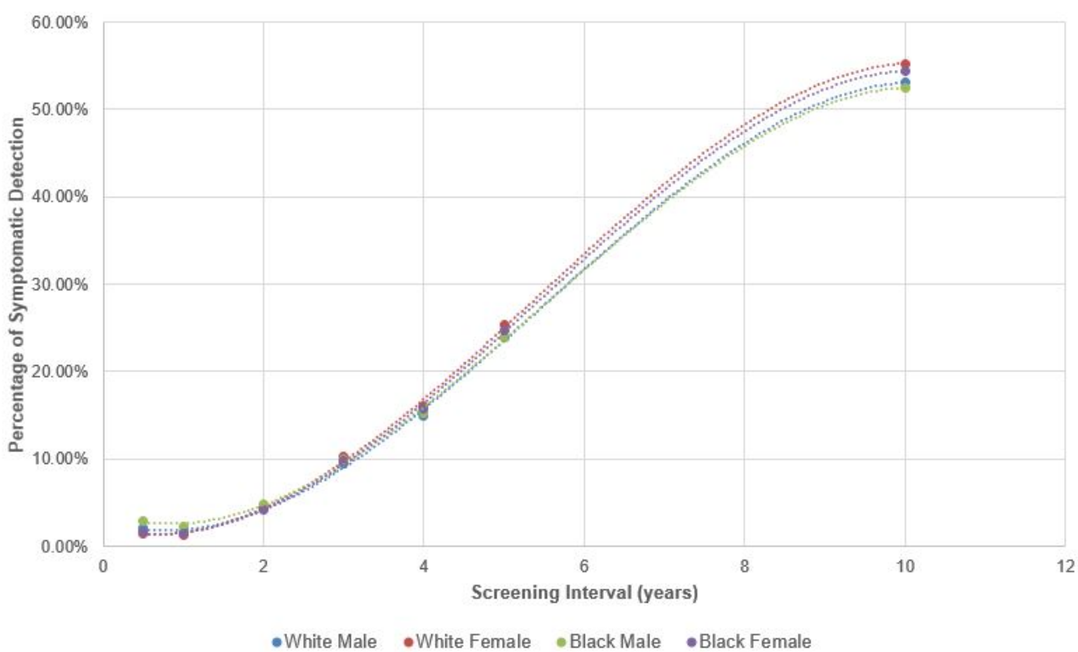

Figure 3.6 The Proportion of Pancreatic Cancer Cases that would be Detected Symptomatically for each Gender and Race

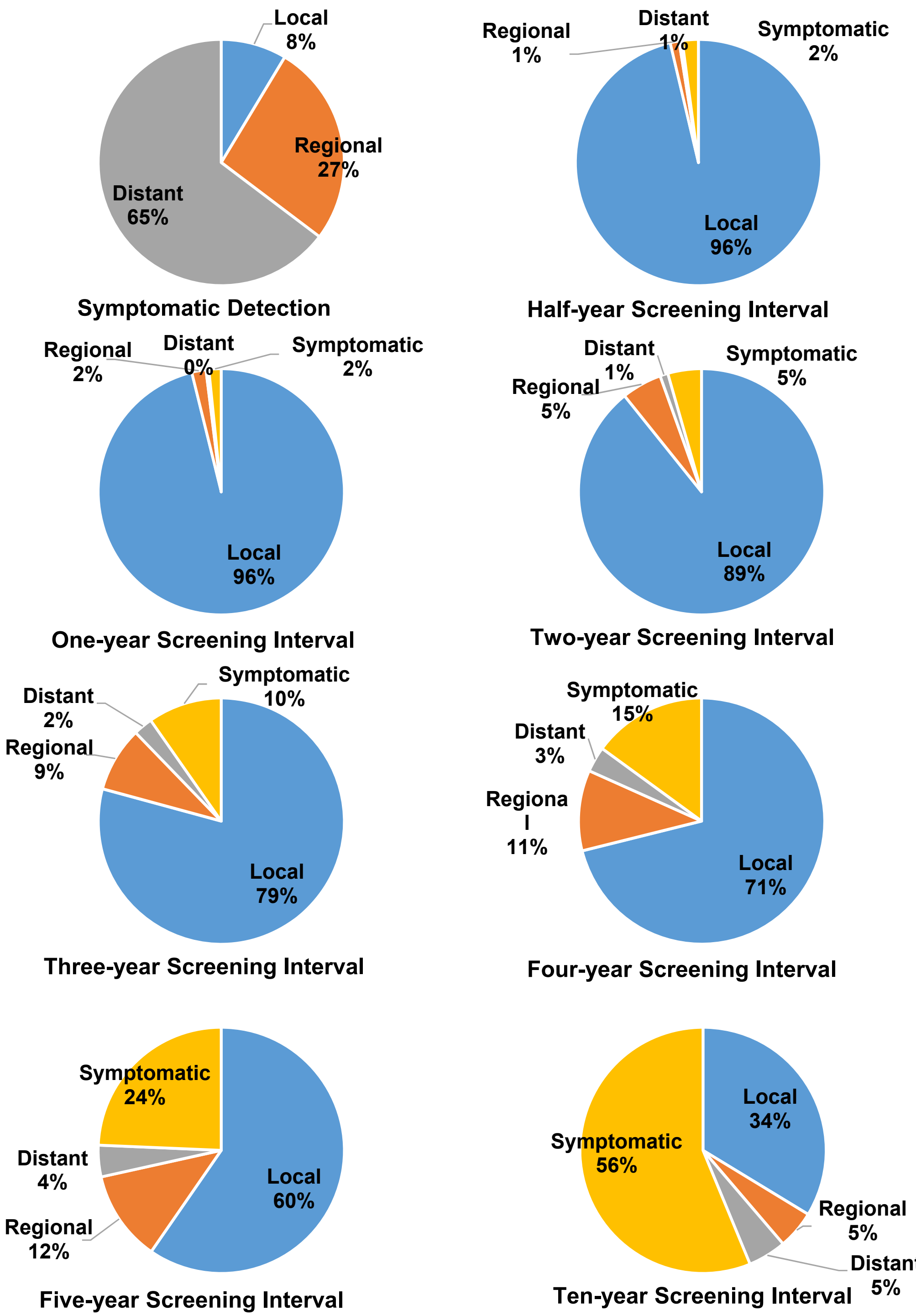

Figure 3.7 Distributions of Cancer Stage at Detection Symptomatically and under Different Screening Intervals for White Male

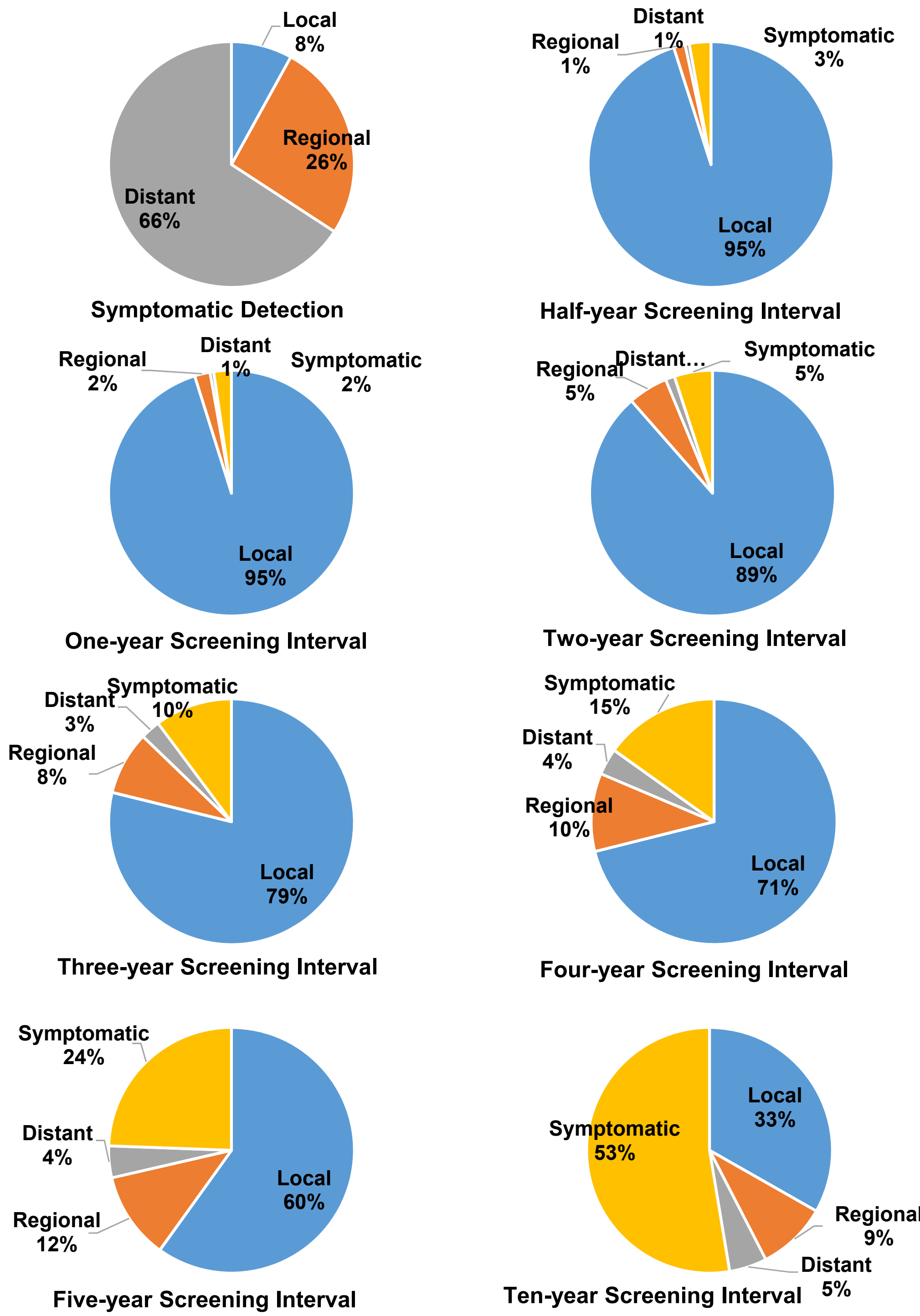

Figure 3.8 Distributions of Cancer Stage at Detection Symptomatically and under Different Screening Intervals for Black Male

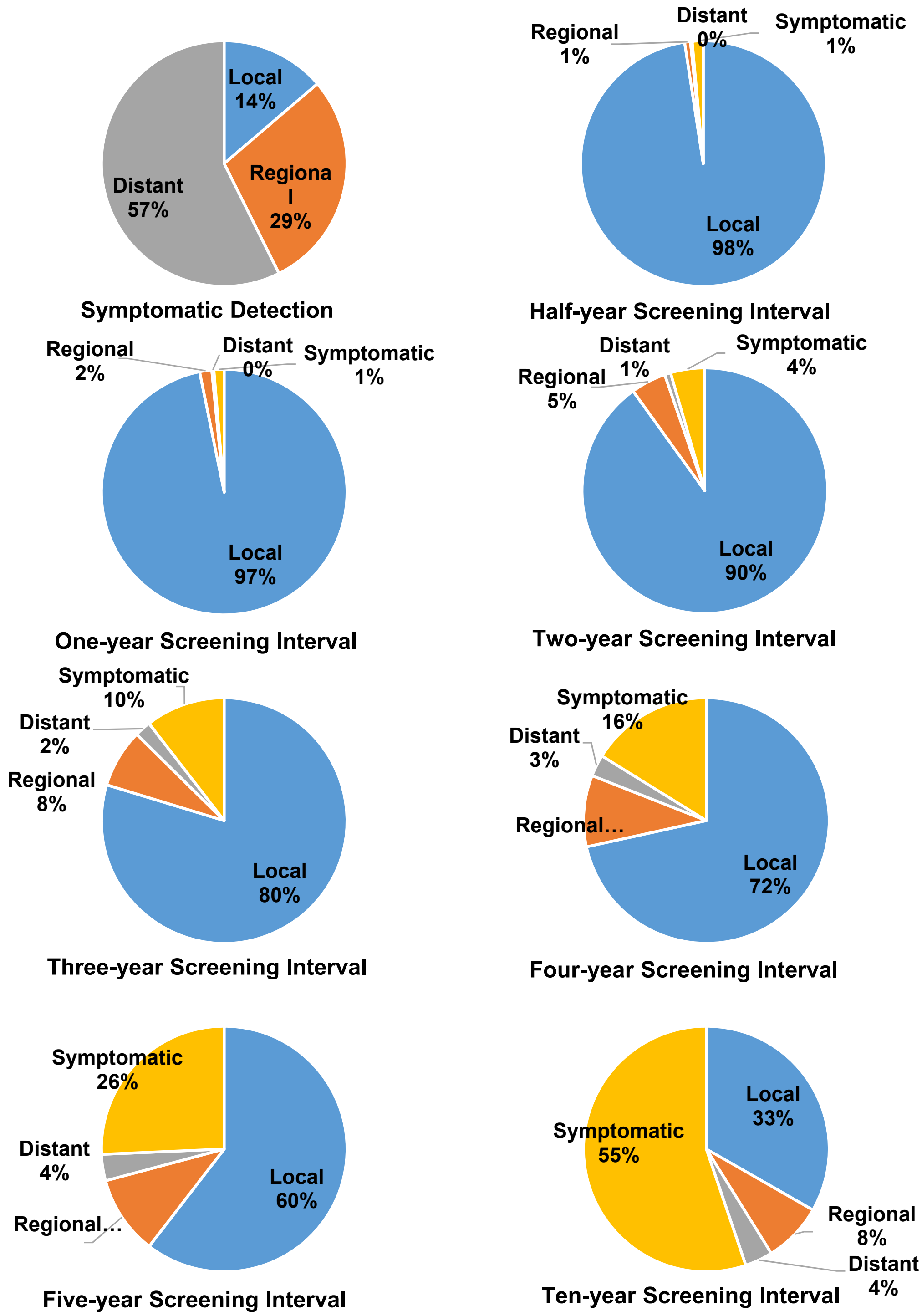

Figure 3.9 Distributions of Cancer Stage at Detection Symptomatically and under Different Screening Intervals for White Female

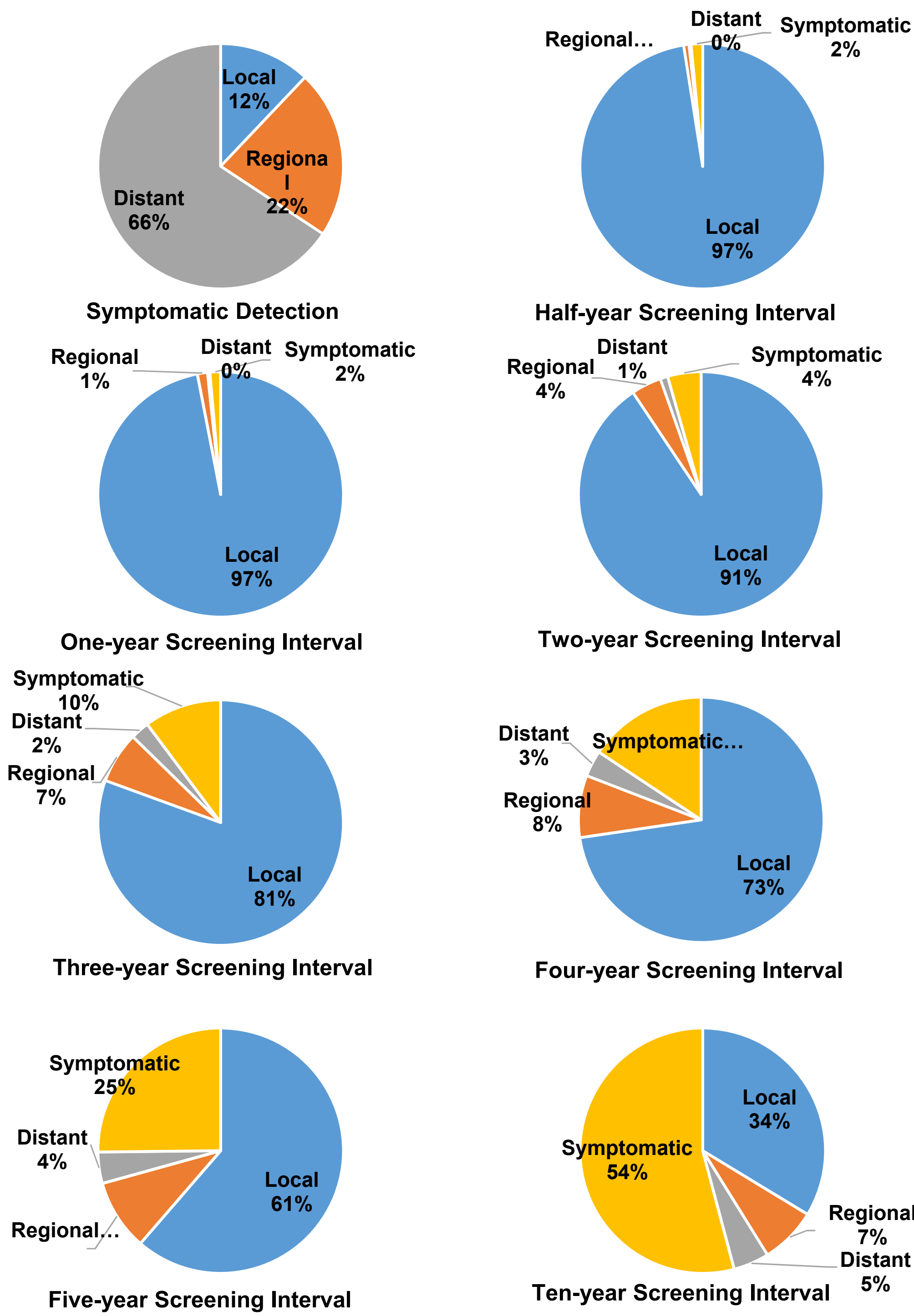

Figure 3.10 Distributions of Cancer Stage at Detection Symptomatically and under Different Screening Intervals for Black Female

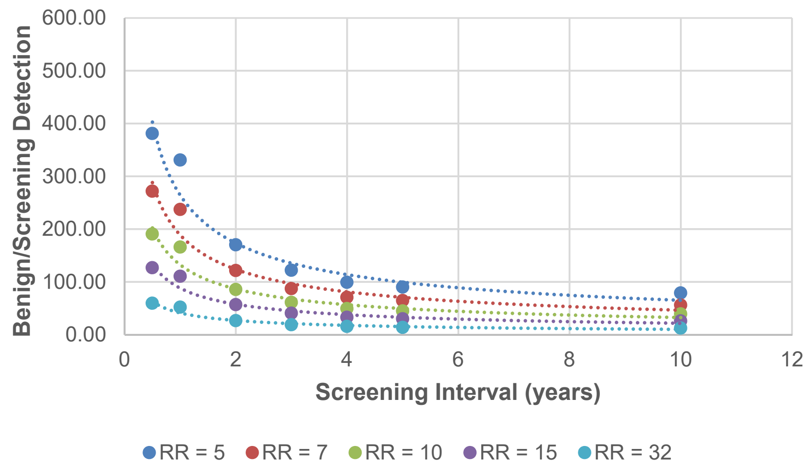

(a) White Male

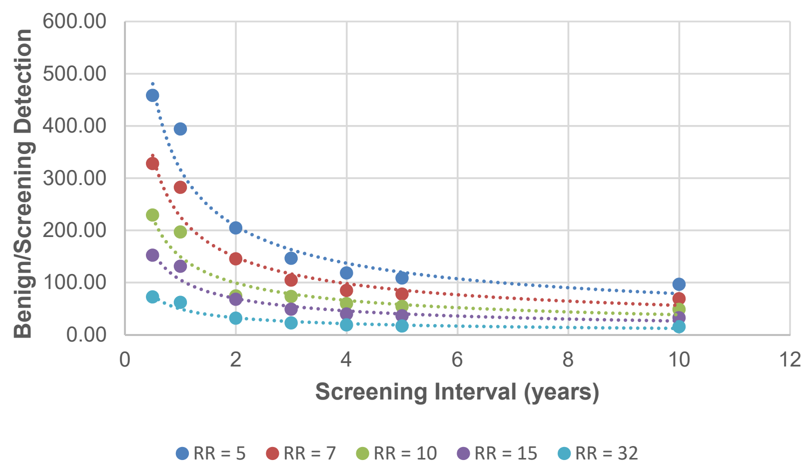

(b) White Female

Figure 3.11 The Number of Benign Screenings to One Screening Detection

shortest screening interval that has $T_{effort} = 100$, 150, or 200 across all subgroups, we consistently get half a year screening interval if the patient has a relative risk of 32 (i.e., three first degree members with pancreatic cancer). Table 3.2 summarizes the minimum screening interval given a maximum benign to screening detection for each race, gender, and relative risk. This suggests that screening policies can be personalized to the patient demographic and relative risk that can in other ways be expressed as risk factors and comorbidites.

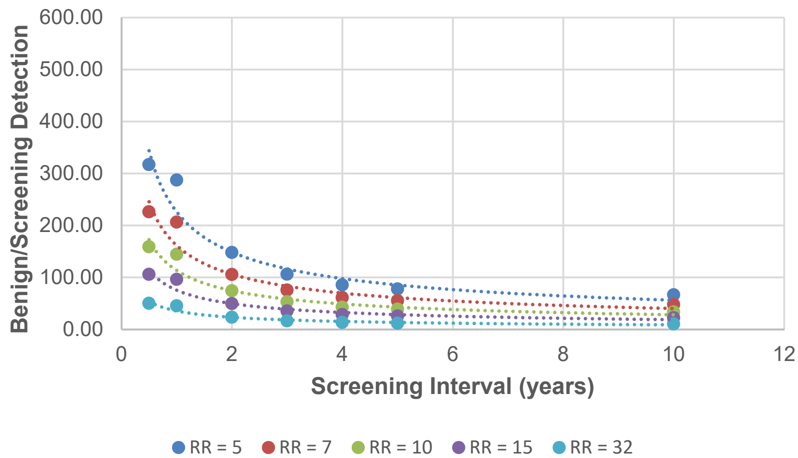

(c) Black Male

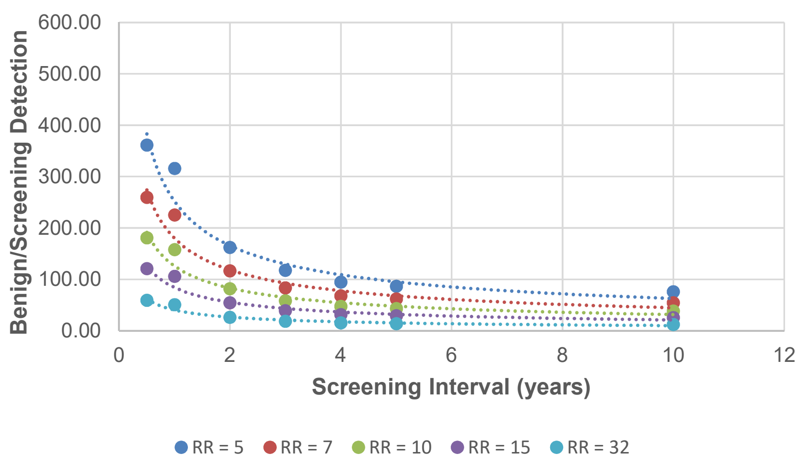

(d) Black Female

Figure 3.11 (continued) The Number of Benign Screenings to One Screening Detection

Table 3.2 The Shortest Screening Interval Under a Certain Benign to Screening Detection Ratio Threshold

		Shortest Screening Interval (years)		
Race/Gender	Relative Risk	$T_{effort} = 200$	$T_{effort} = 150$	$T_{effort} = 100$
White Male	5	2	3	4
	7	2	2	3
	10	0.5	2	2
	15	0.5	0.5	2
	32	0.5	0.5	0.5
White Female	5	3	3	10
	7	2	2	4
	10	1	2	2
	15	0.5	1	2
	32	0.5	0.5	0.5
Black Male	5	2	2	4
	7	2	2	3
	10	0.5	1	2
	15	0.5	0.5	1
	32	0.5	0.5	0.5
Black Female	5	2	3	4
	7	2	2	3
	10	0.5	2	2
	15	0.5	0.5	2
	32	0.5	0.5	0.5

3.5 Discussion and Conclusion

In Chapter 2, we developed a pancreatic cancer progression model. In this chapter, we complemented the progression model with incidence rates incorporating patients' relative risk, the possibility of any cause of death, and incorporation of screening. We measured the incidence rate within the different populations and the effect of screening interval on false positive rates and stage distributions at detection.

The stage distributions at detection for a certain screening interval did not change for the different populations. This can be explained by revisiting the effect of race and gender on the tumor timeline. In Table 2.13, we summarized the average resulting tumor timeline by race and gender where the resulting timelines did not vary significantly. On the other hand, the screening effort associated with false positive screenings and the benign to screening detection ratio differs by population and screening interval. Analyzing the stage distribution at detection suggests that a half-year screening interval is not beneficial as it yields the same outcome as annual screening with more effort. Combining that result with the benign to screening detection effort, annual screening for patients with a relative risk of 32 (at least three FDRs with pancreatic cancer) performs best. The same conclusion is valid for a Black male with a relative risk of 15. For the other groups, a policy recommendation depends on the amount of effort (T_{effort}) a policy maker is willing to spend.

From Table 3.2, we can infer that employing a screening policy with a certain predetermined effort would result in White females having less frequent screenings compared to the other populations. From the literature, White females are the demographic that is least expected to be at high risk for pancreatic cancer, while Black males were projected to be the highest at risk. The suggested screening interval for Black males is at least as aggressive, if not more, than the suggested screening interval for other demographic groups at different relative risk and maximum benign to screening detection values. These results are based on the benign to screening detection curves in Figure 3.11, where the curves for Black male are the lowest and for White female are the highest.

Screening for pancreatic cancer should be personalized considering a bound on the amount of effort required to detect one pancreatic cancer via screening. Personalization should incorporate relative risk first then race and gender. Relative risk has a larger effect on the shortest screening interval under a threshold for effort spent. Endoscopic Ultrasound is an invasive procedure and that makes the required effort to screen more significant the larger the number of benign screenings for each screening detection. This study can be expanded to include cost or additional effort such as patient effort to undergo the screening, medical costs versus incentive to screen, and finally the potential treatment of the cancer after it is detected. The next chapter incorporates the resectability of the disease upon detection in the evaluation of the true benefit of screening.

CHAPTER

4

PANCREATIC CANCER SCREENING AND RESECTABILITY PREDICTIONS TO MAXIMIZE EXPECTED SURVIVAL

4.1 Introduction

Pancreatic cancer has one of the lowest 5-year survival rates among the different cancers. This is mostly attributed to the late diagnosis of the disease and to the fact that the only true cure for the disease is resectability. Currently, only 15 to 20 percent of pancreatic cancer patients are presenting with a resectable disease upon diagnosis. Without a formal screening policy implemented, the low resectability and survival rates will continue to result in late symptomatic detection after the tumor has metastasized.

Patients that presented with resectable pancreatic cancer and successfully underwent surgery were estimated to have a 5-year survival probability of 7.3-22% [Kuh04; Roe18]. The post resection survival rates are improving with technological advances and the increased frequency of total pancreatectomy as a treatment option for pancreatic disorders [Kuh04; Sep17]. Kuhlmann et al. showed that resection survival rates can improve if the patient's tumor size was smaller at the point of resection [Kuh04]. This makes screening for pancreatic cancer more relevant given that studies have shown improved survival due to resection especially at earlier stages [Roe18].

Chapters 2 and 3 introduced a pancreatic cancer progression model, a resectability prediction tool, and a discrete event simulation screening model. In this chapter, we combine the work to produce a screening simulation model that predicts resectability of tumors at detection by screening policy. We also expand the resectability prediction tool and introduce a new measure of effort for evaluating different screening policies.

4.2 Literature Review

There is a vast literature on cancer screening, and we narrowed our search to colorectal, breast, and pancreatic cancer screening models. We studied the screening policies tested and the policy evaluation metrics used. In this section, we also review the survival rates of pancreatic cancer with and without resection.

Loeve et al. developed a colorectal cancer screening simulation model, MISCAN-COLON, and they estimated the annual cost of screening as well as the mortality reduction under two screening policies [Loe99]. Tafazzoli et al. presented a discrete event simulation model for colorectal cancer screening, and they estimated the cost-effectiveness ratio to compare different policies [Taf09]. Tafazzoli's work used a cost-effectiveness ratio which is defined as the difference in cost of two policies divided by the difference in effect (benefit) of the two policies [Taf09]. Li et al. developed a partially observable Markov chain for colorectal cancer screening where they estimated the cumulative quality-adjusted life years and the cumulative cost of a screening policy for a certain period of time [Li14].

A breast cancer screening model based on a Monte Carlo simulation was used to test different screening strategies [For09]. The model used estimates of the difference in screening detection and symptomatic detection under different screening intervals to evaluate screening policies [For09]. Maillart et al. assessed the effect of dynamic screening policies for breast cancer assuming a perfect screening modality [Mai08]. They estimated the lifetime mortality risk of a patient versus the expected number of mammograms in a screening policy, and they identified the efficient screening policies by creating efficiency frontiers [Mai08]. Tejada et al. built a screening and treatment model for breast cancer, and they estimated the quality-adjusted life years under treatment post screening detection as well as the treatment and screening costs [Tej14]. Ayer et al. developed a partially observable Markov decision process for personalized mammography screening policies for breast cancer, where the input to their model was a previously validated microsimulation model of breast cancer natural history, treatment, and death [Aye]. The model used quality expected life years as the objective to maximize, and it identified screening policies based on patient's age [Aye].

There are clinical studies that evaluated the survival of pancreatic cancer patients after they underwent resection (total pancreatectomy or the Whipple procedure). Distler et al. evaluated the survival of 195 patients that underwent pancreatic head resection where eight of the patients died

Table 4.1 Patient Survival Post Pancreatic Resection, [Roe18]

Stage	Explanation	Survival Probability, %		
		1-year	3-year	5-year
IA	≤ 2cm, no lymph node involvement	87.6	52.6	39.3
IB	2-4cm, no lymph node involvement	90.8	45.4	34.1
IIA	> 4cm, no lymph node involvement	77.1	46.7	27.6
IIB	any size, spread to 1-3 lymph nodes	81.4	36.8	21.1
III	any size, tumor involves celiac axis or major artery	78.6	10.5	23.2

within 30 days post operation [Dis13]. Distler et al. estimated the 3-year survival to be 31.5% and the 5-year survival to be 11.9% after pancreatic head resection [Dis13]. Kuhlmann et al. peformed a similar analysis where they studied the survival of 160 patients post resection, and the median survival time concurred with the findings of other similar studies [Kuh04]. They found the post resection 3-year survival to be 32%, 18.5%, and 0.05% if the patient had a tumor with diameter 0-2cm, 2-4cm, and 4-6cm, respectively [Kuh04]. Van Roessel et al. studied the survival of pancreatic cancer patients post resection as well, where their cohort consisted of 1525 patients with non-metastatic disease across multiple health centers [Roe18]. A summary of the survival probability based on tumor stage is in Table 4.1. Since this study had the largest patient cohort, and it is the most recent, we use their estimated survival rates in our evaluation analysis.

4.3 Methods

We developed a discrete event simulation model that evaluates screening policies and predicts the resectability of a patient upon cancer detection and that patient's five-year survival. The simulation model design concept was similar to that presented in Chapter 3. The model initiates with sets of patients at age 35 years old and cancer free, and a screening policy was employed on that population. We created ten homogeneous populations for each race, gender, and relative risk, as well as ten heterogeneous populations with randomly generated race, gender, and risk factors according to the prevalence of each in the US population. Every experiment corresponding to a screening policy was employed on all ten populations and an average result was stored. The goal of the experiments on both homogeneous and heterogeneous populations was to test the effect of screening on a subpopulation and the population as a whole. SEER reports the overall average five-year survival rate that we utilize to compare the effect of a policy on a population [NCISP].

4.3.1 Incidence Rate

SEER incidence rates of pancreatic cancer that are race, gender, and age specific are shown in Figure 4.1. We fit the incidence rates in each of the groups by age with the polynomial function

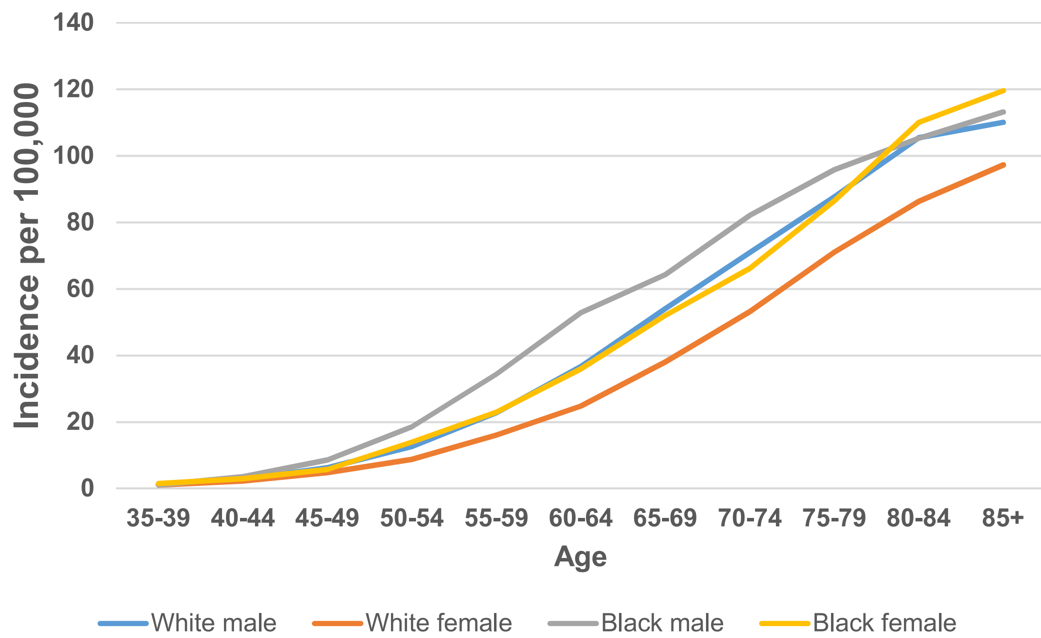

Figure 4.1 SEER Incidence Rate per 100,000 per year for Pancreatic Cancer

$f(x) = a + bx + cx^2 + dx^3 + ex^4$. Similar to the methodology in Chapter 3, we use the incidence rate as a probability measure to determine if a patient develops pancreatic cancer at a certain age.

However, SEER reported the incidence rates as an average of different causes of the cancer. Therefore, we first analyze the pancreatic cancer population and its etiology. The percentage and prevalence of each cause are summarized in Table 4.2. The reported percentages only account for about 60% of the PC population, and the remaining 40% are assumed to be from unknown causes. We use the prevalence in the population of each of the risk factors, along with their relative risks, to create a patient in a heterogeneous population. We assume independence between the different risk factors. We grouped the hereditary factors summarized in Table 4.4 and calculated a weighted average of the hereditary factors' relative risk based on their associated prevalence. We found the average relative risk of the hereditary factors to be 3.66 when we take the conservative lower bound of all of the ranges summarized in Table 4.4. We use Tables 4.2 and 4.3 to create a patient profile in a heterogeneous population.

4.3.1.1 Screening Modalities

In Chapter 3, we assumed the most accurate screening modality, Endoscopic Ultrasound (EUS), for the screening experiments. However, multiple studies on screening high-risk patients have used Magnetic Resonance Imaging (MRI) as their first screening modality and Endoscopic Ultrasound

Table 4.2 Causes of PC as a Percentage of PC Population

Risk Factor	**Relative Risk, [Bec14]**	**Percentage of PC Population, [II16]**	**Percentage of General Population**
Smoking, Male	1.7-2.2	26.2	15.8, [Cen17c]
Smoking, Female	1.7-2.2	31.0	12.2, [Cen17c]
Obesity, Male	1.5	12.8	Table 4.3
Obesity, Female	2.8	11.5	Table 4.3
Diabetes	1.8-2.0	9.7	Table 4.3
Chronic Pancreatitis	13.3	1.3	0.05
Hereditary Factors	2-132 (3.66)[4.4]	5-10	Table 4.4

Table 4.3 Diabetes and Obesity Prevalence in Population based on Race and Gender

	White Male	White Female	Black Male	Black Female
Diabetes [Cen17b]	8.1	6.8	12.2	13.2
Obesity [Hal15]	37.9	38.0	36.9	54.8

Table 4.4 Familial Risk Factors of PC with their Prevalence in the Population

Risk Factor	**Relative Risk, [Bec14]**	**Prevalence in Population**
BRCA1/BRAC2	2-3.5	1/5,000 [Inh]
Lynch Syndrome	8.6	Unknown
Familial adenomatous polyposis	4.5-6	1-9/100,000 [Orp]
Peutz-Jeghers Syndrome	132	1-9/1,000,000 [Orp]
Familial atypical multiple mole melanoma pancreatic carcinoma syndrome	47	Unknown
Hereditary Pancreatitis	69	3/1,000,000 [Sol93]
Cystic Fibrosis	3.5	1-9/100,000 [Orp]
Familial Pancreatic Cancer	4.5-32	1-9/1,000,000 [Orp]

(EUS) as a confirming test. Zhang et al. reported MRI senstivity and specificity at 89% and 89%, respectively, and EUS sensitivity and specificity at 88% and 96%, respectively. In this chapter, we perform two sets of experiments where the screening modality is EUS or MRI.

4.3.1.2 Resectability Prediction

In Chapter 2, we presented a resectability prediction tool where the input of the tool included the patient's cancer stage. In this chapter, we explored creating three disjoint tools for each cancer stage and hence the cancer stage was removed from the input variable. Following the previous analysis in Chapter 2, we created a binary input vector with the i^{th} element equal to one if the i^{th} property is satisfied. The properties considered in constructing the three new tools are tumor volume and patient's age. We fit each model using Ridge Regression, a tool that accounts for the relationships between the input variables assuming multicollinearrity. With the discretized intervals for age and tumor volume, we do not have independent input variables and hence the use of Ridge Regression. Moreover, we used a binary output variable when training the model, and Ridge Regression returned a range of values when the tool is used for resectability prediction.

The resulting output of the tools ranged from -0.2 to 1.2 since Ridge Regression is a type of linear fit, although the training set's output was either zero or one. Therefore, we assigned a value of zero for the negative results and a value of one for the greater than one results when using the tools in our simulation. A value that is between zero and one is required in our model since we are estimating the probability of resectability upon tumor detection. As we have explored in Chapter 2, we trained the original model using SVC, SVR, and Logistic Regression but the resulting output was predominantly zeros and ones. We created the same structure as presented in Chapter 2 where we divided the data 80% for training and 20% for testing. Table 4.5 summarizes the accuracy measures of each of the tools produced using the 20% proportion of data that was reserved for testing. To calculate the accuracy measures presented in Table 4.5, we assumed any value that is greater than 0.5 corresponds to a resectable cancer and a value that is below 0.5 is a nonresectable cancer. The highest predicted value for the distant stage resectability prediction tool was 0.3, and hence all patients with distant stage PC were predicted to be unresectable.

Table 4.5 Accuracy Measures for the Resectability Prediction Models, by Stage (%)

	Original	**Local**	**Regional**	**Distant**
Sensitivity	49.94	73.68	60.91	0
Specificity	91.07	74.15	62.67	100
Positive Predictive Value	67.65	68.56	61.96	0
Negative Predictive Value	82.95	78.65	61.63	100
AUC of ROC (max of 1)	0.71	0.75	0.62	0.50

There are trade-offs between the original model and the segmented models based on the tumor stage. For example, the sensitivity increases from the original model to the local and regional models but drops to zero for the distant model, while the opposite occurs with specificity. We calculated the area under the curve of the receiver operating characteristic curve (AUC of ROC), which is the plot between the predicted output and the true values. We used a binary representation of the predicted outputs such that a value of one was assigned for a predicted value greater than 0.5, and a value of zero was assigned otherwise to calculate the AUC values of every tool. An AUC value that is closer to one means a higher accuracy (a 100% accuracy corresponds to an AUC of ROC value equal to 1). Given the tradeoffs between the original model and the segmented models, we choose to continue this chapter with the segmented models as the tools used to predict resectability upon detection.

4.3.1.3 Evaluation Measures

Our model incorporates the probability of resectability upon detection by screening or symptomatic detection. We use the probability of resection in our evaluation measure since it inherently informs the "success" of detection by screening. Our benefit measure is the distribution of the probability of survival of the patient upon detection. In our analysis, we evaluate the 5-year survival rate of patients under certain policies. From the literature, we have the survival rates of pancreatic cancer patients with resection [Roe18]. We estimate an average of the unresectable pancreatic 5-year survival at 3.4% for all cancer sizes [Bil07]. Our resection prediction tool provides a probability of resection upon detection. For each simulated patient that develops pancreatic cancer, we calculate:

$$\begin{aligned}\mathbf{P}(\text{survival}|\text{tumor size}) = {} & \mathbf{P}(\text{survival}|\text{tumor size, resection}) \times \mathbf{P}(\text{resection}|\text{tumor size}) \\ & + \mathbf{P}(\text{survival}|\text{tumor size, no resection}) \times \mathbf{P}(\text{no resection}|\text{tumor size}), \quad (4.1)\end{aligned}$$

and we calculate the average 5-year survival for all simulated cancer patients to estimate the 5-year survival under a certain policy.

We evaluate the effort of screening by considering the number of benign screenings performed in the population, the number of **Productive Screenings**, and the number of **Unproductive Screenings**. We define a screening detection to be **productive** when tumor was found by screening at a resectable stage, and we define an **unproductive** screening detection of a tumor detected by screening but at an unresectable stage. Therefore, we express Effort as follows:

$$
\begin{aligned}
\text{Effort} &= \frac{\text{Benign Screenings} + \text{Unproductive Screenings}}{\text{Productive Screenings}} \\
&= \frac{\text{Benign Screenings} + (\text{Screening Detections} \times \mathbf{P}(\text{no resection}))}{\text{Screening Detections} \times \mathbf{P}(\text{resection})} \\
&= \frac{\text{Benign Screenings} + \sum_{\text{Screening}} \mathbf{P}(\text{no resection})}{\sum_{\text{Screening}} \mathbf{P}(\text{resection})} \\
&= \frac{\text{Benign Screenings} + \sum_{\text{Screening}} 1 - \mathbf{P}(\text{resection})}{\sum_{\text{Screening}} \mathbf{P}(\text{resection})}
\end{aligned}
\tag{4.2}
$$

We use the average 5-year survival and the effort to measure the effect and burden of a screening policy. We evaluate all 5-year survival and effort pairs to establish an efficient frontier for each of the homogeneous populations as well as the heterogeneous population. We further evaluate the efficient policies.

4.3.2 Simulation Model Steps

For each experiment, we run the following simulation and steps described. We first create a population of patients, either homogeneous or heterogeneous, and then we apply a screening policy to that population. We test screening policies on homogeneous populations to study the differences in their effect and how screening personalization could occur. We also test screening policies on heterogeneous populations to study the effect of a one-policy-fits-all and to assess the volume of patients that would be missed by screening high-risk patients only.

We first describe the process by which we create a homogeneous population of a certain race, gender, and relative risk.

<u>Process for Creating Homogeneous Populations:</u>

Step 1 Set population's race, gender, relative risk, and cancer free start age of 35 years old.

Step 2 Increase the patient's age by one year and using the patient's race, gender, age, and relative risk determine:

1. If the patient is alive and cancer free, repeat Step 2.
2. If the patient dies from any cause, proceed to Step 4.
3. If the patient develops pancreatic cancer, proceed to Step 3.

Step 3 Create the cancer:

1. Generate tumor inverse growth rate for the patient, r.

2. Generate tumor volume at symptomatic detection, d.
3. Generate tumor volume at transition from local stage to regional stage, n.
4. Generate tumor volume at transition from regional stage to distant stage, m.

Step 4 Record the following for each patient created in the population:

1. If patient died before cancer, record their age of death.
2. If patient developed cancer, record:
   - Age of cancer.
   - Inverse growth rate, r, of the tumor for that patient.
   - At transition from local stage to regional stage, record tumor size and age of patient.
   - At transition from regional stage to distant stage, record tumor size and age of patient.
   - At symptomatic detection, record tumor size, patient's age, stage of tumor, and resectability of tumor.

We also describe the process by which we create a heterogeneous population that encompasses different races, genders, and relative risks as per their prevalence in the US population.

Process for Creating Heterogeneous Populations:

Step 1 Start the patient at age 35 years old and cancer free.

Step 2 Generate the patient's race and gender with the White:Black ratio as 76.6:13.4 and the Male:Female ratio as 49.2:50.8 [U.S].

Step 3 Generate the patient's medical profile of relevant risk factors with the prevalence distribution in Tables 4.2 and 4.3.

Step 4 Increase the patient's age by one year and using the patient's race, gender, age, and relative risk determine:

1. If the patient is alive and cancer free, repeat Step 4.
2. If the patient dies from any cause, proceed to Step 6.
3. If the patient develops pancreatic cancer, proceed to Step 5.

Step 5 Create the cancer:

1. Generate tumor inverse growth rate for that patient, r.
2. Generate tumor volume at symptomatic detection, d.

3. Generate tumor volume at transition from local stage to regional stage, n.
4. Generate tumor volume at transition from regional stage to distant stage, m.

Step 6 Record the following for each patient created in the population:

1. If patient died before cancer, record their age of death.
2. If patient developed cancer, record:
   - Age of cancer.
   - Inverse growth rate, r, of the tumor for that patient.
   - At transition from local stage to regional stage, record tumor size and age of patient.
   - At transition from regional stage to distant stage, record tumor size and age of patient.
   - At symptomatic detection, record tumor size, patient's age, stage of tumor, and resectability of tumor.

After the populations have been created, we employ every screening policy experiment on them and average the output to summarize the effort needed to employ the screening policy and the corresponding five-year survival.

Screening Policy Implementation Simulation Steps:

Step 1 Set the screening start age, screening end age, screening interval, and screening modality to test a certain policy.

Step 2 Looping through each patient in the population, we categorize whether the patient died cancer free or developed cancer.

Step 3 If the patient died cancer free:

- If age of death is after the screening start age and after the screening end age, the patient receives all benign screenings and the number of false positive outcomes (of the benign screenings) is randomly generated based on the specificity of the screening modality.
- If age of death is after the screening start age but before the screening end age, the patient receives benign screenings until his death and number of false positive outcomes (of the benign screenings) is randomly generated.
- If age of death is before the screening start age, the patient receives no screenings.

Step 4 If the patient developed cancer:

- If the patient's age when the cancer is detectable after the screening start age and the screening end age, the patient receives benign screening during the screening period, number of false positive results is generated, and the cancer is symptomatically detected.

- If the patient's age when the cancer is detectable after the screening start age but before the screening end age, the patient receives benign screening from the screening start age until their cancer age. The next screening after the patient's cancer is determined as follows:
    1. if symptomatic detection occurs before the next screening, then the cancer is symptomatically detected.
    2. if symptomatic detection occurs after the next screening, then the number of screenings until symptomatic detection or the screening end age (which ever comes first) is calculated. Looping through the screenings:
        (a) If the modality detects the tumor, the age at detection is recorded and the tumor is deemed to be detected by screening.
        (b) Any false negative result is recorded in the procedure.
        (c) If the patient underwent the screenings and the tumor was not detected, then symptomatic detection occurs.
    3. if the tumor start age is after the last screening in the policy, then symptomatic detection occurs.
- If the patient's age when the cancer is detectable before the screening start age:
    1. If the patient's symptomatic detection age is also before the screening start age, then the cancer is symptomatically detected and the patient does not receive any screening during the screening period.
    2. Otherwise, the next screening is at the screening start age. The number of screenings until symptomatic detection or the screening end age (the minimum of both) is calculated. Looping through the screenings:
        (a) If the modality detects the tumor, the age at detection is recorded and the tumor is deemed to be detected by screening.
        (b) Any false negative result is recorded in the procedure.
        (c) If the patient underwent the screenings and the tumor is not detected, then symptomatic detection occurs.

Step 5 Calculate the screening Effort using Equation 4.2 and the five-year survival rate of the policy using Equation 4.1.

The simulation steps are used to loop through different screening experiments, where the effort and five-year survivals are recorded to compare the experiments.

4.3.3 Experiment Design

A homogeneous population was set with predetermined race, gender, and relative risk. We restrict the race to White or Black, and we alter the relative risk between 5, 7, 10, 15, or 32. A heterogeneous population composed of individuals with different risks, race and gender according to the prevalence and demographic of the US population was created. As for the screening policies, each has a defined screening start age, screening end age, screening interval, and screening modality. We set:

- the screening start age at 40, 45, 50, 55, or 60 years old,
- the screening end age at 70, 75, 80, 85, or 90 years old,
- the screening interval at 1, 2, 3, 4, 5, or 10 years, and
- the screening modality at MRI or EUS.

The CAPS guidelines suggested that a screening start age should be set at 50 years old [CMHFHR13], and hence the experiment design in Chapter 3. However, given the difference in incidence age distribution by race and gender, we expect that homogeneous groups will respond differently to the varying screening start ages. In Chapter 3, we set the screening end age at 100 years old. In this Chapter, we test the effect of different screening end ages. The question of when to stop screening is tied to the resectability of the tumor upon detection. Some guidelines deem patients of age ≥ 70 years old to have unresectable pancreatic cancer due to post surgical complications that could lead to mortality [Tam14]. However, Judge Ginsburg underwent successful resection at age 75 years old and the SEER data includes many patients of age ≥ 70 years old that underwent resection. Therefore, with our resectability prediction tools, we allow the screening end age to be as high as 90 years old and we test the difference in effort versus five-year survival rates accordingly. For the set of homogeneous populations, we evaluate 6,000 different experiments because of the resulting number of homogeneous populations. On the other hand, the heterogeneous populations 300 experiments are evaluated.

4.4 Results

We created ten homogeneous populations for each race, gender, and relative risk of size 100,000 each and ten heterogeneous populations of size 1,000,000 each. The screening policies were applied to all populations and the average outcome was recorded. We focus on the relationship between the average five-year survival and the effort exerted by a certain policy on a certain population. Given a screening modality, there are 150 unique screening policies tested on a population where the screening start age, the screening end age, and the screening interval differ. Therefore, every screening policy has an average five-year survival probability and effort pair for every population.

First, we eliminate the inefficient policies. An inefficient policy is one that has a lower five-year survival and a higher effort than another policy.

4.4.1 Screening Policy Evaluation for Homogeneous Populations

Each of the homogeneous populations generated contained a different number of cancer patients due to the differences in incidence rates by race and gender. The average number of cancer patients in each cohort of the homogeneous populations is summarized in Table 4.6.

Table 4.6 The Average Number of Cancer Patients per 100,000 in the Homogeneous Populations Created

Relative Risk	White Male	White Female	Black Male	Black Female
5	10,014	5,240	8,041	7,780
7	14,027	7,321	11,300	10,875
10	20,041	10,534	16,138	15,599
15	29,943	15,641	24,160	23,280
32	62,910	33,507	51,263	49,329

We first analyze the result of the screening policies applied on the homogeneous populations. Figure 4.2 shows the effort and five-year survival pairs for each race and gender cohort with different relative risks using MRI as the screening modality (the Figures where EUS is the screening modality are in Appendix B). Each point on the graph corresponds to a screening policy with a set screening start age, screening end age, and screening interval. The effort decreases as the relative risk of the patients increases since there are more cancer patients in the higher risk population. We set the scale of the Effort axis for each of the charts separately as opposed to maintaining the same scale to properly show the trend within a chart. If we were to set the same scale to view the effect of the relative risk on effort, then the charts with the higher relative risks will appear as a horizontal line instead of a scatter. The five-year survival of females is lower than the five-year survival of males due to the older age distribution of females which negatively impacts the resectability at detection. Moreover, Black males are the youngest pancreatic cancer cohort and have the highest achievable five-year survival rates. The resectability prediction tool takes the age of the patient as an input, and the higher the age, the lower the probability of resectability. Therefore, we expect the younger patients to have a higher average five-year survival.

As it is apparent in the charts in Figure 4.2, most policies are relatively inefficient. Therefore, we filter the policies by removing the policies that have a lower five-year survival and a higher effort than another policy. Summaries of the efficient policies are in Tables 4.7, 4.8, 4.9, 4.10, and 4.11. Figure 4.3 is a scatter plot of the five-year survival versus Effort efficient frontiers by race, gender, and relative risk. The scale in Figure 4.3 was unified to portray the different outcomes of policies on

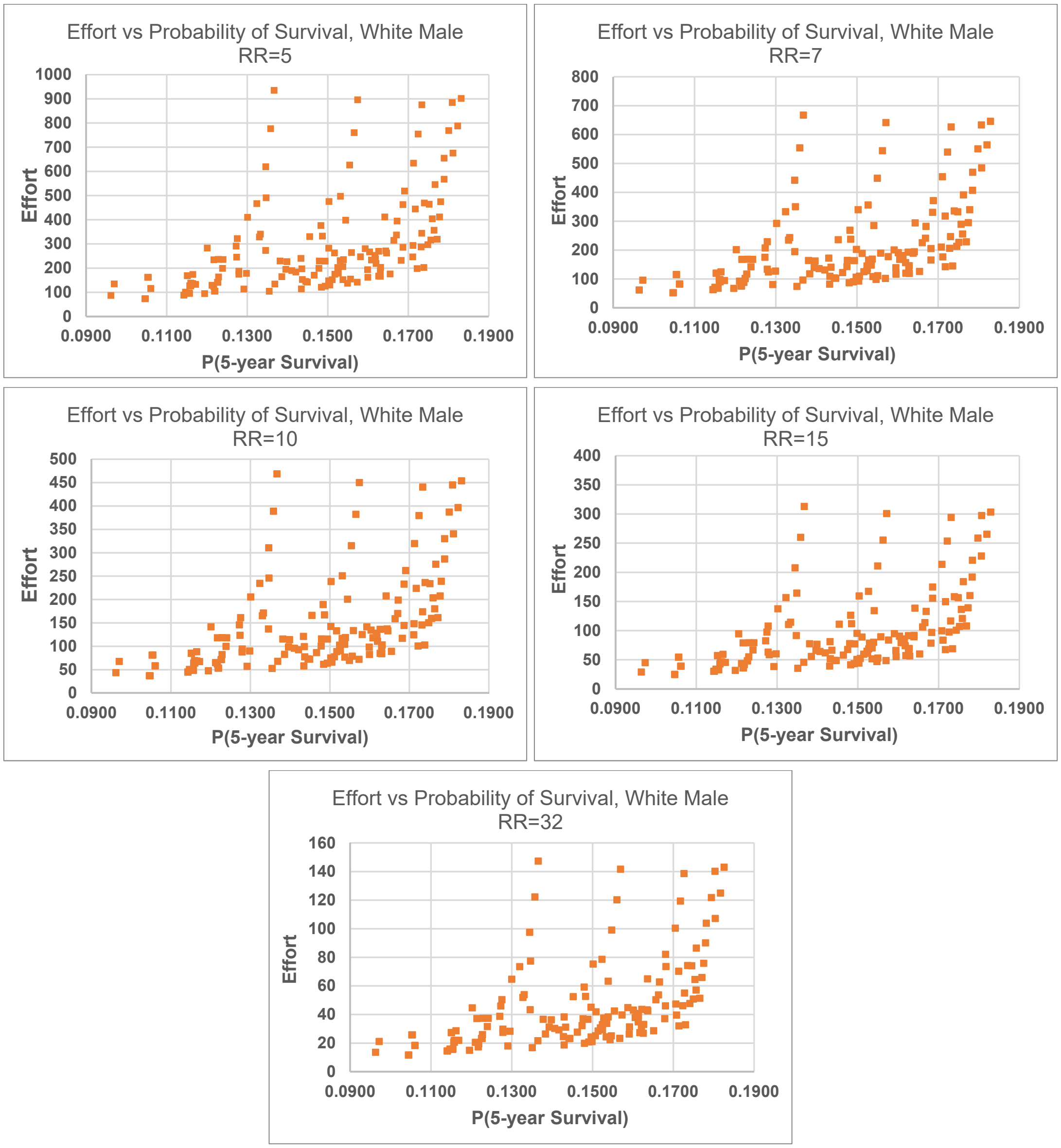

(a) White Male

Figure 4.2 Effort against five-year survival of the different screening policies on homogeneous populations using MRI

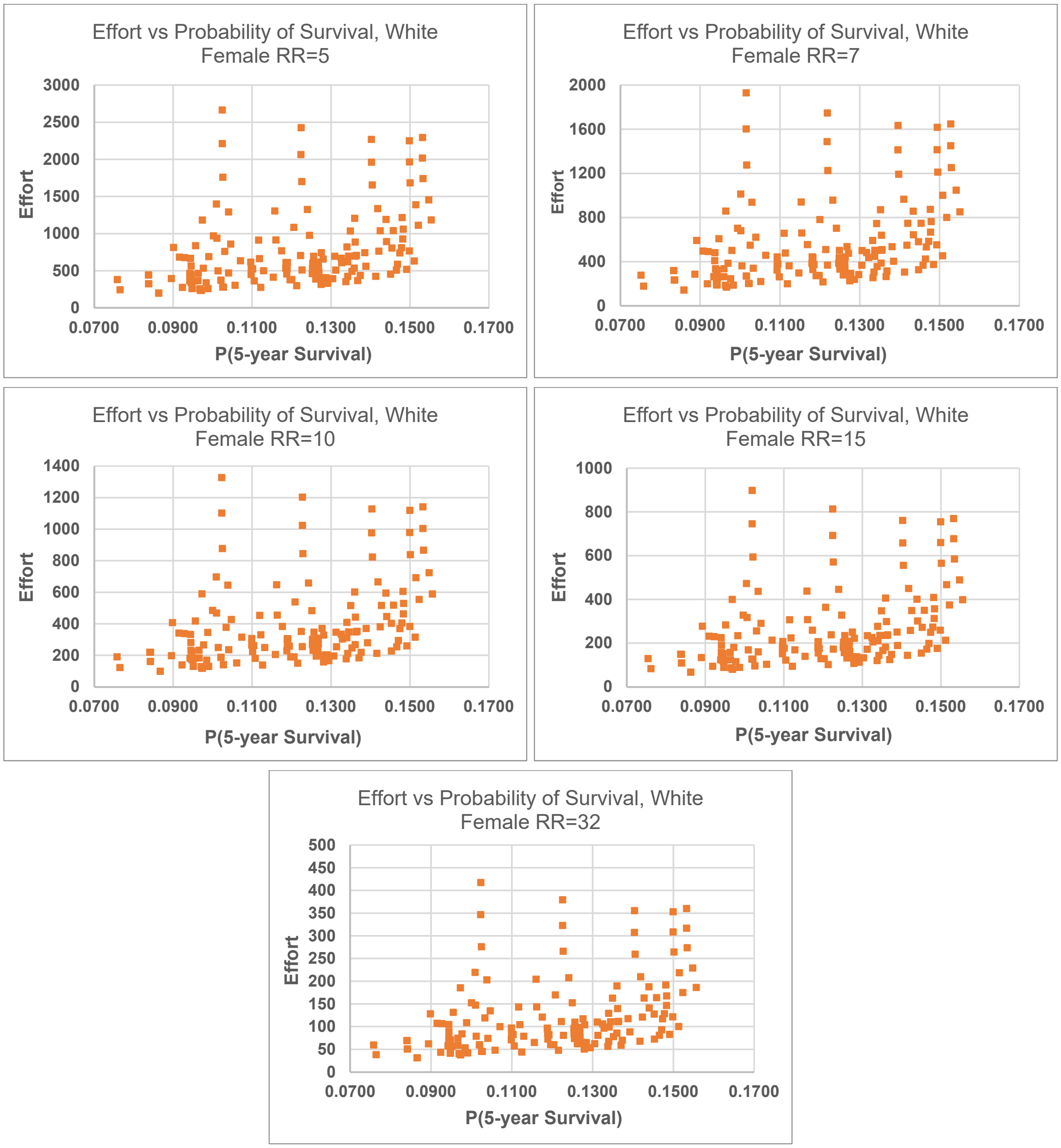

(b) White Female

Figure 4.2 (continued) Effort against five-year survival of the different screening policies on homogeneous populations using MRI

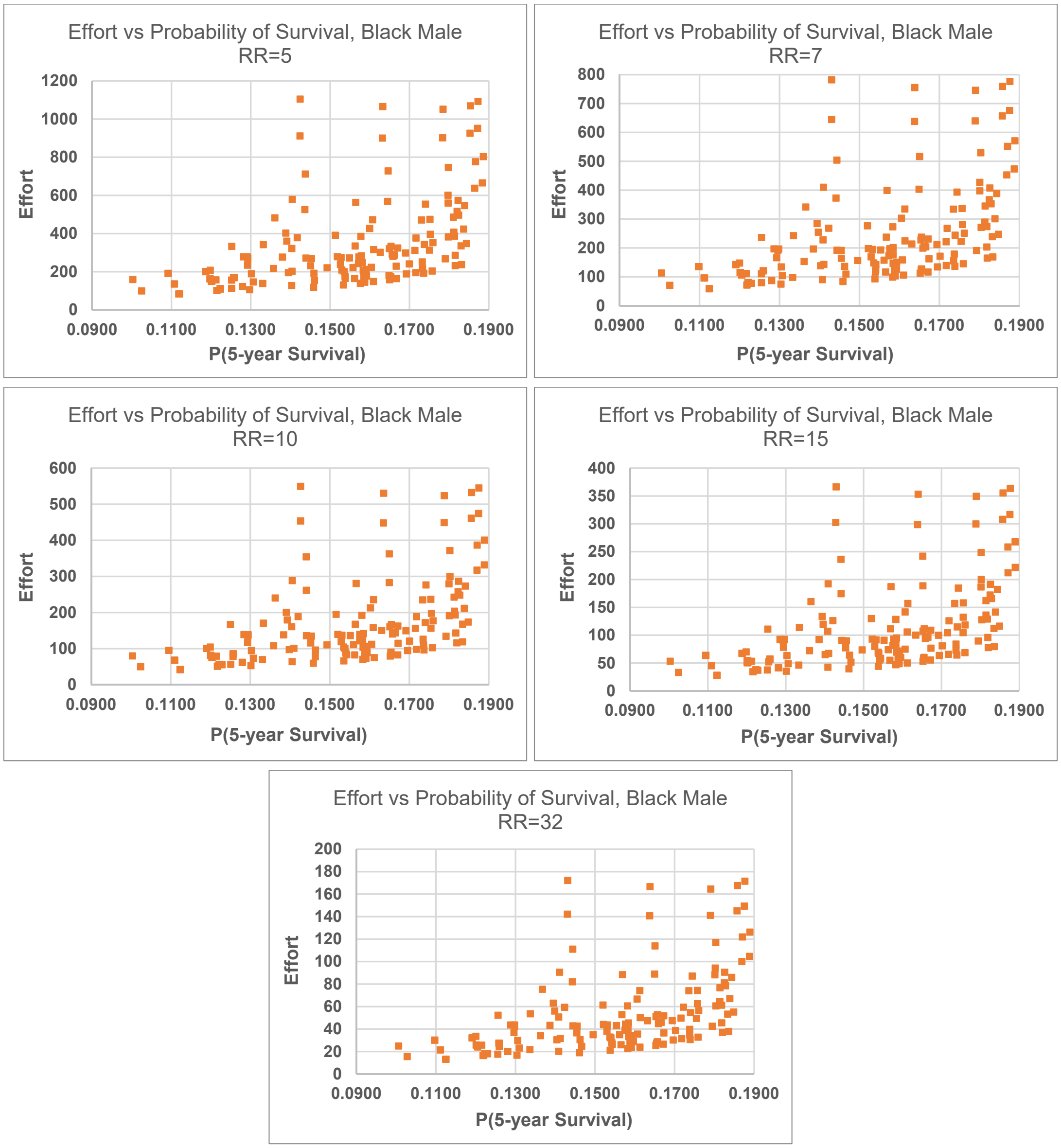

(c) Black Male

Figure 4.2 (continued) Effort against five-year survival of the different screening policies on homogeneous populations using MRI

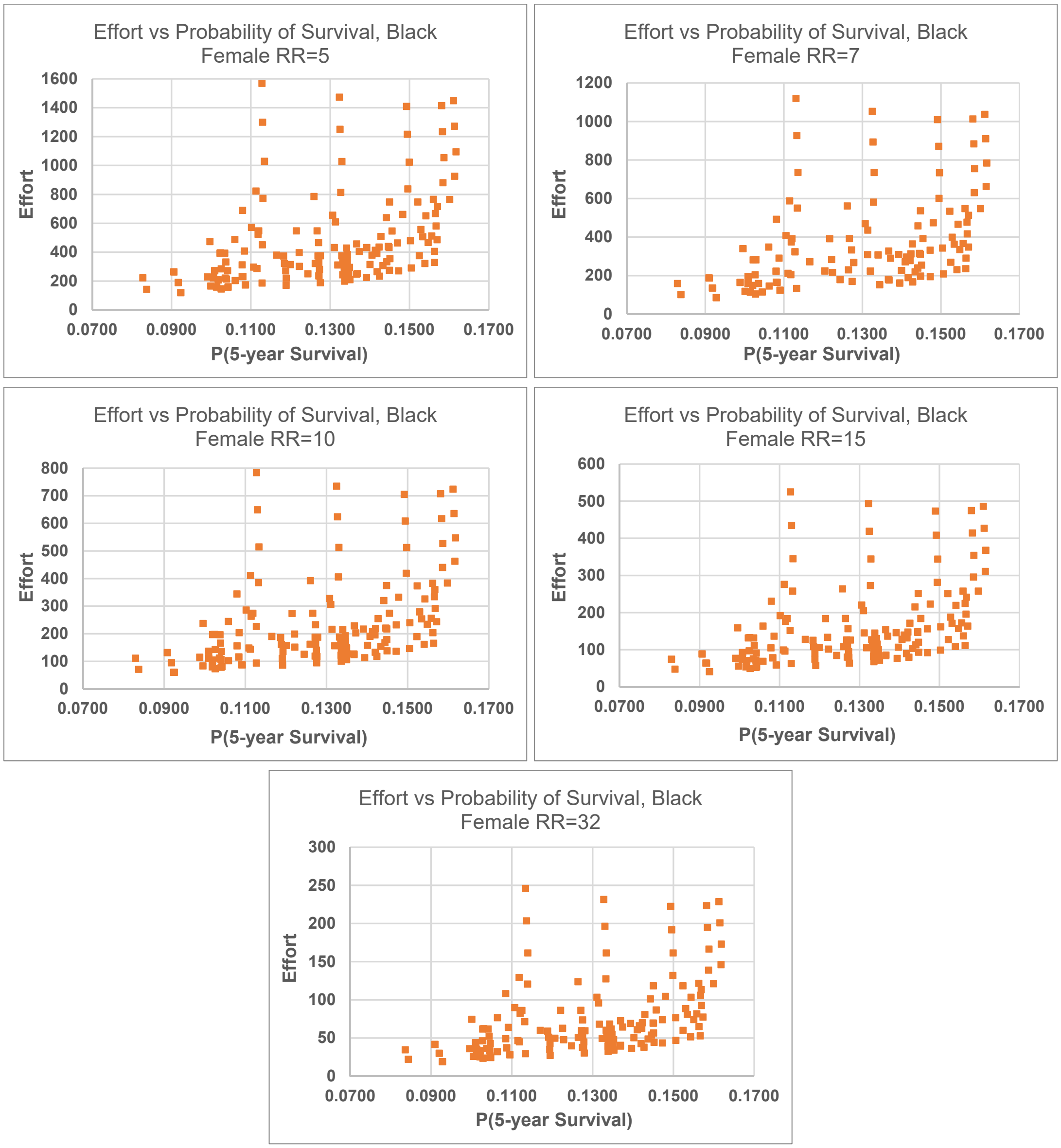

(d) Black Female

Figure 4.2 (continued) Effort against five-year survival of the different screening policies on homogeneous populations using MRI

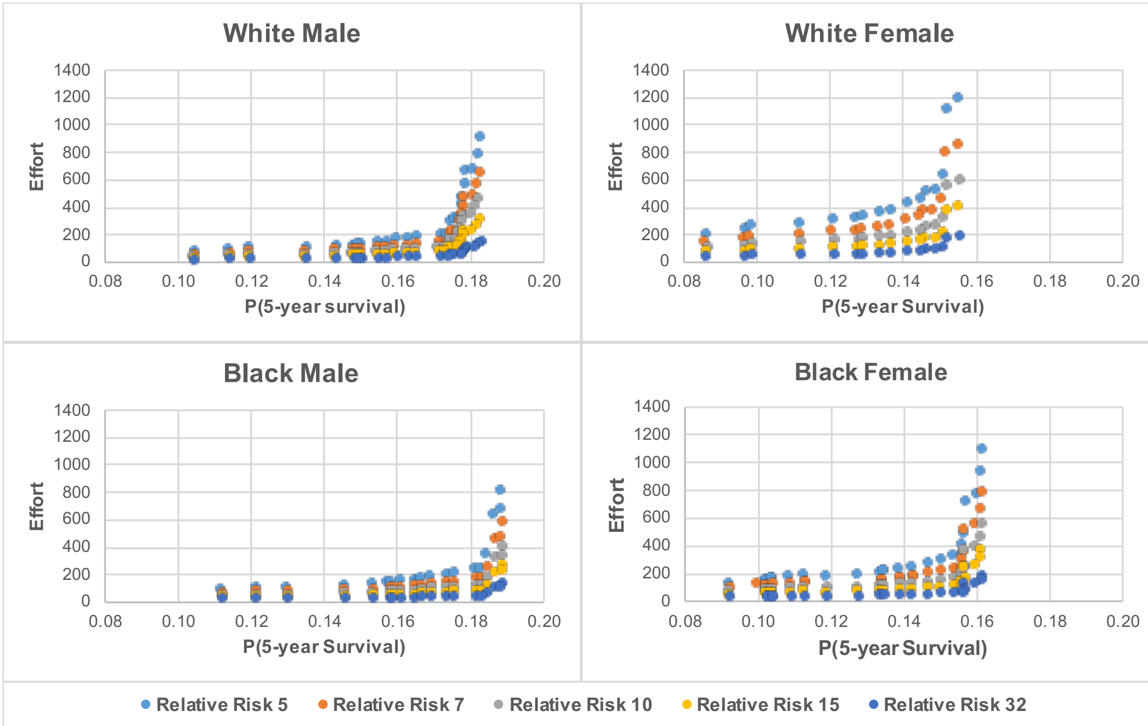

Figure 4.3 Efficient Frontiers by Race, Gender, and Relative Risk

race and gender. The Effort was higher for the lower risk cohorts since the number of cancer patients is lower. The scatter points in Figure 4.3 with equal five-year survivals correspond to the same policy. The elimination of inefficient policies was based on the average five-year survivals and the effort. We note that the 95% confidence interval for the probability of five-year survival is approximately ±0.001 across the different populations and policies. Each table includes the screening policy, the range of five-year survival rates across the different relative risks using different screening modalities, and the effort to screen for every relative risk.

We notice that the efficient policies for White Males include the most aggressive screening policy of yearly screenings with a screening starting age of 40 years old and a screening end age of 90 years old. On the other hand, that policy was not found to be an efficient policy for the other cohorts. We believe that this aggressive policy could have been considered efficient if we had used the confidence interval surrounding the average of the probability of five-year survival when defining the efficient policies. However, since we define efficient policies using the mean five-year survival probabilities only, we do not claim that two policies are statistically different if one was labeled efficient and the other was not if their survival probabilities were within each other's 95% confidence intervals.

White females are an older cohort in the pancreatic cancer population than males. As a result, the efficient screening policies summarized in Table 4.8 have a screening start age that is mostly 60

Table 4.7 Efficient Screening Policies for White Male using MRI or EUS

Screening Interval	Screening Start Age	Screening End Age	Five-year Survival, %		Effort under different Relative Risks				
			MRI	EUS	5	7	10	15	32
Yearly	40	90	18.29-18.36	18.25-18.35	903	647	454	303	143
	45	90	18.17-18.27	18.16-18.26	789	565	397	265	125
	50	85	17.82-17.92	17.81-17.90	655	470	330	221	104
	50	90	18.04-18.14	18.03-18.13	676	485	340	228	107
	55	90	17.80-17.90	17.79-17.89	568	407	287	192	90
Two Years	40	90	17.75-17.85	17.72-17.82	475	340	239	160	76
	45	90	17.71-17.80	17.68-17.77	412	295	208	139	66
	55	90	17.38-17.50	17.38-17.50	297	213	150	101	48
Three Years	40	85	17.50-17.58	17.43-17.53	317	227	160	107	51
	40	90	17.66-17.77	17.62-17.71	320	229	161	108	51
	55	85	17.14-17.24	17.09-17.18	199	143	100	67	32
	55	90	17.30-17.41	17.26-17.36	203	145	103	69	33
	60	85	16.26-16.34	16.21-16.29	167	119	84	56	27
	60	90	16.51-16.58	16.46-16.53	176	126	89	60	29
Four Years	55	85	15.91-16.03	15.86-15.96	162	117	82	55	26
	60	80	14.99-15.07	14.93-15.01	130	93	66	44	21
	60	85	15.43-15.52	15.37-15.45	137	99	70	47	22
	60	90	15.68-15.74	15.61-15.68	142	102	72	48	23
Five Years	60	70	11.94-12.03	11.90-11.98	95	68	47	32	15
	60	75	13.51-13.57	13.45-13.50	104	75	53	35	17
	60	80	14.30-14.35	14.23-14.30	115	82	58	39	19
	60	85	14.82-14.87	14.75-14.81	121	87	61	41	20
	60	90	14.91-14.98	14.82-14.91	126	90	64	43	21
Ten Years	60	70	10.45-10.51	10.40-10.47	74	53	37	25	12
	60	80	11.40-11.48	11.37-11.43	89	63	45	30	14

Table 4.8 Efficient Screening Policies for White Female using MRI or EUS

Screening Interval	Screening Start Age	Screening End Age	Five-year Survival, %		Effort under different Relative Risks				
			MRI	EUS	5	7	10	15	32
Yearly	60	85	15.18-15.23	15.16-15.25	1114	801	554	374	175
	60	90	15.51-15.57	15.51-15.56	1185	852	589	398	186
Two Years	60	90	15.08-15.13	15.05-15.13	632	454	314	213	100
Three Years	55	85	14.59-14.66	14.56-14.63	510	368	254	172	81
	55	90	14.85-14.92	14.81-14.89	520	376	259	176	83
	60	85	14.12-14.17	14.08-14.12	427	307	212	144	68
	60	90	14.47-14.53	14.43-14.48	455	327	227	154	72
Four Years	60	85	13.33-13.39	13.28-13.33	355	256	177	120	57
	60	90	13.66-13.71	13.60-13.65	369	265	184	125	59
Five Years	60	75	11.19-11.27	11.14-11.21	278	200	138	93	44
	60	80	12.08-12.16	12.02-12.09	301	217	150	102	48
	60	85	12.75-12.81	12.68-12.76	317	227	157	107	51
	60	90	12.87-12.95	12.83-12.88	332	239	165	112	53
Ten Years	60	70	8.60-8.66	8.57-8.64	200	144	99	67	31
	60	80	9.66-9.73	9.63-9.69	236	171	118	80	38
	60	90	9.83-9.91	9.79-9.87	259	188	129	88	42

years old with 55 years old being the earliest screening. All screening policies that have a screening start age of 40, 45, or 50 years old were found to be inefficient for White females. A similar result was found in Black male and Black female cohorts where all policies with a screening start age of 40 or 45 years old were found to be inefficient. This result could also be due to the use of the average five-year survival rather than the 95% confidence interval.

Moreover, the efficient policies for White Male, White Female, and Black Male were consistent across the different relative risks and both screening modalities. On the other hand, that was not the case for Black females. For example, Table 4.10 shows that the screening policy starting at age 60 and ending at age 90 years old with a two-year screening interval is only considered to be efficient for patients with a relative risk of 5 or 7. Some of the differences could be due to simulation and the generation of the random variables pertaining to screening at the different steps. For example, the number of false negative screenings that would require a cancer patient to go through screening again may be a factor.

We further analyze the set of efficient policies for each cohort by assuming a maximum allowable effort of 200 and choosing the policy with the maximum survival rate. From Figure 4.3, we note that the corresponding policies will not be equivalent across the cohorts. Table 4.12 summarizes the efficient policies for each race, gender, and relative risk cohort that requires a maximum effort of 200 and maximizes the five-year survival rate. The policies in the table are expressed as the screening

Table 4.9 Efficient Screening Policies for Black Male using MRI or EUS

Screening Interval	Screening Start Age	Screening End Age	Five-year Survival, %		Effort under different Relative Risks				
			MRI	EUS	5	7	10	15	32
Yearly	50	90	18.86-18.89	18.85-18.88	803	571	400	268	126
	55	85	18.65-18.71	18.63-18.70	638	453	317	212	100
	55	90	18.84-18.89	18.83-18.88	666	474	332	222	105
Two Years	55	90	18.44-18.49	18.40-18.46	348	247	174	116	55
Three Years	55	85	18.15-18.21	18.09-18.15	232	165	116	78	37
	55	90	18.32-18.36	18.25-18.30	237	169	119	79	38
	60	85	17.36-17.40	17.29-17.34	192	137	96	64	31
	60	90	17.57-17.60	17.52-17.55	204	145	102	69	33
Four Years	55	85	16.92-16.97	16.83-16.90	189	13	94	63	30
	60	80	16.09-16.13	16.03-16.06	149	106	75	50	24
	60	85	16.50-16.53	16.42-16.46	158	113	79	53	25
	60	90	16.68-16.72	16.61-16.65	165	117	82	55	27
Five Years	60	70	12.97-13.04	12.95-12.22	106	75	53	35	17
	60	75	14.58-14.62	14.52-14.56	118	84	59	40	19
	60	80	15.34-15.39	15.27-15.31	131	93	66	44	21
	60	85	15.76-15.83	15.75-15.76	140	99	70	47	23
	60	90	15.87-15.91	15.79-15.83	145	104	73	49	24
Ten Years	60	70	11.21-11.25	11.16-11.21	84	59	42	28	13
	60	80	12.15-12.19	12.10-12.13	102	72	51	34	16

interval, screening start age, and screening end age, respectively. There are more invasive policies for males than females as well as for higher relative risk than lower relative risk, where the higher number of cancer patients reduces the effort required for a certain screening policy. The most invasive resulted policy was for White Males with a relative risk of 32, and the least invasive resulted policy was for White Females with a relative risk of 5. We switch the analysis and search for the screening policies that achieve a five-year survival rate of 15%. Table 4.19 summarizes the efficient policies that would need to be employed to achieve approximately a 15% five-year survival rate. White Females require the most aggressive screening (i.e., screening every two to three years), while Black Males require the least aggressive screening (i.e., screening every five years).

We examine the set of screening policies that were found to be efficient for all homogeneous cohorts by looking at the distribution of cancer stage at detection under each of the common policies. The percentage of patients that would be detected at each stage, either symptomatically or by screening, are summarized in Table 4.14. We consider the screening policies that have a screening start age of 60 years old and a screening end age of 85 and 90 years old with the screening intervals of three years, four years, and five years. For a certain screening interval, we compare the percentage of

Table 4.10 Efficient Screening Policies for Black Females by Relative Risk using MRI

Screening Interval	Screening Start Age	Screening End Age	Relative Risk	Five-year Survival, %	Effort under different Relative Risks				
					5	7	10	15	32
Yearly	50	90	All	16.16-16.19	1096	785	548	368	173
	55	90	All	16.14-16.18	927	663	463	311	146
	60	85	5, 10, 15	15.67-15.71	717	514	359	241	113
	60	90	5, 7, 32	16.01	765	548	384	257	121
Two Years	55	90	All	15.69-15.74	486	349	243	164	77
	60	90	5, 7	15.64	406	291	204	137	65
Three Years	55	85	All	15.39-15.43	322	231	161	108	51
	55	90	All	15.63-15.67	330	236	165	111	53
	60	85	All	14.70-14.73	271	195	136	92	43
	60	90	All	15.03-15.07	291	209	146	99	47
Four Years	60	75	7	11.33	187	133	94	63	29
	60	80	7, 32	13.44	212	152	107	72	34
	60	85	All	13.91-13.96	226	161	113	76	36
	60	90	All	14.24-14.28	235	168	118	79	38
Five Years	60	70	5, 10, 15, 32	10.41-10.48	156	118	78	52	24
	60	75	All	11.33-11.95	172	133	86	58	27
	60	80	All	12.75- 13.44	189	152	95	64	30
	60	85	All	13.36-13.95	199	161	100	68	32
	60	90	All	13.50-14.28	210	168	106	71	34
Ten Years	55	85	7	10.91	174	124	87	59	28
	60	70	All	9.24-9.29	121	86	60	40	19
	60	80	All	10.26-10.29	146	104	73	49	24
	60	90	5, 7, 10, 15	10.43-10.45	161	115	81	55	26

Table 4.11 Efficient Screening Policies for Black Females by Relative Risk using EUS

Screening Interval	Screening Start Age	Screening End Age	Relative Risk	Five-year Survival, %	Effort under different Relative Risks				
					5	7	10	15	32
Yearly	50	90	All	16.15-16.18	1096	786	548	368	173
	55	90	All	16.13-16.17	927	664	463	311	146
	60	85	5, 7	15.70	717	514	360	241	113
	60	90	All	15.96-16.00	766	549	384	258	121
Two Years	55	90	All	15.67-15.71	487	349	244	164	77
	60	90	5, 7	15.60	407	291	204	137	65
Three Years	55	85	All	15.35-15.38	323	232	162	109	52
	55	90	All	15.57-15.61	331	237	166	112	53
	60	85	All	14.64-14.69	272	195	137	92	44
	60	90	All	14.97-15.01	293	209	147	99	47
Four Years	60	80	32	13.39	214	153	107	72	34
	60	85	All	13.88-13.91	226	162	114	77	36
	60	90	All	14.18-14.21	236	169	118	80	38
Five Years	60	70	All	10.37-10.44	157	112	78	52	25
	60	75	All	11.85-11.90	172	123	86	58	27
	60	80	All	12.67-12.74	189	136	95	64	30
	60	85	All	13.30-13.33	201	144	101	68	32
	60	90	All	13.441-13.47	211	151	106	72	34
Ten Years	60	70	All	9.20-9.26	121	86	60	40	19
	60	80	All	10.21-10.25	147	105	74	50	24
	60	90	10, 15	10.38-10.39	162	116	81	55	27

Table 4.12 Efficient Policies labeled with the Screening Interval, Screening Start Age, and Screening End Age with a Maximum Effort of 200 and the Corresponding Five-year Survival Rate for each Cohort

		Relative Risk				
		5	**7**	**10**	**15**	**32**
White Male	Policy	3, 55, 85	3, 55, 90	3, 40, 90	1, 55, 90	1, 40, 90
	Five-year Survival	17.22%	17.36%	17.66%	17.83%	18.36%
White Female	Policy	10, 60, 70	5, 60, 75	4, 60, 90	3, 55, 90	1, 60, 90
	Five-year Survival	8.64%	11.19%	13.71%	14.91%	15.57%
Black Male	Policy	3, 60, 85	3, 55, 90	2, 55, 90	2, 55, 90	1, 50, 90
	Five-year Survival	17.36%	18.34%	18.48%	18.49%	18.89%
Black Female	Policy	5, 60, 85	3, 60, 85	3, 55, 90	2, 55, 90	1, 50, 90
	Five-year Survival	13.36%	14.73%	15.64%	15.71%	16.19%

Table 4.13 Efficient Policies that Achieve 15% Five-year Survival

	Screening Interval	Screening Start Age	Screening End Age	Average 15% Survival Rate
White Male	4	60	80	15.04
	5	60	90	14.93
White Female	2	60	90	15.11
	3	55	90	14.90
Black Male	5	60	75	14.60
	5	60	80	15.37
Black Female	3	60	90	15.04

patients that would be detected at local using screening. For the screening policies with a three-year screening interval, the difference is about 10% for males and 15% for females across both races when the screening end age is changed from 85 years old to 90 years old. With a four-year or a five-year screening interval, the differences in the percentage of patients detected at local using screening are 7%, 7-8%, 10%, and 11% for Black male, White male, Black female, and White female, respectively. If we focus on the screening policies that have a screening start age of 60 and a screening end age of 90, the difference in the percentage of patients detected at local via screening when the screening interval changes from three years to four years is around 7% for White males, Black males, and Black females, while it is around 9% for White females. When the screening interval increases from four years to five years, the difference in the percentage of patients that are detected at local by screening drops by 3% for males and 1.5% for females.

Examining the proportions of cancer patients that would be detected at local stage via screening can be considered as a part of the reward to screen. The literature describes a resectable pancreatic cancer as one that is confined to the pancreas, and SEER defines local stage as a tumor that is confined to the pancreas. Therefore, it could be interpreted that local stage means resectable disease. However, as we have seen in the SEER data, not all patients with local tumors were recommended for surgery, hence our resectability prediction tools. With potential advances in pancreatic cancer treatments, the value of detecting more patients in the local stage should increase improving the five-year survival rates.

4.4.2 Screening Policy Evaluation for Heterogeneous Populations

As we evaluate the same set of screening policies on the heterogeneous population, we also report the average cancer statistics of the population. Table 4.15 summarizes the average number of cancer free patients, cancer patients, and cancer patients that are younger than a certain age in a heterogeneous population of one million. The cancer patients counts reported are consistent with the screening start and end ages of the different screening policies to highlight the number of patients that would

Table 4.14 Distribution of cancer detection by stage and mechanism (%) in each cohort under common screening strategies with certain screening interval, start age (second row) and end age (third row)

			Screening Policy									
			Three Years				Four Years		Five Years			
			55	55	60	60	60	60	60	60	60	60
			85	90	85	90	85	90	75	80	85	90
White Male	Sympt.	Local	3.54	2.52	4.41	2.61	4.93	3.65	9.36	7.20	5.20	3.96
		Regional	2.69	1.87	3.45	1.94	3.86	2.74	7.28	5.61	3.95	2.9
		Distant	13.86	9.87	18.40	10.82	20.21	14.71	39.20	29.04	20.80	15.34
	Screen	Local	78.46	84.12	72.39	83.01	68.71	76.24	42.21	55.33	66.43	73.58
		Regional	0.85	0.97	0.87	1.02	1.38	1.61	1.13	1.62	2.06	2.41
		Distant	0.60	0.66	0.49	0.61	0.91	1.04	0.81	1.20	1.55	1.81
White Female	Sympt.	Local	4.46	3.11	5.19	2.51	5.75	3.98	10.59	8.38	5.95	4.17
		Regional	3.53	2.41	4.09	1.91	4.48	2.97	8.46	6.56	4.54	2.97
		Distant	17.70	11.81	20.73	9.32	22.36	14.57	44.70	33.10	22.44	14.04
	Screen	Local	72.89	81.04	68.77	84.61	65.09	75.69	34.61	49.38	63.47	74.33
		Regional	0.87	0.99	0.76	1.00	1.37	1.65	0.94	1.49	2.07	2.58
		Distant	0.55	0.65	0.46	0.66	0.95	1.14	0.71	1.10	1.52	1.91
Black Male	Sympt.	Local	2.91	2.09	3.87	2.31	4.44	3.33	8.60	6.47	4.82	3.76
		Regional	2.23	1.54	2.98	1.70	3.35	2.46	6.79	4.99	3.55	2.66
		Distant	11.39	7.77	15.92	9.17	17.63	12.77	35.69	26.08	18.50	13.58
	Screen	Local	82.03	87.08	75.96	85.31	72.33	78.84	46.86	59.62	69.58	75.97
		Regional	0.86	0.91	0.79	0.92	1.34	1.53	1.17	1.62	2.02	2.3
		Distant	0.58	0.61	0.48	0.60	0.91	1.06	0.89	1.21	1.52	1.73
Black Female	Sympt.	Local	4.46	3.15	5.30	2.79	5.92	4.19	10.80	8.43	6.18	4.42
		Regional	3.47	2.43	4.19	2.11	4.57	3.15	8.60	6.61	4.67	3.19
		Distant	16.98	11.46	20.71	10.30	22.28	15.01	42.60	32.21	22.41	14.68
	Screen	Local	73.80	81.49	68.63	83.28	65.12	75.10	36.39	50.32	63.41	73.62
		Regional	0.81	0.92	0.74	0.96	1.26	1.53	0.95	1.41	1.93	2.36
		Distant	0.48	0.55	0.42	0.56	0.86	1.02	0.67	1.03	1.39	1.72

Table 4.15 Average Counts of Cancer Free and Cancer Patients at Different Ages in the Sets of Heterogeneous Populations by Race and Gender

	White Male	**White Female**	**Black Male**	**Black Female**
Average Cancer Free	400606	410265	70500	70284
Average Cancer	18179	22072	2788	5306
Cancer Patients Age < 40	4411	12716	774	2219
Cancer Patients Age $\in [40,45)$	177	0	6	9
Cancer Patients Age $\in [45,50)$	333	4	37	32
Cancer Patients Age $\in [50,55)$	592	120	100	85
Cancer Patients Age $\in [55,60)$	966	359	166	152
Cancer Patients Age $\in [60,65)$	1386	699	237	243
Cancer Patients Age $\in [65,70)$	1793	1064	284	349
Cancer Patients Age $\in [70,75)$	2116	1414	328	459
Cancer Patients Age $\in [75,80)$	2234	1652	316	523
Cancer Patients Age $\in [80,85)$	1993	1681	275	513
Cancer Patients Age $\in [85,90)$	1379	1344	173	405
Cancer Patients Age ≥ 90	800	1020	93	319

be covered or missed by screening.

We conducted five different experiments, where we performed the screening experiments on the entire population or on the set of patients with a relative risk that is greater than or equal to 3, 5, 7, or 10. Figure 4.4 shows the results of these experiments where the effort and the five-year survival values are for the whole population and not just the patients being screened using MRI as the screening modality, and the same figure with EUS as the screening modality is in Appendix B. Table 4.16 summarizes the size and the average number of patients in each cohort. From Table 4.16, we can deduce that there are 12,172 cancer patients out of 864,561 individuals with a relative risk less than three, which is 1.4% and is equivalent to the general lifetime risk that is reported by SEER. Even though a screening policy for high-risk patients would only miss some pancreatic cancer patients, a population wide screening policy would relatively be highly inefficient. From the experiment runs and as reported in Figure 4.4, the effort of screening is highest in the population wide screening as to be expected where it can reach a value of 4000 as opposed to 350 for patients with a relative risk of 5 or higher. We also notice that the effort to screen is similar when screening patients with a relative risk of 5 or higher, but the corresponding five-year survival rate of the population does not reach 11% due to the lower risk cancer patients that are not receiving screening. Therefore, an argument can be made that increasing the population's five-year survival to 17% may be worth the screening effort.

The current structure of relative risk sampling in the heterogeneous population simulation does not allow for a wide range of values for relative risks as shown in Table 4.16. We consider smoking,

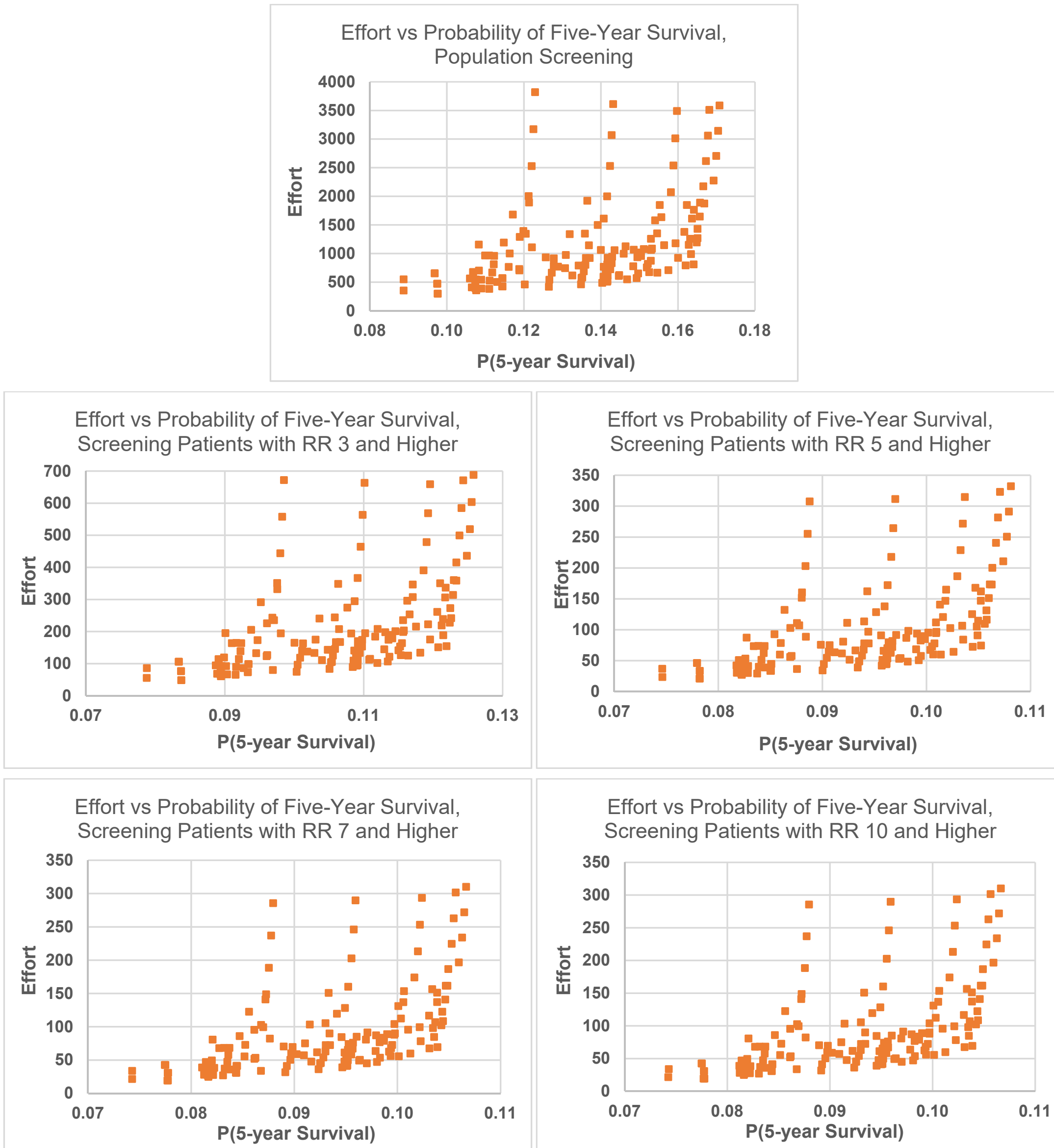

Figure 4.4 Effort against five-year survival of the different screening policies on a heterogeneous population using MRI

Table 4.16 Average Number of Cancer Patients per 1,000,000 in a Heterogeneous Population

	Size of Subpopulation	**Cancer Patients**
All Population	1,000,000	28,342
With $RR \geq 3$	135,439	16,170
With $RR \geq 5$	54,602	11,467
With $RR \geq 7$	50,147	11,091
With $RR \geq 10$	50,137	11,080

diabetes, obesity, chronic pancreatitis, and hereditary factors only, and the resulting patient profiles are derived from the estimates of the prevalence of these conditions within the population. For example, chronic pancreatitis and Lynch syndrome have relative risks that are higher than other risk factors, but only chronic pancreatitis has sufficient information about its prevalence available to be included here. We acknowledge this limitation due to the information provided in the literature about the known causes of pancreatic cancer as well as the prevalence of each of the risk factors. We were able to study the effect of screening on a heterogeneous population with respect to age, race, gender, and some risk factors that are known to cause pancreatic cancer.

We conduct the same analysis as before where we introduce a 200 maximum effort allowed for screening, and we summarize the corresponding efficient screening policies in Table 4.18. We note that a population wide screening cannot be performed with a screening effort of less than 200, and the highest achievable corresponding five-year survival is 12% when screening patients with a relative risk ≥ 3. We also consider screening policies with a certain minimum five-year survival rate; however, we cannot achieve 15% when screening subpopulations. Therefore, we consider a minimum five-year survival rate of 10% and report the corresponding policies with the least effort.

4.5 Conclusion

In this chapter, we expanded on the resectability tool and incorporated the concept into our screening evaluation discrete-event simulation model. We compared a large set of experiments with varying screening start age, screening end age, screening interval, and screening modality. The experiments were evaluated by estimating the five-year survival of pancreatic cancer under a certain screening policy against the effort it takes to perform that policy. We identify a screening policy as efficient if there is not another policy with a higher average five-year survival and a lower effort. We identify the efficient policies for each population which eliminated over 100 policies for each cohort.

In testing the different policies on a heterogeneous population, we show that screening policies on the population level would be inefficient. The effort of screening the whole population is very high as compared to screening high-risk patients only. However, screening a high-risk subpopulation

Table 4.17 Efficient Screening Policies for a Heterogeneous Population by Relative Risk using MRI

Screening Interval	Screening Start Age	Screening End Age	Relative Risk	Five-year Survival, %
Yearly	40	90	All	10.67-17.08
	45	90	All	10.65-17.05
	50	90	All	10.65-17.00
	55	85	3 and higher	10.49-12.33
	55	90	All	10.60-16.93
	60	90	All	10.49-16.69
Two Years	45	90	All	10.46-16.57
	55	90	All	10.43-16.49
Three Years	40	90	All	10.44-16.51
	55	85	All	10.31-16.20
	55	90	All	10.39-16.41
	60	85	All	10.02-15.47
	60	90	All	10.13-15.76
Four Years	55	85	All	9.83-14.97
	60	80	All	9.51-14.17
	60	85	All	9.70-14.68
	60	90	All	9.80-14.93
Five Years	60	70	All	8.31-11.10
	60	75	All	8.92-12.65
	60	80	All	9.24- 13.49
	60	85	All	9.46-14.04
	60	90	All	9.50-14.16
Ten Years	55	85	$\geq 5, \geq 10$	8.44-8.51
	55	90	$\geq 3, \geq 7$	8.44-9.33
	60	70	Full population, $\geq 5, \geq 10$	7.78-9.76
	60	75	$\geq 3, \geq 7$	7.78-8.37
	60	80	$\geq 3, \geq 5, \geq 7$	8.17-8.94
	60	85	Full population, $\geq 7, \geq 10$	8.16-10.77

Table 4.18 Efficient Policies with a Maximum Effort of 200 and the Corresponding Five-Year Survival Rate in a Heterogeneous Population Screening

	Screening Interval	Screening Start Age	Screening End Age	Five-Year Survival
All Population	N/A	N/A	N/A	N/A
With $RR \geq 3$	3	55	90	12.2%
With $RR \geq 5$	1	55	85	10.6%
With $RR \geq 7$	1	55	90	10.6%
With $RR \geq 10$	1	55	90	10.6%

Table 4.19 Efficient Policies that Achieve 10% Five-year Survival

	Screening Interval	**Screening Start Age**	**Screening End Age**	**Average 15% Survival Rate**
All Population	10	60	70	9.76
	10	60	80	10.76
With $RR \geq 3$	5	60	75	10.03
	10	55	85	9.33
With $RR \geq 5, \geq 7, \geq 10$	3	60	85	10.06
	3	60	90	10.17
	4	55	85	9.87

would only improve their survival rate but not the whole population's survival as we can infer from the screening experiments. In other words, a yearly screening of high-risk Black females from 50 years old to 90 years old would yield a five-year survival of 16% of high-risk Black females only. When the screened homogeneous population is viewed as part of the heterogeneous population, the heterogeneous population five-year survival would be enhanced but not to 16% since there would be pancreatic cancer patients that were not screened. However, screening high-risk populations is the stepping stone to early detection of pancreatic cancer.

Generally, the five-year survival can improve from the current 8.5% as reported by SEER to a maximum of 19% under some screening policies for high-risk Black males. Although this is a 100% increase in five-year survival, it will remain relatively low even under screening until technology advances and surgeries, such as pancreatectomy and Whipple, yield higher post resection survival rates. Moreover, we show that the screening modality does not affect the five-year survival rates or the effort as it is currently defined. Therefore, it would be safe to screen using MRI and when needed a diagnosis confirmation using EUS can be performed since a suspected mass can be biopsied with FNA (fine-needle aspiration).

However, the specificity of MRI is 89% while the specificity of EUS is 96%, which would result in a higher false positive rate when using MRI to screen rather than EUS. Although EUS is more accurate, it is an invasive procedure that requires the patient to be sedated. Moreover, taking a biopsy from the pancreas using FNA would scar tissue surrounding the target being biopsied. Therefore, there are trade-offs when a policy maker decides on which screening modality to use. We acknowledge that the false positive rates can be incorporated into the calculation of the effort required to screen.

This chapter introduced the evaluation of screening policies using estimates of effort and five-year survival of homogeneous populations and heterogeneous population. The five-year survival was evaluated using a resectability prediction tool. In addition, the concept of productive screening was introduced and used to evaluate the effort associated with a screening policy.

CHAPTER

5 CONCLUSION

This dissertation explored the problem of early diagnosis of pancreatic cancer. The silent disease is often diagnosed after it has metastasized which drastically narrows treatment options. The low 8.5% five-year survival rate makes pancreatic cancer one of the deadliest cancers. Experts call for pancreatic cancer screening as a gateway to enhance survival rates since early detection can lead to higher survival. To identify screening policies for pancreatic cancer, we first built a disease progression model to understand and simulate the timeline of the tumor using SEER data for pancreatic cancer. The SEER database is the largest source of pancreatic cancer data. However, the database mainly consisted of unique patients and hence our inability to construct patient trajectories. Therefore, we used a progression model framework that utilizes patient data at diagnosis. The progression model was parameterized to race, age, and gender using different underlying assumptions regarding the inverse growth rate. Our findings confirmed with the literature that pancreatic cancer is a late symptom disease, where there is a window for screening and detecting the tumor before metastasis. To the best of our knowledge, our progression model is the first to use population level data to model the progression of pancreatic cancer.

We overlaid the progression model with different screening policies by creating sets of homogeneous populations with different relative risks. For the first set of experiments, we set the screening start age at 50 years old, the screening end age at 100 years old, and the screening modality to Endoscopic Ultrasound (EUS). We varied the screening interval to half a year, a year, two years, three years, four years, five years, and ten years. We studied the effect each screening policy has on a homogeneous population with a certain race, gender, and relative risk. We estimated the number of benign screenings (the number of screenings where a cancer-free patient underwent screening) and the ratio of benign screenings to the number of cancers detected by screening. We also examined the frequency at which a cancer free patient undergoing screening receives a false positive result given the specificity of EUS. We found there is merit to personalizing screening policies by relative risk, race, and gender as a screening policy imposes different effort depending on the homogeneous population.

However, we understand that not all tumors that were detected by screening are curable. Therefore, we developed resectability prediction tools that use a patient's age, tumor size, and tumor stage to estimate a probability of resectability. We use the prediction tool to estimate the probability of resectability at detection, either symptomatically or by screening, to accordingly evaluate the probability of five-year survival for that patient. We performed a new set of experiments where we varied the screening start age, screening end age, screening interval, and screening modality. We tested the screening policies on homogeneous and heterogeneous populations. We estimated each population's average five-year survival and the effort required to screen under every screening policy tested. For each population, we identified the set of efficient screening policies where the five-year survival of that policy is greater and its effort is less than that of another policy's.

While there are pancreatic cancer progression models in the literature, our contribution is a model that provides distributions for tumor volume at transition from one state to another in the progression of the tumor. We developed a screening policy evaluation tool that uses the tumor progression model where an extensive search for effective screening policies can be performed. The output of the tool includes the tumor stage at which a patient's cancer is detected, and this informs policy makers about the effectiveness of a screening policy. To avoid overestimation of the effectiveness of a screening policy, our work is the first to introduce a resectability prediction tool. The resectability prediction evaluates a patient's condition upon detection without modeling the patient's treatment path. The resectability prediction was used to estimate the population average five-year survival rate. During our literature search, we did not find cancer screening models that aim to increase the five-year survival rate while minimizing the effort to screen.

Extensions to this dissertation

Performing our analyses, we understand the problem of early detection of pancreatic cancer and its complexity when determining who and when to screen. We created a foundation where the problem can be optimally answered. The simulation models were built using SEER data; a snapshot of patients data rather than longitudinal data. This indicates that there maybe opportunities for improvement given the right type of data. We can estimate the inverse growth rate and be better informed on the distribution it follows. A tumor progression model could incorporate a patient's relative risk as we believe comorbidities can influence the growth behavior of the tumor. A resectability prediction model can evolve to a treatment prediction model and include the possible effects of radiotherapy and surgery. We believe we have just scratched the surface in modeling pancreatic cancer progression, screening, and treatment prediction. There are a few directions that we can venture into to expand on the work presented in this dissertation.

The Progression Model

In this work, we were heavily governed by the available data. A pancreatic cancer longitudinal dataset with patient history and tumor progression would help construct a progression model that is also personalized to relative risk. We could answer questions like: if a patient had chronic pancreatitis prior to their cancer, does his/her cancer progress faster than a patient without chronic pancreatitis? We can attempt to translate the effect of comorbidities on cancer progression to the inverse growth rate the patient can have and proceed with the same methodology as presented in Chapter 2. With longitudinal data, we can also better understand the tumor doubling time behavior and hence the inverse growth rate, whether it is based on age, race, gender, or relative risk.

Effort

We defined effort as either (i) the ratio of benign screenings to screening detections, or as (ii) the ratio of benign screenings plus unsuccessful screening detections to successful screening detections. The effort to screen can include other aspects such as the physical act of screening. For example, EUS is an invasive procedure that requires sedation and a companion to discharge the patient, while MRI is an imaging mechanism that does not require sedation. Therefore, there is room to model the effort of using a certain screening modality versus another from a burden on patients perspective. Moreover, the rate at which false negative and false positive results occur can also be considered an effort as they would differ by screening modality according to their specificity. The effort can be expressed in monetary terms as well, where the cost of each procedure, the time each takes, and the side effects of each could be modeled. With converting the effort into cost, the survival years can in turn be converted into cost as well with the common measure of Quality Adjusted Life Years (QALYs). The monetary aspect has the advantage of evening the scale of the effort and the benefit of screening. As we chose to divert from the monetary measures, we can view the complexity of accuracy measuring the cost of every component especially with the time involved with screening when using EUS as the screening modality.

Treatment Prediction

In our work, we view treatment as resection of the tumor, and we developed a resectability prediction tool. Although resection is considered to be the true cure of pancreatic cancer, radiation and chemotherapy are also being used. Neoadjuvant therapy is gaining popularity, where a patient is first treated with chemotherapy then resection [HL17]. Some believe there is benefit in neoadjuvant therapy before surgery, where the tumor size could be reduced and a borderline resectable cancer could become resectable [HL17]. The resectability prediction tool can be expanded to become a treatment prediction tool and include the pre-surgical step of neoadjuvant therapy. From our work, the probability of resectability can be viewed as an overall measure of the patient's condition at different points in the cancer. However, borderline resectable tumors are not well defined in our model since we do not have a direct way to identify the borderline resectability from the SEER data. With the introduction of neoadjuvant therapy prior to resection, we need a treatment model that can account for the borderline resectable. The model would allow for time-adjusted survival rate of borderline resectable tumor depending on the rate at which neoadjuvant therapy reduces the size of the tumor.

Personalized Survival Rates

This dissertation used average survival rates that were not gender, race, or age specific to calculate the probability of survival of a patient given their resectability status. SEER reports average survival rates by gender, race, and age of pancreatic cancer patients. However, the rates were not specific to tumor size, stage, or whether the patients underwent resection. Moreover, the reported survival rates differed by gender, race, and age. There are studies that used the SEER data to show that there are treatment disparities based on race and gender. However, the differences in survival rates cannot be entirely attributed to the treatment disparities found in the data, where the tumor could behave differently in different races and genders. The survival rates need to be revisited and personalized to race, gender, and age to better evaluate the effect of a screening policy on each of the cohorts tested in Chapter 4.

Other Potential Extensions: Pancreatic Cysts

Once a screening policy is in place for pancreatic cancer, it is possible to detect pancreatic cysts through the screening. Pancreatic cysts are lesions that can be benign or cancerous, where most cysts are harmless. The challenge of the optimal management of pancreatic cysts can stem from pancreatic cancer screening.

Since there is a chance that pancreatic cysts are in fact pre-cancerous, resection becomes a treatment option as a precaution measure. Cyst resection decisions stem from the potential progression of the cyst. If it is believed that the cyst will not grow or become cancerous, then a decision for cyst management can be to do nothing. Optimal pancreatic cyst management can be viewed under the umbrella of pancreatic cancer screening since high-risk patients for pancreatic cancer are also at risk for pancreatic cysts. Therefore, when high-risk patients are screened, we need to develop optimal management policies when cysts are detected. A pancreatic cyst management model that maximizes a patient's expected quality of life under the constraints of the potential progression of the cyst and burden of resection could be built to help inform the guidelines for cyst management.

In conclusion, pancreatic cancer is a silent and deadly disease. There is room for screening to improve survival. This dissertation presents discrete-event simulation models of tumor progression and screening policy evaluation tools for pancreatic cancer. This work builds a foundation for future research in this area.

BIBLIOGRAPHY

[Abo] *About the Pancreas - The National Pancreas Foundation*.

[AS12] Al-Sukhni, W. et al. "Screening for Pancreatic Cancer in a High-Risk Cohort: An Eight-Year Experience". *J Gastrointest Surg* **16** (2012), pp. 771–783.

[Ame] American Cancer Society. *Signs and Symptoms of Pancreatic Cancer*.

[Atk83] Atkinson, E. N. et al. "On Estimating the Growth Function of Tumors". *Mathematical Biosciences* **67**.2 (1983), pp. 145–166.

[Aye] Ayer, T. et al. "OR Forum-A POMDP Approach to Personalize Mammography Screening Decisions". *Operations Research* **60**.5 (), pp. 1019–1034.

[Bec14] Becker, A. E. et al. *Pancreatic ductal adenocarcinoma: Risk factors, screening, and early detection*. 2014.

[Bil07] Bilimoria, K. Y. et al. "Validation of the 6th edition AJCC pancreatic cancer staging system". *Cancer* **110**.4 (2007), pp. 738–744.

[Can] Canto, M. I. et al. "Screening for Early Pancreatic Neoplasia in High-Risk Individuals: A Prospective Controlled Study" ().

[CMHFHR13] Canto MI Harink F Hruban RH, e. a. "International Cancer of the Pancreas Screening Consortium summit in the management of patients with increased risk for familial pancreatic cancer". *Gut* **62**.80 (2013), pp. 339–347.

[Cen17a] Centers for Disease Control. *National Diabetes Statistics Report, 2017 Estimates of Diabetes and Its Burden in the United States Background*. Tech. rep. 2017.

[Cen17b] Centers for Disease Control and Prevention. *Current Cigarette Smoking Among Adults in the United States | CDC*. 2017.

[Cen17c] Centers for Disease Control and Prevention. *National Diabetes Statistics Report, 2017 Estimates of Diabetes and Its Burden in the United States Background*. Tech. rep. 2017.

[Com14] Comas, M. et al. "Budget Impact Analysis of Switching to Digital Mammography in a Population-Based Breast Cancer Screening Program: A Discrete Event Simulation Model". *PLoS ONE* **9**.5 (2014), e97459.

[Cuc16] Cucchetti, A. et al. "Estimation of the Survival Benefit Obtainable From Screening for the Early Detection of Pancreatic Cancer". *Pancreas* **45**.5 (2016), pp. 714–719.

[DC14] Del Chiaro, M. et al. *Early detection and prevention of pancreatic cancer: Is it really possible today?* 2014.

[Dha15] Dhar, P. et al. "Pancreatic cancer in chronic pancreatitis". *Indian journal of surgical oncology* **6**.1 (2015), pp. 57–62.

[Dis13] Distler, M. et al. "Evaluation of survival in patients after pancreatic head resection for ductal adenocarcinoma". *BMC Surgery* **13**.12 (2013), pp. 1–8.

[For09] Forastero, C. et al. "Optimization of Screening Programmes for Breast Cancer". *World Congress on Medical Physics and Biomedical Engineering, IFMBE Proceedings, volume 25/2*. Munich, Germany: Springer, Berlin, Heidelberg, 2009, pp. 762–765.

[Fou17] Fountzilas, C. *Do Pancreatic Cysts Become Cancerous? | Roswell Park Comprehensive Cancer Center*. 2017.

[Fur01] Furukawa, H et al. "Growth rate of pancreatic adenocarcinoma: initial clinical experience." *Pancreas* **22**.4 (2001), pp. 366–9.

[Gd18] Gordon-dseagu, V. L. et al. "Pancreatic cancer incidence trends: evidence from the Surveillance, Epidemiology and End Results (SEER) population-based data". *International Journal of Epidemiology* November 2017 (2018), pp. 427–439.

[Gre10] Greuter, M. J. et al. "The validation of a simulation model incorporating radiation risk for mammography breast cancer screening in women with a hereditary-increased breast cancer risk". *European Journal of Cancer* **46**.3 (2010), pp. 495–504.

[Hae12] Haeno, H. et al. "Computational Modeling of Pancreatic Cancer Reveals Kinetics of Metastasis Suggesting Optimum Treatment Strategies". *Cell* **148**.1-2 (2012), pp. 362–375.

[Hal15] Hales, C. M. et al. *Prevalence of Obesity Among Adults and Youth: United States, 2015-2016 Key findings Data from the National Health and Nutrition Examination Survey*. Tech. rep. Centers for Disease Control and Prevention, 2015.

[Har16] Harinck, F et al. "A multicentre comparative prospective blinded analysis of EUS and MRI for screening of pancreatic cancer in high-risk individuals". *Gut* **65**.9 (2016), pp. 1505–1513.

[HL17] Heinrich, S. & Lang, H. "Neoadjuvant Therapy of Pancreatic Cancer: Definitions and Benefits." *International journal of molecular sciences* **18**.8 (2017).

[Hol14] Holmer, R. et al. "Interleukin-6: A villain in the drama of pancreatic cancer development and progression". *Hepatobiliary and Pancreatic Diseases International* **13**.4 (2014), pp. 371–380.

[201a] *How Cancer Is Diagnosed - National Cancer Institute*. 2015.

[Hru00] Hruban, R. H. et al. "Progression model for pancreatic cancer." *Clinical cancer research : an official journal of the American Association for Cancer Research* **6**.8 (2000), pp. 2969–72.

[II16] Ilic, M. & Ilic, I. "Epidemiology of pancreatic cancer". *World Journal of Gastroenterology* **22**.44 (2016), pp. 9694–9705.

[Inh] *Inherited Gene Mutations Information | Susan G. Komen®*.

[KLB] Kingma, D. P. & Lei Ba, J. "Adam: A Method for Stochastic Optimization".

[Kuh04] Kuhlmann, K. et al. "Surgical treatment of pancreatic adenocarcinoma". *European Journal of Cancer* **40**.4 (2004), pp. 549–558.

[LL14] Lee, E. S. & Lee, J. M. "Imaging diagnosis of pancreatic cancer: a state-of-the-art review." *World journal of gastroenterology* **20**.24 (2014), pp. 7864–77.

[Len14] Lennon, A. M. et al. "The early detection of pancreatic cancer: What will it take to diagnose and treat curable pancreatic neoplasia?" *Cancer Research* **74**.13 (2014), pp. 3381–3389.

[Li14] Li, Y. et al. "Using a partially observable Markov chain model to assess colonoscopy screening strategies âĂŞ A cohort study". *European Journal of Operational Research* **238**.1 (2014), pp. 313–326.

[Lin] Lindquist, C. M. et al. "Pancreatic cancer screening" ().

[Loe99] Loeve, F. et al. "The MISCAN-COLON Simulation Model for the Evaluation of Colorectal Cancer Screening". *Computers and Biomedical Research* **32**.1 (1999), pp. 13–33.

[Lop14] Lopez, N. E. et al. "Borderline resectable pancreatic cancer: Definitions and management". *World Journal of Gastroenterology* **20**.31 (2014), pp. 10740–10751.

[Lou14] Louzoun, Y. et al. "A mathematical model for pancreatic cancer growth and treatments". *Journal of Theoretical Biology* **351** (2014), pp. 74–82.

[Mai08] Maillart, L. M. et al. "Assessing Dynamic Breast Cancer Screening Policies". *Operations Research* **56**.6 (2008), pp. 1411–1427.

[McA17] McAllister, F. et al. "Current Status and Future Directions for Screening Patients at High Risk for Pancreatic Cancer." *Gastroenterology & hepatology* **13**.5 (2017), pp. 268–275.

[NCISP] National Cancer Institute Surveillance, E. & Program, E. R. *Pancreatic Cancer - Cancer Stat Facts*. Tech. rep.

[Nip17] Nipp, R. et al. "Disparities in cancer outcomes across age, sex, and race/ethnicity among patients with pancreatic cancer". *Cancer Medicine* (2017).

[Not16] Notta, F. et al. "A renewed model of pancreatic cancer evolution based on genomic rearrangement patterns". *Nature* **538**.7625 (2016), pp. 378–382.

[Old17] Oldfield, L. E. et al. "Molecular Events in the Natural History of Pancreatic Cancer". *Trends in Cancer* **3**.5 (2017), pp. 336–346.

[Orp] *Orphanet*.

[Pan15] Pandharipande, P. V. et al. "Targeted Screening of Individuals at High Risk for Pancreatic Cancer: Results of a Simulation Model". *Radiology* **275**.1 (2015), pp. 177–187.

[Ped11] Pedregosa, F. et al. "Scikit-learn: Machine Learning in Python". *Journal of Machine Learning Research* **12**.Oct (2011), pp. 2825–2830.

[Pet18] Peters, M. L. B. et al. "Progression to pancreatic ductal adenocarcinoma from pancreatic intraepithelial neoplasia: Results of a simulation model". *Pancreatology* **18**.8 (2018), pp. 928–934.

[PRM18] Phan, J. & Raman Muthusamy, V. "Managing Incidental Pancreatic Cysts". *Current Gastroenterology Reports* **20**.7 (2018), p. 32.

[Ple07] Plevritis, S. K. et al. "A natural history model of stage progression applied to breast cancer". *Statistics in Medicine* **26**.3 (2007), pp. 581–595.

[Por13] Poruk, K. E. et al. "Screening for pancreatic cancer: why, how, and who?" *Annals of surgery* **257**.1 (2013), pp. 17–26.

[Rah14] Rahib, L. et al. *Projecting cancer incidence and deaths to 2030: The unexpected burden of thyroid, liver, and pancreas cancers in the united states*. 2014.

[Rai10] Raimondi, S. et al. "Pancreatic cancer in chronic pancreatitis; aetiology, incidence, and early detection". *Best Practice & Research Clinical Gastroenterology* **24**.3 (2010), pp. 349–358.

[Raj14] Rajapakshe, R. et al. "Development of a Micro-Simulation Model for Breast Cancer to Evaluate the Impacts of Personalized Early Detection Strategies". *Breast Imaging. IWDM. Lecture Notes in Computer Science*. vol 8539. Springer, Cham, 2014, pp. 372–379.

[Rob07] Roberts, S. et al. “Development of a simulation model of colorectal cancer”. *ACM Transactions on Modeling and Computer Simulation* **18**.1 (2007), pp. 1–30.

[Roe18] Roessel, S. van et al. “International Validation of the Eighth Edition of the American Joint Committee on Cancer (AJCC) TNM Staging System in Patients With Resected Pancreatic Cancer”. *JAMA Surgery* **153**.12 (2018), e183617.

[Saa18] Saad, A. M. et al. “Trends in pancreatic adenocarcinoma incidence and mortality in the United States in the last four decades ; a SEER-based study”. *BMC Cancer* (2018), pp. 1–11.

[Sal15] Salvatore, T. et al. “Pancreatic cancer and diabetes: A two-way relationship in the perspective of diabetologist”. *International Journal of Surgery* **21** (2015), S72–S77.

[Sch14] Schulte, A. et al. “Cigarette smoking and pancreatic cancer risk: More to the story than just pack-years”. *European Journal of Cancer* **50**.5 (2014), pp. 997–1003.

[Sep17] Seppänen, H. et al. “The Results of Pancreatic Resections and Long-Term Survival for Pancreatic Ductal Adenocarcinoma: A Single-Institution Experience”. *Scandinavian Journal of Surgery* **106**.1 (2017), pp. 54–61.

[She17] Shen, S. et al. “A Bayesian model for estimating multi-state disease progression”. *Computers in Biology and Medicine* **81** (2017), pp. 111–120.

[Soc] Social Security. *Actuarial Life Table*. Tech. rep.

[Sol93] Solomon, S. et al. *PRSS1-Related Hereditary Pancreatitis*. 1993.

[Sun14] Sun, S. et al. “A new approach for estimating the progression of pancreatic cancer”. *2014 8th International Conference on Systems Biology (ISB)*. IEEE, 2014, pp. 118–123.

[Taf09] Tafazzoli, A. et al. “Probabilistic cost-effectiveness comparison of screening strategies for colorectal cancer”. *ACM Transactions on Modeling and Computer Simulation* **19**.2 (2009), pp. 1–29.

[Tam14] Tamburrino, D. et al. *Selection criteria in resectable pancreatic cancer: A biological and morphological approach*. 2014.

[Tan12] Tanaka, M. et al. “International consensus guidelines 2012 for the management of IPMN and MCN of the pancreas”. *Pancreatology* **12**.3 (2012), pp. 183–197.

[Tej14] Tejada, J. J. et al. “Combined DES/SD model of breast cancer screening for older women, II: screening-and-treatment simulation Combined DES/SD model of breast cancer screening for older women, II: screening-and-treatment simulation”. *IIE Transactions* **46** (2014), pp. 707–727.

[Tej15] Tejada, J. J. et al. “Combined DES/SD model of breast cancer screening for older women, I: Natural-history simulation Combined DES/SD model of breast cancer screening for older women, I: Natural-history simulation”. *IIE Transactions* **47** (2015), pp. 600–619.

[Tem17] Tempero, M. A. et al. “Pancreatic Adenocarcinoma, Version 2.2017, NCCN Clinical Practice Guidelines in Oncology.” *Journal of the National Comprehensive Cancer Network : JNCCN* **15**.8 (2017), pp. 1028–1061.

[201b] *The Basics of Endoscopic Ultrasound*. 2017.

[Tum11] Tummala, P. et al. “Imaging of pancreatic cancer: An overview.” *Journal of gastrointestinal oncology* **2**.3 (2011), pp. 168–74.

[U.S] U.S. Census Bureau. *American FactFinder - Results*.

[Ver10] Verna, E. C. et al. “Pancreatic cancer screening in a prospective cohort of high-risk patients: a comprehensive strategy of imaging and genetics.” *Clinical cancer research : an official journal of the American Association for Cancer Research* **16**.20 (2010), pp. 5028–37.

[Vin11] Vincent, A. et al. “Pancreatic cancer”. *The Lancet* **378**.9791 (2011), pp. 607–620.

[Wee14] Weekes, S. L. et al. “A Multicompartment Mathematical Model of Cancer Stem Cell-Driven Tumor Growth Dynamics”. *Bulletin of Mathematical Biology* **76**.7 (2014), pp. 1762–1782.

[Wu18] Wu, W. et al. “Rising trends in pancreatic cancer incidence and mortality in 2000 âĂŞ 2014”. *Clinical Epidemiology* (2018), pp. 789–797.

[Xu14] Xu, Z. et al. *Pancreatic cancer and its stroma: A conspiracy theory*. 2014.

[YID13] Yachida, S & Iacobuzio-Donahue, C. A. *Evolution and dynamics of pancreatic cancer progression*. 2013.

[Yac10] Yachida, S. et al. “Distant metastasis occurs late during the genetic evolution of pancreatic cancer”. *Nature* **467**.7319 (2010), pp. 1114–1117.

[YL13] Yadav, D. & Lowenfels, A. B. “The epidemiology of pancreatitis and pancreatic cancer.” *Gastroenterology* **144**.6 (2013), pp. 1252–61.

[Zak15] Zakhari, S. “Chronic alcohol drinking: Liver and pancreatic cancer?” *Clinics and Research in Hepatology and Gastroenterology* **39** (2015), S86–S91.

[Zho17] Zhou, H. et al. “Racial disparities in pancreatic neuroendocrine tumors survival: a SEER study”. *Cancer Medicine* (2017), pp. 2745–2756.

[Zho10] Zhou, J. et al. “Incidence rates of exocrine and endocrine pancreatic cancers in the United States”. *Cancer Causes & Control* **21**.6 (2010), pp. 853–861.

APPENDICES

APPENDIX

A GROWTH MODEL DERIVATIONS

The unconditional joint distributions of volume and stage at symptomatic detection are derived below when R follows a uniform distribution. The unconditional distribution of volume at symptomatic detection is:

$$
\begin{aligned}
f_D(d) &= \int_a^b \frac{1}{b-a}\left(\frac{\mathrm{d}}{\mathrm{d}d}\left(1-e^{-\gamma r(d-c_0)}\right)\right)\mathrm{d}r \\
&= \int_a^b \frac{1}{b-a}\gamma r e^{-\gamma r(d-c_0)}\mathrm{d}r \\
&= \frac{1}{b-a}\cdot\left[\frac{a\cdot e^{-\gamma\cdot a(d-c_0)} - b\cdot e^{-\gamma\cdot b(d-c_0)}}{d-c_0}\right. \\
&\qquad\qquad \left. + \frac{e^{-\gamma\cdot a(d-c_0)} - e^{-\gamma\cdot b(d-c_0)}}{\gamma(d-c_0)^2}\right]
\end{aligned}
\tag{A.1}
$$

The unconditional joint distribution of volume at symptomatic detection and the local stage at detection:

$$
\begin{aligned}
f_{D,I}(d,0) &= \int_a^b \frac{1}{b-a}\gamma r e^{-(\gamma+\eta)r(d-c_0)}\mathrm{d}r \\
&= \frac{1}{b-a}\left[\frac{\gamma r e^{-(\gamma+\eta)r(d-c_0)}}{-(\gamma+\eta)(d-c_0)}\bigg|_a^b - \int_a^b \frac{\gamma e^{-(\gamma+\eta)r(d-c_0)}}{-(\gamma+\eta)(d-c_0)}\mathrm{d}r\right] \\
&= \frac{1}{b-a}\left[\frac{\gamma\cdot a\cdot e^{-(\gamma+\eta)a(d-c_0)} - \gamma\cdot b\cdot e^{-(\gamma+\eta)b(d-c_0)}}{(\gamma+\eta)(d-c_0)}\right. \\
&\qquad\left. + \frac{\gamma\cdot e^{-(\gamma+\eta)a(d-c_0)} - \gamma\cdot e^{-(\gamma+\eta)b(d-c_0)}}{(\gamma+\eta)^2(d-c_0)^2}\right]
\end{aligned}
\tag{A.2}
$$

The unconditional joint distribution of volume at symptomatic detection and the regional stage at detection:

$$
\begin{aligned}
f_{D,I}(d,1) &= \int_a^b \frac{1}{b-a}\cdot\frac{\eta\gamma}{\eta-\omega} r[e^{-(\gamma+\omega)r(d-c_0)} - e^{-(\gamma+\eta)r(d-c_0)}]\mathrm{d}r \\
&= \frac{1}{b-a}\cdot\frac{\eta\gamma}{\eta-\omega}\left[\frac{\gamma r e^{-(\gamma+\omega)r(d-c_0)}}{-(\gamma+\omega)(d-c_0)}\bigg|_a^b - \frac{\gamma r e^{-(\gamma+\eta)r(d-c_0)}}{-(\gamma+\eta)(d-c_0)}\bigg|_a^b\right. \\
&\qquad\left. + \int_a^b \frac{e^{-(\gamma+\omega)r(d-c_0)}}{-(\gamma+\omega)(d-c_0)} - \frac{e^{-(\gamma+\eta)r(d-c_0)}}{-(\gamma+\eta)(d-c_0)}\mathrm{d}r\right] \\
&= \frac{1}{b-a}\cdot\frac{\eta\gamma}{\eta-\omega}\left[\frac{a\cdot e^{-(\gamma+\omega)a(d-c_0)} - b\cdot e^{-(\gamma+\omega)b(d-c_0)}}{(\gamma+\omega)(d-c_0)}\right. \\
&\qquad + \frac{b\cdot e^{-(\gamma+\eta)b(d-c_0)} - a\cdot e^{-(\gamma+\eta)a(d-c_0)}}{(\gamma+\eta)(d-c_0)} \\
&\qquad\left. - \frac{e^{-(\gamma+\omega)r(d-c_0)}}{-(\gamma+\omega)(d-c_0)}\bigg|_a^b + \frac{e^{-(\gamma+\eta)r(d-c_0)}}{-(\gamma+\eta)(d-c_0)}\bigg|_a^b\right] \\
&= \frac{1}{b-a}\cdot\frac{\eta\gamma}{\eta-\omega}\left[\frac{a\cdot e^{-(\gamma+\omega)a(d-c_0)} - b\cdot e^{-(\gamma+\omega)b(d-c_0)}}{(\gamma+\omega)(d-c_0)}\right. \\
&\qquad + \frac{b\cdot e^{-(\gamma+\eta)b(d-c_0)} - a\cdot e^{-(\gamma+\eta)a(d-c_0)}}{(\gamma+\eta)(d-c_0)} \\
&\qquad + \frac{e^{-(\gamma+\omega)a(d-c_0)} - e^{-(\gamma+\omega)b(d-c_0)}}{(\gamma+\omega)^2(d-c_0)^2} \\
&\qquad\left. + \frac{e^{-(\gamma+\eta)b(d-c_0)} - e^{-(\gamma+\eta)a(d-c_0)}}{(\gamma+\eta)^2(d-c_0)^2}\right]
\end{aligned}
\tag{A.3}
$$

The discretized version of each distribution was also derived to substitute into the likelihood function. The probability of symptomatic detection volume to be in a certain interval and the detection stage at local is:

$$\begin{aligned}\mathbf{P}(D \in (d_k, d_{k+1}), I=0) &= \int_{d_k}^{d_{k+1}} f_{D,I}(x,0)dx \\ &= \frac{1}{b-a} \cdot \left[\frac{\gamma(b-a)}{\gamma+\eta} + \frac{\gamma \cdot e^{-(\gamma+\eta)b(x-c_0)} - \gamma \cdot e^{-(\gamma+\eta)a(x-c_0)}}{(\gamma+\eta)^2(x-c_0)} \right]_{x=d_k}^{d_{k+1}}\end{aligned} \tag{A.4}$$

The probability of symptomatic detection volume to be in a certain interval and the detection stage at regional is:

$$\begin{aligned}\mathbf{P}(D \in (d_k, d_{k+1}), I=1) &= \int_{d_k}^{d_{k+1}} f_{D,I}(x,1)dx \\ &= \frac{1}{b-a} \cdot \frac{\eta\gamma}{\eta-\omega} \cdot \left[\frac{b-a}{\gamma+\omega} + \frac{a-b}{\gamma+\eta} + \frac{e^{-(\gamma+\omega)b(x-c_0)} - e^{-(\gamma+\omega)a(x-c_0)}}{(\gamma+\omega)^2(x-c_0)} \right. \\ &\qquad \left. + \frac{e^{-(\gamma+\eta)a(x-c_0)} - e^{-(\gamma+\eta)b(x-c_0)}}{(\gamma+\eta)^2(x-c_0)} \right]_{x=d_k}^{d_{k+1}}\end{aligned} \tag{A.5}$$

The probability of symptomatic detection volume to be in a certain interval and the detection stage at distant is:

$$\begin{aligned}\mathbf{P}(D \in (d_k, d_{k+1}), I=2) &= \int_{d_k}^{d_{k+1}} f_{D,I}(x,2)dx \\ &= \frac{1}{b-a} \cdot \left[\frac{e^{-\gamma b(x-c0)} - e^{-\gamma a(x-c0)}}{\gamma(x-c_0)} \right. \\ &\qquad + \frac{\gamma \cdot \omega \cdot e^{-(\gamma+\eta)b(x-c0)} - \gamma \cdot \omega \cdot e^{-(\gamma+\eta)a(x-c0)}}{(\eta-\omega)(\gamma+\eta)^2(x-c_0)} \\ &\qquad \left. + \frac{\gamma \cdot \eta \cdot e^{-(\gamma+\omega)a(x-c0)} - \gamma \cdot \eta \cdot e^{-(\gamma+\omega)b(x-c0)}}{(\eta-\omega)(\gamma+\omega)^2(x-c_0)} \right]_{x=d_k}^{d_{k+1}}\end{aligned} \tag{A.6}$$

APPENDIX

B

CHAPTER 4 FIGURES

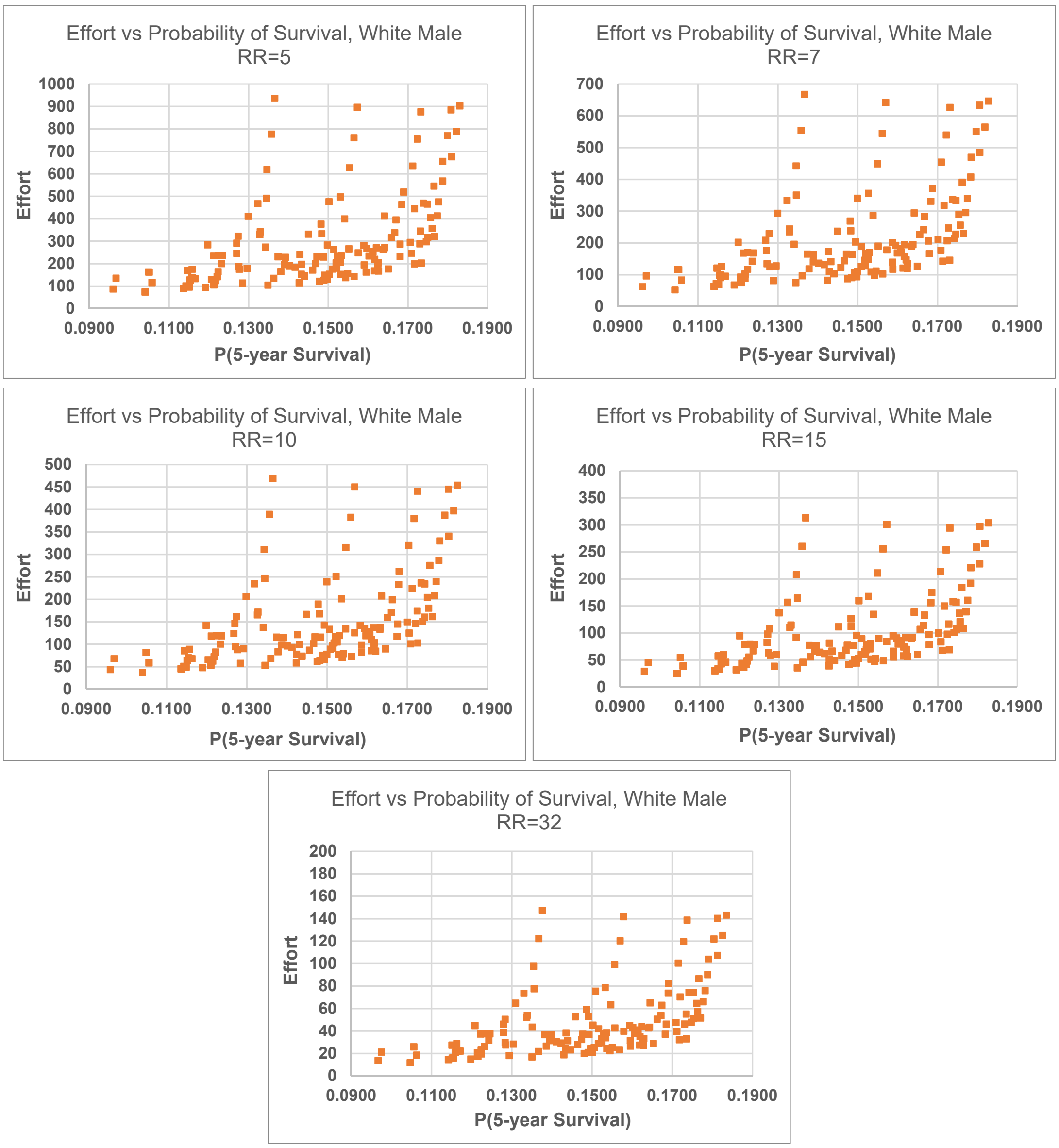

(a) White Male

Figure B.1 Effort against five-year survival of the different screening policies on homogeneous populations using EUS

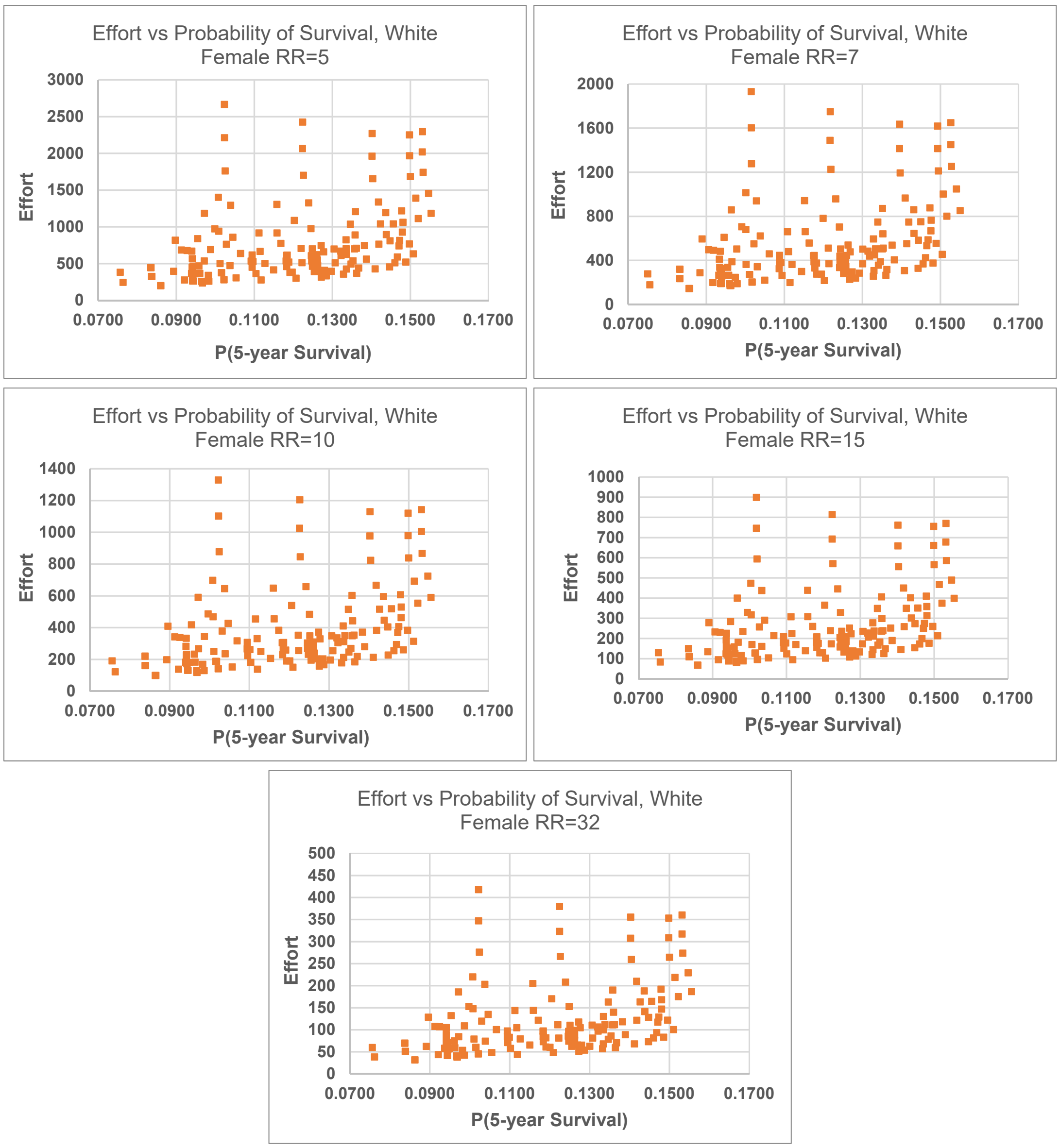

(b) White Female

Figure B.1 (continued) Effort against five-year survival of the different screening policies on homogeneous populations using EUS

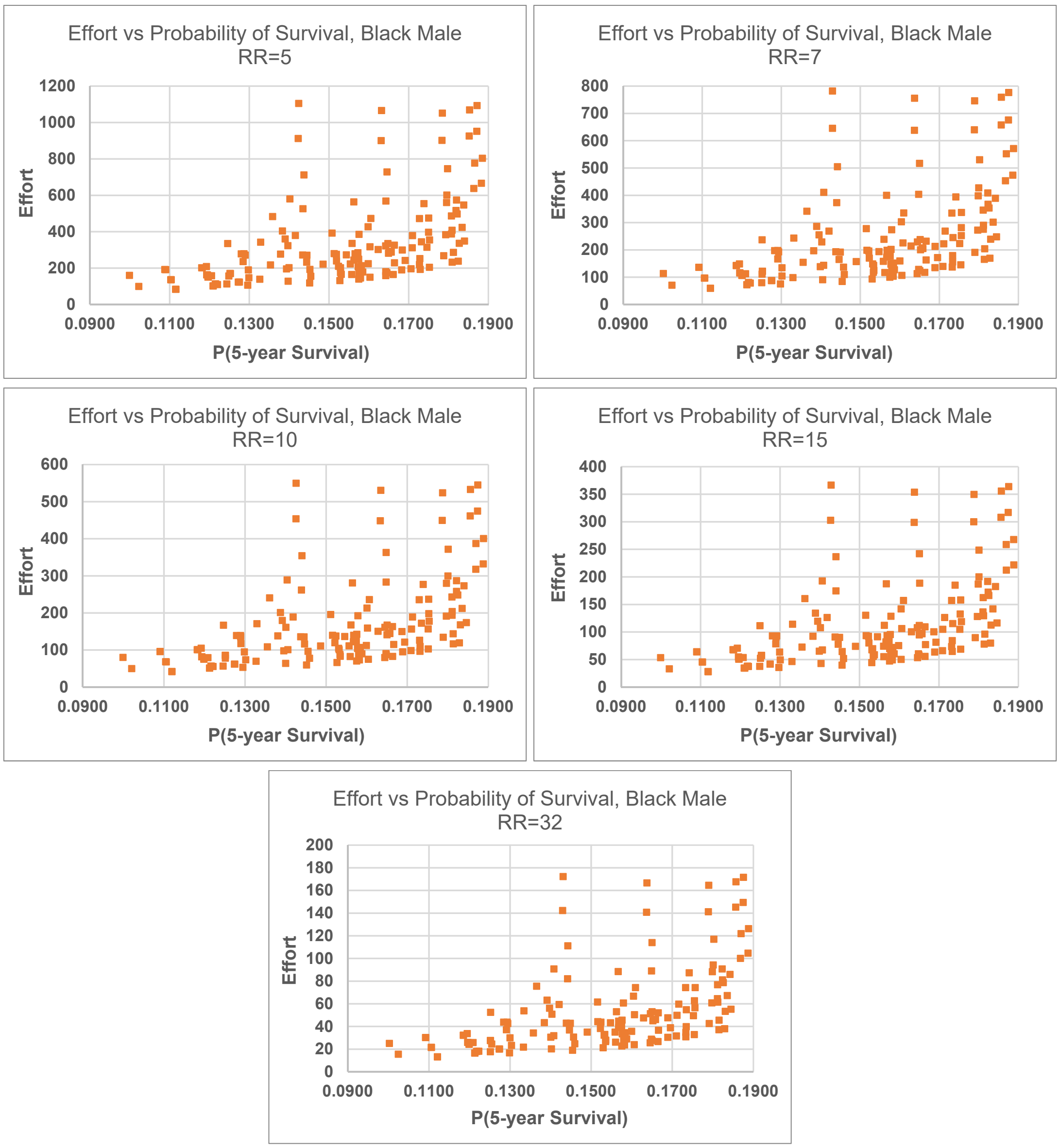

(c) Black Male

Figure B.1 (continued) Effort against five-year survival of the different screening policies on homogeneous populations using EUS

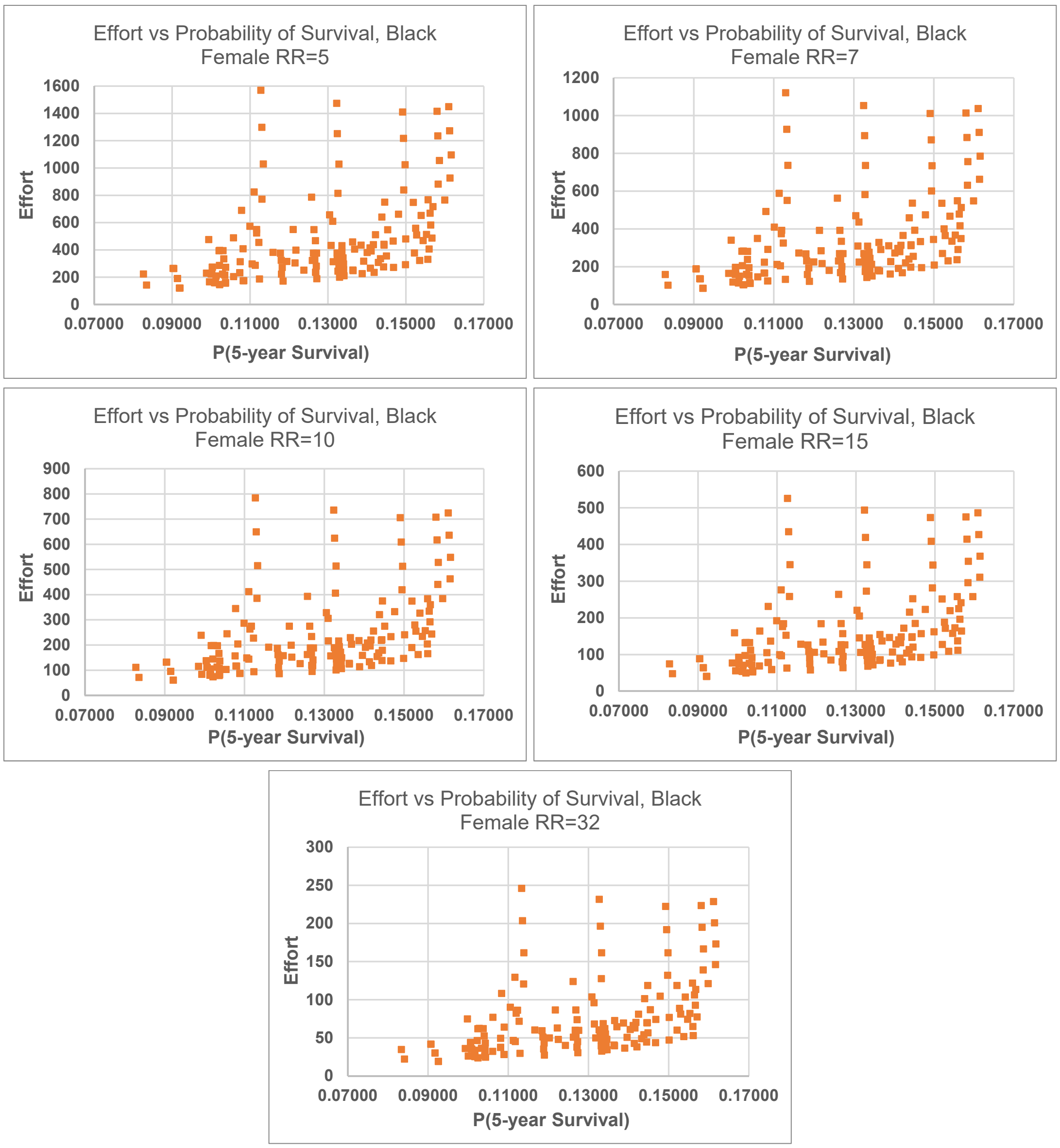

(d) Black Female

Figure B.1 (continued) Effort against five-year survival of the different screening policies on homogeneous populations using EUS

Figure B.2 Effort against five-year survival of the different screening policies on a heterogeneous population using EUS